2019

Synthetic biology approaches to improve cell-based cancer immunotherapy

BOSTON UNIVERSITY

COLLEGE OF ENGINEERING

Dissertation

SYNTHETIC BIOLOGY APPROACHES TO IMPROVE CELL-BASED CANCER IMMUNOTHERAPY

by

JANG HWAN CHO

B.S.E., Duke University, 2013

Submitted in partial fulfillment of the

requirements for the degree of

Doctor of Philosophy

2019

Approved by

First Reader

Wilson W. Wong, Ph.D.
Assistant Professor of Biomedical Engineering

Second Reader

James J. Collins, Ph.D.
Termeer Professor of Medical Engineering and Science
Massachusetts Institute of Technology

Third Reader

Ahmad Khalil, Ph.D.
Assistant Professor of Biomedical Engineering

Fourth Reader

John T. Ngo, Ph.D.
Assistant Professor of Biomedical Engineering

Fifth Reader

Andrew Emili, Ph.D.
Professor of Biology
Boston University, College of Arts and Sciences

Professor of Biochemistry
Boston University, School of Medicine

DEDICATION

I would like to dedicate this work to my family.

ACKNOWLEDGMENTS

I sincerely thank everyone who helped me to succeed during my graduate studies. First of all, I want to acknowledge my academic advisors, Dr. Wilson Wong and Dr. Jim Collins. When I first came to Boston University, I remember myself not knowing anything about cellular immunotherapy. I simply wanted to pursue in the field of synthetic biology. I was naïve enough not to realize how much they were related to each other. After my first-year lab rotation, Wilson told me that adoptive immunotherapy is a field of opportunity and "we are limited by our imagination". I was convinced by his passion and eagerness to contribute to the field of cellular immunotherapy. Throughout my Ph.D. career, Wilson was very helpful in every aspect.

I was also very fortunate to be mentored by Dr. Jim Collins. I have to admit that it was many of his studies that really inspired me to work in the synthetic biology field and influenced me to come to Boston University Ph.D. program. I sincerely appreciate his mentorship and advice during my time at Boston University: not only regarding academic matters but also personal issues as well. Jim always listens to his students and helps as much as he could.

I also like to acknowledge all my graduate committee members: Dr. Wilson Wong, Dr. Jim Collins, Dr. Ahmad (Mo) Khalil, Dr. John Ngo, and Dr. Andrew Emili for their academic support.

Also, I would like to acknowledge everyone who helped me in the laboratory. I want to especially thank Dr. Atsushi Okuma. As the only immunologist in Wong lab, he always inspired and instructed me with topics in immunology that I was not familiar with

at the time. I very much enjoy having discussions with him in the lab. I want to recognize Dr. Dalal Al-Rubaye, and international Master exchange students: Teresa Wiese, and Silvia Beghi who all came from outside of the United States to help with different projects. I also thank Katri Sofjan for helping me with several ongoing projects. I also like to acknowledge Dr. Devin R. Burrill for initial guidance on protein purifications. I want to recognize Jeong Min Park for protein purifications during her summer research at the Wong lab. I also would like to thank the member from Wong lab for their help: Huishan Li, Deboki Chakravarti, Ben Weinberg, Nicole Wong, Matthew Brenner, Seunghee Lee, Justin Letendre, and Chloe Ding.

Moreover, I want to thank members of the Khalil and Collins laboratories for all the great discussions. I also want to thank Szilvia Kiriakov for maintaining the Attune flow cytometer. I want to recognize Patrick Autissier and Brian Tilton at BU Flow Cytometry Core for cell sorting help. Also, I acknowledge Dr. Thomas Balon from the BU animal facility for IVIS imaging assistance. I also want to thank Christen Bailey who always answered my questions about the administrative work.

Lastly, I want to thank my family: my supportive spouse So Lim, my wonderful children Wujin and Yenna, my brother Jun Hwan, and my wonderful parents and parents-in-law for always supporting me throughout my life.

SYNTHETIC BIOLOGY APPROACHES TO IMPROVE

CELL-BASED CANCER IMMUNOTHERAPY

JANG HWAN CHO

Boston University College of Engineering, 2019

Major Professors: Wilson Wong, Assistant Professor of Biomedical Engineering

and

James J. Collins, Termeer Professor of Medical Engineering and Science, Massachusetts Institute of Technology

ABSTRACT

Adoptive T cell immunotherapy is a promising anti-cancer therapy that has the potential to become the ultimate therapeutic agents to treat a variety of diseases. Recently, chimeric antigen receptor (CAR) expressing T cells has demonstrated to be a very effective approach to treat B cell cancer patients. Despite optimistic results, there are several improvements that need to be made to enhance the safety and efficacy of current CAR T cell therapy. Fortunately, different synthetic biology tools can be implemented to overcome many of the current deficiencies of CAR T cell therapy. Here, we develop anti-Axl CAR and synNotch receptors to target Axl which is a tyrosine kinase receptor that is commonly overexpressed in many cancers and considered as one of important cancer therapeutic targets. Next, we develop a *s*plit, *u*niversal, and *pr*ogramm*a*ble (SUPRA) CAR system that can be used to switch targets without re-engineering T cells, fine-tune T cell activation level, and sense and logically respond to multiple antigens. These multiple features are useful in mitigating tumor relapse, limiting CAR-T induced toxicities, and enhancing

tumor specificity. Orthogonal SUPRA CARs are also used to control different cell types and signaling domains, enabling diverse immune responses from SUPRA CAR T cells. Lastly, we demonstrate that SUPRA CAR can redirect the activity of both innate and adaptive immune cell types. We also expand the logic capabilities of SUPRA CAR T cells by integrating three inputs in a single immune cell. We also show intercellular logic gate by engineering immune cell-cell interaction. We further demonstrate controlling endogenous immune cell polarization using SUPRA CAR T cells. These wide-ranges of SUPRA CAR applications imply its versatility as a platform for engineering cell-cell interactions with advanced logic functions to enhance efficacy and safety of cell-based cancer immunotherapy.

CITATION TO PREVIOUSLY PUBLISHED WORK

Portions of this dissertation are from the material that has been published or is in the preparation process for publication.

Chapter 1 was published as:

Brenner, M.J., Cho, J.H., Wong, N.M.L., and Wong, W.W. (2018). Synthetic biology: immunotherapy by design. *Annu. Rev. Biomed. Eng.* 20.

Chapter 2 was published as:

Cho, J.H., Okuma, A., Al-Rubaye, D., Intisar, E., Junghans, R.P., and Wong, W.W. (2018). Engineering Axl specific CAR and SynNotch receptor for cancer therapy. *Sci. Rep.* 8, 3846.

Chapter 3 was published as:

Cho, J.H., Collins, J.J., and Wong, W.W. (2018a). Universal chimeric antigen receptors for multiplexed and logical control of T cell responses. *Cell* 173, 1426–1438.e11.

TABLE OF CONTENTS

LIST OF FIGURES

LIST OF ABBREVIATIONS

CAR ..... Chimeric Antigen Receptor

CRS ..... Cytokine Release Syndrome

IFN- γ ..... Interferon gamma

IL-2 ..... Interleukin 2

scFv ..... single-chain variable fragment

TCR ..... T Cell Receptor

Tconv ..... conventional T cells

TIL ..... Tumor Infiltrating Lymphocyte

TME ..... Tumor Micro Environment

Treg ..... regulatory T cells

CHAPTER ONE: SYNTHETIC BIOLOGY APPROACHES TO ENHANCE CANCER IMMUNOTHERAPY

1.1 Introduction

1.1.1 Synthetic Biology Tools to Engineer Mammalian Cells

Synthetic biology is a multidisciplinary field where it merges physics, biology, genetic engineering, chemistry, and electrical and computer engineering to program cellular functions more efficiently and reliably for therapeutic and research applications [1–4]. As synthetic biology focuses on engineering cells with novel functions that do not exist in nature, it has a strong emphasis on designing reliable and programmable synthetic genetic circuits that can provide precise control of gene of interests in a spatiotemporal manner. Early synthetic biology research was focused on programming synthetic gene circuits in prokaryotes where many of gene circuits were inspired by electrical circuits including the construction of genetic toggle switch [5], oscillators [6,7], and Boolean logic gates [8]. Many of previous gene circuits in bacteria were based on relatively simple mathematical models. These efforts to recapitulate the complex cellular phenotypes with simple synthetic components advanced our understanding of engineering cell with predictable and reliable functions.

The field of mammalian synthetic biology focuses on developing tools and novel gene circuits to control and reprogram different functions of mammalian cells [9]. These tools include devices for controlling RNA and protein expression, synthetic transcription factors

capable of carrying out user-defined gene expression programs, tools for editing the genome, and tools that enable rewiring of signaling pathways.

Many RNA devices have been developed to tune gene expression and to perform logic based on RNA interference or miRNAs [10,11]. Other types of RNA control devices include RNA aptamers and ribozymes used to regulate the stability of mRNA transcripts. Additionally, synthetic biologists have created tools to control protein activity and turnover that could be harnessed for cellular immunotherapy. Degron domains, which affect the regulation of protein degradation, have been used to control the degradation kinetics, and thus levels, of protein in the cell [12,13]. Alternatively, ligand-inducible domains can be used to control the degradation or dimerization of proteins of interest in a tunable manner [14–16]. Recently, Lim and colleagues demonstrated the use of heterodimerization domains to develop CARs that can be controlled by small molecules, effectively creating an ON switch. Furthermore, light-inducible dimerization domains could be useful in cellular therapy to enable spatiotemporal control of cell activity [17–22].

On the transcription level, there are many tools available for regulation, such as DNA binding domains developed by fusing natural transcription factors (e.g. TetR and GAL4) to transcriptional activator or repressor domains [23,24]. Synthetic transcription factors could also be designed to regulate endogenous transcription using zinc fingers (ZFs) [25,26], transcription activator-like effectors (TALEs) [27–29], or clustered regularly interspaced short palindromic repeat-associated systems (CRISPR/Cas) [30–32]. Additionally, these systems enable highly specific and efficient genome editing at defined genomic loci [33,34]. These tools are already being used to enhance cellular

immunotherapies. For example, a recent study demonstrated that CD19 CARs precisely integrated at the endogenous T cell receptor a-constant (TRAC) locus using CRISPR/Cas9 resulted in uniform expression of the CAR and increased T cell potency [35]. Further, evidence suggests that simultaneous genomic disruption of integration of an HIV-specific CAR into the CCR5 locus helps engineered T cells resist HIV infection [36].

Another main goal of synthetic biology is to rewire cell-sensing pathways to create novel input-output relationships. In order to achieve this goal, synthetic receptors have been developed that can couple specific inputs (e.g. small molecules or surface antigens) with user-defined outputs (e.g. transcription programs or cell signaling) have been developed (**Figure 1.4.1, Receptor Engineering**). One of the first classes of synthetic receptors is activated solely by synthetic ligands (RASSLs). RASSLs are genetically engineered G-protein-coupled receptors (GPCRs) receptors that can respond to synthetic ligands with native GPCR signaling [37]. Additionally, Tango receptors have been developed to enable transcriptional output from three different classes of receptors (GPCRs, receptor tyrosine kinases, and steroid hormone receptors) [38]. Tango receptors tether synthetic transcription factors to the membrane using linkers containing a protease cleavage sequence (PCS). Upon ligand-binding, the receptor recruits a signaling protein fused to the appropriate protease, which subsequently cleaves the transcription factor from the receptor and allows it to carry out a defined transcription program. Moreover, the modular extracellular sensor architecture (MESA) has been used to sense soluble ligands through ligand-induced dimerization of a transcription factor-bearing receptor chain and a protease-bearing receptor chain. The MESA system has recently been used to rewire

human T cells to sense vascular endothelial growth factor (VEGF) and to produce interleukin 2 or other programmable transcriptional outputs using dCas9 system (28). This particular input-output function demonstrates how synthetic receptors can be used to direct the immune system to respond against normally immunosuppressive cues. Furthermore, synthetic receptors built upon a minimal proteolytic core of the Notch receptor (synNotch) allow for the programming of both inputs and outputs useful for cell-based therapies [39].

As one of key goal in synthetic biology is to engineer human cells to treat disease, the variety of synthetic biology tools are used to assemble more effective and precise synthetic gene circuits for various therapeutic purposes [4,9]. Very recently, there have been several foods and drug administration (FDA) approved drugs utilizing different mammalian synthetic biology tools. In 2017, the FDA approved the first *in vivo* gene therapy, Vortigern neparvovec, for the treatment of Leber's congenital amaurosis, which is an inherited disease causing progressive blindness [40]. Voretigene neparvovec is an engineered adeno-associated virus serotype 2 (AAV2) vector that contains Retinal pigment epithelium-specific 65 kDa protein (RPE65) cDNA. In addition, FDA approved first therapy using small interfering RNA (siRNA) technology to treat people with hereditary transthyretin-mediated amyloidosis [41]. By using siRNA, it inhibits translation of abnormal form of transthyretin, a transport protein in the body that carries thyroid hormone and retinol-binding protein. Also, recent clinical trials using CRISPR/Cas genome editing technology to treat blood disorder β- thalassemia started [42]. Lastly, multiple clinical trials demonstrated the efficacy of using synthetic receptors called chimeric antigen receptors (CARs) to treat blood cancer. CD19 CAR expressing T cells or CD19 CAR-T cells have

been tremendously successful in treating acute lymphoblastic leukemia with complete remission rate up to ~90% in both children and adults. Two CD19 CAR-T cell therapies are now FDA approved including Novartis' Kymriah (tisagenlecleucel) to treat acute lymphoblastic leukemia and Gilead's Yescarta (axicabtageneciloleucel) to treat large B-cell lymphoma [43]. All of these examples demonstrate applications of synthetic biology tools to engineer human cells to treat different diseases. In the following section, I will describe the cancer immunotherapy research field in more detail and elaborate on how synthetic biology can be used to improve its efficacies.

1.1.2 Brief Overview of Cancer Immunotherapy

Immunotherapy is a type of cancer treatment that involves the use of patient immune systems and it is one of the most effective cancer treatment today [44,45]. There are several types of immunotherapy such as the use of cancer vaccines, monoclonal antibodies, cytokines, and adoptive cell-based therapy. Personalized cancer vaccines have demonstrated to be very effective when cancer neoantigens were used in melanoma patients [46,47]. Cancer neoantigens are promising targets for the vaccine because they are highly immunogenic and tumor specific. In another example, autologous antigen presenting cells (APCs), which are a group of endogenous immune cells including dendritic cells and macrophages, have been used to treat prostate cancer. After patients' APCs are collected, these isolated cells are stimulated with cancer antigen called prostatic acid phosphatase (PAP). Then, the APCs process and display antigens to stimulate CD4+ helper

cells and CD8+ cytotoxic T cells in the patient body. This therapy is called Sipuleucel-T (also known as Provenge) and is FDA approved to treat metastatic prostate cancer [48].

Furthermore, various cytokines, small proteins that are crucial for intercellular signaling, are being utilized as immunotherapy agents. These cytokines include Interleukin-2 (IL-2) that has been successfully used to patients with advanced renal cancer and melanoma [49]. Also, variety of different cytokines including Granulocyte colony-stimulating factor (G-CSF), Granulocyte-macrophage colony-stimulating factor (GM-CSF), Interferon alpha-2b (IFN-α 2b), IL-8, IL-12, and IL-15 are currently being tested in clinical trials to treat different types of cancers including breast cancer, ovarian cancer, prostate cancer, brain tumors, and Acute Myeloid Leukemia (AML) [49].

Furthermore, specific types of monoclonal antibodies called checkpoint inhibitors have illustrated to be a very potent anti-cancer therapy [50]. Checkpoint inhibitor therapy targets inhibitory immune checkpoints, which downregulates immune cell function when activated. Tumors often activate inhibitory checkpoint molecules on immune cells to protect themselves from being targeted and checkpoint inhibitors prevent interaction between checkpoint molecules and their ligand expressed on tumor cells. There are several types of FDA approved checkpoint inhibitors including CTLA-4 blockade (Ipilimumab), PD-1 inhibitors (Nivolumab and Pembrolizumab), and PD-L1 inhibitors (Atezolizumab, Atezolizumab, and Durvalumab) [50]. These checkpoint blockers are demonstrated to be very effective against lung cancer, melanoma, kidney cancer, bladder cancer, and Hodgkin's lymphoma. Although very promising, there are several clinical data suggesting that only subsets of patients get benefit from these checkpoint inhibitor therapies.

Cellular immunotherapy is another pillar of immunotherapy that has shown to be very effective for different types of cancers [35,51–53]. Traditionally, tumor-infiltrating T cells (TILs) were isolated from the patient tumor, expanded *ex vivo,* and then re-infused back into patients to treat metastatic melanoma [54,55]. However, the protocol of TIL therapy is often complicated, time-consuming, and labor intensive. Furthermore, finding effective or potent TILs that will function well *in vivo* is not trivial. In order to overcome this issue, researchers have successfully re-directed T cell activity by expressing synthetic receptors called chimeric antigen receptors (CARs) through genetic engineering.

CARs are genetically engineered synthetic receptors composed of extracellular single chain variable fragment (scFv) fused to intracellular T cell signaling domains that include co-stimulatory domains (such as CD28 and 4-1BB) and CD3ζ signaling domain [56]. When CAR-expressing T cells bind to tumor antigens expressed on tumor surface, they initiate anti-tumor immune responses such as cytokine production and tumor cytotoxicity. Unlike T cell receptor (TCR) activation, CAR activation is MHC-independent, but CARs can only target antigens expressed on cell surfaces. CAR-T cell therapy against CD19, a transmembrane protein expressed on B lineage cells, has shown to be very potent in multiple clinical trials and there are now FDA approved CD19 CAR-T cell drugs.

It was the iteration of CAR design that really improved its clinical efficiency [56]. Early CAR design is composed of scFv that can bind to tumor antigens, fused to CD3ζ signaling domain. However, this first-generation CAR-T cell failed to suppress tumor burden in the patient. Mainly, these first generation engineered CAR-T cells lacked proliferation and persistence *in vivo*. To overcome this issue, in second generation CAR design, CD28 co-

stimulatory domain was fused in tandem with CD3ζ signaling domain and this approach significantly increase persistence, anti-tumor effect, cytokine secretion, and proliferation *in vivo*. Later, different co-stimulatory domains such as 4-1BB are also included in CAR designs. In third generation CAR, multiple co-stimulatory domains were fused in tandem to further increase T cell functions *in vivo*.

Immune cells are an ideal platform to treat different human disease for several reasons. First, immune cells can move through the patient body to constantly sense and signal pathogens or abnormal physiologies. Moreover, they can infiltrate a variety of tissue types and proliferate at the site of inflammation and recruit different types of immune cell types. In addition, they have memory phenotypes that can be crucial in recurring inflammations. Lastly, these immune cells can have multiple functions from cytotoxicity of tumor cells to secretion of cytokines that can modify local tumor microenvironments. Thus, reprogramming immune cells with novel function has the potential to become the ultimate therapeutic agents to cure many different diseases.

1.2 Current limitations of CAR-T therapy

1.2.1 Safety

Although very promising, CAR-T related toxicities are one of the major concerns in CAR-T therapy. For instance, often when patients receive CD19 CAR-T cells, they undergo symptom called cytokine release syndrome (CRS) [57–59]. CRS occurs when many of the immune cells are overactivated that can lead to the production of inflammatory

cytokines, which in turn can again enhance the activity of host immune cells. It is thought to be coming from the activation of myeloid cells by highly activated engineered T cells. Most of the CRS symptoms are manageable with immunosuppressive agents, but in some cases, it can be lethal and lead to the death of patients [60]. With recent mouse models, researchers are beginning to understand the mechanism of CRS in vivo [61]. To describe briefly, new murine models demonstrated that human or mouse macrophages interact with activated CAR-T cells which then activate endogenous macrophages. Activation of macrophages will further increase the activation level of engineered CAR-T cells to secrete more inflammatory cytokines. As CRS can be toxic in a number of cases, we need a better CAR design to mitigate CRS toxicity in CAR-T treated patients.

Also, current CAR-T cells are not specific enough [62–64]. For example, CD19 is not only expressed on malignant B cells, but it is also expressed on normal B cells. Thus, when patients receive CD19 CAR- T cells, these engineered T cells will kill all the B cells both normal and cancer B cells. This on-target off-tumor responses lead to B cell aplasia in patients who receive CD19 CAR-T therapy. Although B cell aplasia is manageable with immunoglobulin replacement therapy, off-target of CAR-T cells can be very toxic for solid tumors. For instance, Rosenberg and college engineered CAR-T cells against Her2 to treat colon cancer. However, when the patient received Her2 CAR T cells, they reacted with normal lung epithelial cells that express a low level of Her2 which triggered CRS and eventually led to the death of patients [60]. As can be seen from this case, on-target off-tumor response can be toxic and needs to be managed with advanced CAR design.

1.2.2 Efficacy

Although CD19 CAR-T therapy has been very successful, multiple cases of tumor relapse were observed with CD19 CAR-T cell therapy that limits the efficacies of CD19 CAR -T therapy [65–67]. That is, when patients receive CD19 CAR-T therapy, patients will no longer have CD19+ tumor, rather tumors evolve to express other surface proteins such as CD20 and CD22.

Furthermore, even though CAR-T cell therapy is effective against blood tumor, it is not yet effective in treating solid tumors [68–71]. There are several problems. First of all, solid tumors make hard for engineered T cells to penetrate. For instance, chemokines and cytokines secreted by tumor cells make CD8+ T cell trafficking difficult. Also, the low expression level of adhesion molecules such as CXCL9 and CXCL10 in tumor cells prevent T cell trafficking. In addition, tumor cells have a rich extracellular matrix that makes T cell physically difficult to enter into tumor sites. Even if engineered T cells are able to enter tumor location, they often face an array of issues compromising their efficacies due to tumor microenvironment (TME) [72–74]. TME makes engineered CAR-T cell very inefficient because of hypoxia and low nutrients such as lack of glucose and other metabolites (e.g., adenosine) that prevent T cells from proliferating and producing cytokine. Furthermore, there are other immunosuppressive mechanisms including high inhibitory cytokines produced by cancer cells and tumor-associated macrophages (e.g., TGF-b, IL-4, and IL-10), expression of cell surface markers (e.g., PD-L1), and accumulation of regulatory T cells in TME that interfere proper T cell activations. All of

these mechanisms lead to a significant decrease in the efficacy of CAR-T therapy to treat a solid tumor.

1.3 Synthetic Biology Tools for Cellular Immunotherapy

1.3.1 Tools for improving safety

One of the main limitations of cellular immunotherapy, particularly evident in using CAR T cells to treat solid tumors, is the lack of a single, sufficient tumor-specific antigen, which compromises both the safety and efficacy of the therapy. A dual CAR system that can perform combinatorial antigen detection has been developed to increase the specificity of the engineered T cells (**Figure 1.4.1, Logic Control**). In this design, one CAR contains the CD3ζ signaling domain and the other CAR contains the CD28/4-1BB co-stimulatory domains, such that the T cell will only respond to tumor cells that express both antigens. This novel strategy could help to avoid ON target, OFF tissue toxicities observed in CAR T cell therapy. Another example of combinatorial antigen detection uses the synNotch receptor to build combinatorial antigen-sensing circuits [63]. Binding of the synNotch receptor to the tumor antigen (dark gray) releases an intracellular transcription factor, which will then induce the expression of a CAR specific for a second tumor antigen. Furthermore, dimerizing domains that are responsive to small molecule were used to precisely regulate the timing and strength of T cell response [15].

Tumor antigen escape is another challenge that CAR T cell therapy will need to overcome [75]. In order to mitigate the effect of antigen escape on therapy, bispecific

receptors that can be triggered by CD19 and Her2 or CD19 and CD20 have been developed [76]. Thus, even if tumor cells are able to escape detection of one antigen through loss of expression, the cells will still be recognized via the second antigen. Further, many CARs used in clinical trials have a fixed CAR design that is impossible to alter without reengineering the T cells [77]. To allow for increased control over T cell activation during the course of treatment, several split CAR designs have been introduced [78–81] (**Figure 1.4.1. Safety Control**). In these split designs, adaptor antibodies mediate binding between the antigen and the CAR. These split designs promote temporal control of T cell activity and enhance the flexibility of the therapy by allowing T cells to target multiple antigens without reengineering the receptors.

Although recent multiple leukemia clinical trials with CD19 CAR T cells were successful, limited control over CAR T cell activity could result in severe toxicity including cytokine release syndrome. As the safety concerns are one of the main barriers that keep CAR T cell therapy from extending to other cancers than leukemia, many current CAR designs focus on controlling T cell activation. One example is the use of co-inhibitory domains (e.g. PD-1, or CTLA-4) that enable an antigen-specific inhibitory function of the CAR [82]. Also, T cells were engineered to express modified human caspase-9 fused to human FKBP12 to allow dimerization via small molecule. Dimerization induces apoptosis of engineered T cells by activating human caspase9 [83,84]. Introduction of this kill switch will increase the safety of T cell therapy (**Figure 1.4.1. Safety Control**).

1.3.2 Tools for improving efficacy

In addition to safety and specificity concerns, the efficacy of cellular immunotherapies is limited by the inability of engineered T cells to migrate through solid tumors, particularly in solid tissues with deformed vasculature (**Figure 1.4.1. Effectiveness Control**). In order to increase the migration of T cells to tumors, T cells were engineered to express the chemokine receptor CXCR2. These engineered T cells showed enhanced localization to tumors expressing the chemokine CXCL1 in vivo[85]. Moreover, this trafficking resulted in significantly improved antitumor efficacy in vivo[86]. T cells engineered with photoactivatable chemokine receptor, PA-CXCR4, also showed enhanced directional migration to tumor sites and significantly reduced tumor burden in vivo[87]. Another approach to enhancing engineered T cell migration involves restoration of heparanase expression. Ex vivo expanded T cells were found to underexpress heparanase, an enzyme which promotes the degradation of the extracellular matrix. T cells engineered to express heparanase demonstrated improved tumor penetration and antitumor activity[88].

In the tumor microenvironment, there are many immunosuppressive cues including inhibitory cytokines (e.g. IL-4 and TGF-B) and cell surface markers (e.g. PD-L1) that inhibit the antitumor activity of engineered T cells. Thus, engineering T cells to overcome these immunosuppressive cues will be critical to effective cancer cellular immunotherapy (**Figure 1.4.1. Effectiveness Control**). In one study, blockade of inhibitory TGF-B

signaling through overexpression of a non-functional TGF-B receptor mitigated inhibitory effects[89]. Other approaches include converting immunosuppressive cues into immunostimulatory responses. For example, a fusion of the inhibitory cytokine receptor IL-4 exodomain to the IL-7 receptor endodomain effectively converted the tumor-derived IL-4 inhibitory pathway to IL-7 immune stimulation [90]. T cells have also been engineered to express receptors that comprise the PD-1 exodomain and CD28 endodomain. With this approach, binding of engineered T cells to PD-L1(+) tumor cells resulted in increased cytokine secretion and proliferative capacity of the engineered cells [91]. Furthermore, tumor-specific T cells have been engineered to conditionally secrete immunostimulatory cytokines (e.g. IL-12) in the tumor microenvironment to promote engineered T cell efficacy [92]. However, recent clinical trials indicate a need for better control of IL-12 secretion via novel gene circuit design as it showed severe toxicity in a clinical setting [93]. Lastly, feedback control has been used to regulate the duration and dynamics of the T cell response (**Figure 1.4.1. Dynamic Control**).

1.4 Figure

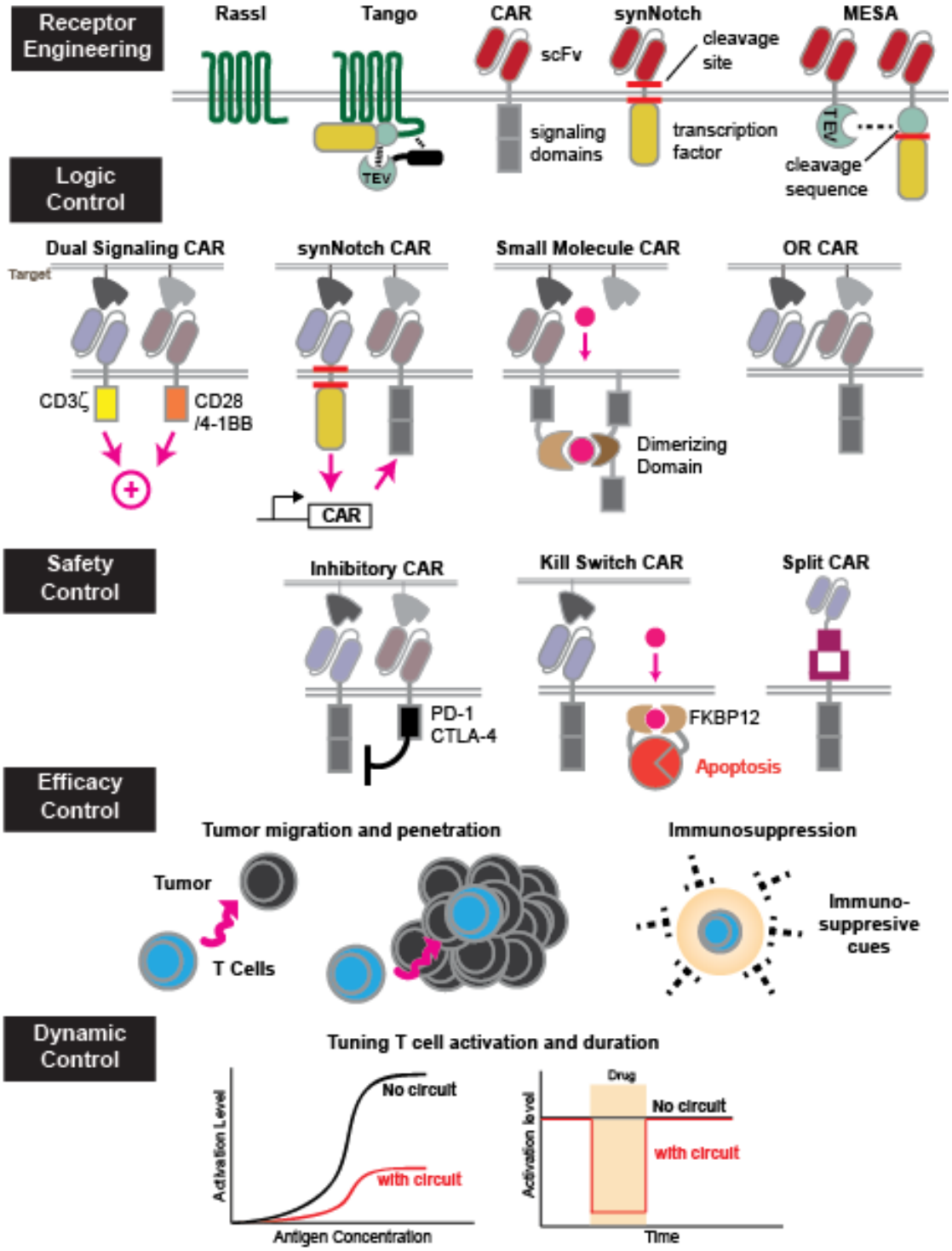

Figure 1.4.1. Applications of synthetic biology in cancer cellular immunotherapy

(A) Receptor Engineering: Different synthetic receptor designs developed to reprogram cells with user-defined input-output relationships.

(B) Logic Control: Different CAR receptor designs that can perform logic to enhance tumor specificity or to tune T cell activity.

(C) Safety Control: Different CAR designs that can mitigate CAR- T cell-related toxicities.

(D) Efficacy Control: Development of novel gene circuits or CARs to increase the effectiveness of CAR T cell therapy by engineering T cell mobility or mitigating immunosuppressive cues in cancer microenvironment.

(E) Dynamic Control: Engineering cells with gene circuits that can tune T cell activation and its duration.

1.5 Acknowledgment

I want to acknowledge Nicole Wong, Matthew Brenner, and Dr. Wilson Wong for their significant contributions including editing published manuscript to complete this chapter.

CHAPTER TWO: ENGINEERING AXL SPECIFIC CAR AND SYNNOTCH RECEPTORS FOR CANCER THERAPY

2.1 Introduction

Receptor tyrosine kinases (RTKs) are transmembrane proteins that sense extracellular ligands. Ligand engagement induces receptor dimerization, which leads to activation of downstream signaling pathways. RTKs regulate a wide range of cellular processes such as cell survival, growth, and differentiation. Moreover, mutation or dysregulation of RTKs has been implicated in many diseases including cancer [94,95].

The Axl protein is a member of the TAM (TYRO3, AXL, and MER) of receptor tyrosine kinases subfamily and involved in the stimulation of cell proliferation [96]. The Axl receptor has been demonstrated to be overexpressed in many human cancers including breast, lung, colon, and pancreatic cancers. High level of Axl expression is associated with poor prognosis in different types of cancer [97–100]. Oncogenic Axl signaling increases cancer cell survival, migration, and invasion [101]. Dysregulation of Axl signaling is also known to enhance the epithelial-mesenchymal transition (EMT) and cause drug resistance to immunotherapy and chemotherapy [102–105]. Since Axl is implicated in many cancer progression and drug resistance, a therapeutic that targets Axl could be a valuable cancer therapy. As such, antibody, small molecule inhibitors, and Axl receptor decoy are in the preclinical and clinical stage for breast, lung for other advanced solid tumors [106].

The transfer of tumor-targeting T cells to patients is a promising approach for cancer immunotherapy. In such an approach, T cells are isolated from the patient, and tumor-

specific receptors such as chimeric antigen receptors (CARs) are introduced into the T cells to redirect their specificity. CARs are composed of an antigen-specific scFv and intracellular signaling domains (CD3ζ and co-stimulatory domains). The binding of scFv to an antigen on cancer cells will stimulate T cell receptor and co-stimulatory pathways, leading to the activation of T cells. CAR-expressing T cells have demonstrated unprecedented efficacy against acute lymphoblastic leukemia (ALL), with around 90% complete remission being observed in clinical trials [107–110]. Despite these encouraging results and the recent FDA approval of anti-CD19 CAR T cells for ALL and lymphoma, more antigen-specific CARs are needed to treat cancer beyond B-cell malignancies. Therefore, the development of CAR against Axl could expand the therapeutic range of CAR T cell therapy.

More recently, Lim and colleagues have created a novel receptor design called synNotch that enables the programming of both input and output via the release of intracellular transcription factor upon antigen-receptor binding [39,63]. Unlike conventional CAR activation which triggers endogenous T cell receptor signaling pathway [56,111], synNotch receptor uses the regulatory notch core portion with an engineered transcription factor that enables programmable inputs and outputs to perform user-defined functions. Because of high programmability, synNotch has been used to reprogram human primary T cell responses both *in vitro* and *in vivo* for enhancing tumor specificity and delivering therapeutic payloads in a tumor antigen-specific manner. As such, synNotch receptor targeting Axl ligand with different output functions, such as producing a defined set of cytokines, will improve cellular immunotherapy to treat various cancers. In this

study, we designed a humanized single-chain variable fragment (scFv) against Axl. Using our Axl scFv, we engineered an Axl CAR and Axl synNotch receptors. In an *in vivo* setting, we demonstrated Axl CAR in human primary T cells for killing tumor cells and Axl SynNotch receptor for producing IL-10 in an antigen-specific manner.

2.2 Results

2.2.1 Design and Characterization of the humanized Axl CAR

Since the receptor tyrosine kinase, Axl, is overexpressed in many different types of cancer, we tested if we can design a humanized single-chain variable fragment (scFv) against Axl that can be used for cellular immunotherapy, especially in the context of CAR and synNotch receptor. From a previously published humanized Axl antibody sequence, we designed an Axl scFv by fusing a variable region of heavy chain to light chain through a GS linker [97,112]. We first tested the functionality of the Axl scFv by using it to create an Axl CAR. The Axl CAR is comprised of the Axl scFv and CD8α hinge region as the extracellular domain, and CD28, 4-1BB, and CD3ζ as the intracellular signaling domains (3rd generation CAR [56,113])**(Figure 2.6.1A**). To verify the activity of the Axl CAR, we stably integrated Axl CAR in Jurkat T cells genome through the electroporation of the PiggyBac transposon system [114]. This Jurkat T cell line also contains an NFAT promoter driving GFP expression for measuring CAR activation. NFAT is a representative transcriptional factor that is known to be activated after T cell receptor (TCR) activation[113]. Therefore, NFAT transcription response is used to measure T cell activation by Axl CAR. After Axl CAR-expressing Jurkat T cells were stimulated with

plate-bound Axl protein, Axl CAR-expressing Jurkat T cells displayed a high level of CD69, which is an early T cell surface activation marker [115], and NFAT transcription reporter activity measured by GFP expression (**Figure 2.6.1B**). In contrast, Jurkat T cells without Axl CAR did not yield high CD69 and NFAT reporter expression.

To test Axl CAR activation under a more physiologically relevant condition, we engineered K562 myelogenous leukemia cells to express the Axl antigen. Axl CAR-expressing Jurkat T cells were then co-cultured *in vitro* with Axl+ K562 cells (**Figure 2.6.2A**). Axl+ K562 cells activated Axl CAR-expressing Jurkat T cells strongly as measured with CD69 and NFAT transcription reporter expression. However, Axl CAR T cells were not activated by Axl- K562 cells (**Figure 2.6.2B**). Furthermore, the basal activity of Axl CAR was minimal as measured by both CD69 and NFAT transcription reporter expression (**Figure 2.6.2B**).

2.2.2 Characterization of Axl CAR in Human Primary CD8+ T cells

After characterizing Axl CAR in Jurkat T cells, we tested whether our Axl CAR is active in human primary T cells. Human primary CD8+ T cells were engineered to express the Axl CAR through lentiviral transduction, and we verified via flow cytometry analysis that more than 80% of the cells expressed the Axl CAR (**Figure 2.6.5A**). To determine whether the Axl CAR is functional in CD8+ T cells, the engineered T cells were activated with plate-bound Axl. High CD69 expression on the T cells confirmed that Axl CAR T cells could be activated from plate-bound Axl protein (**Figure 2.6.3A**). Next, we tested if

engineered T cells can eliminate Axl+ tumor cells. We co-cultured Axl CAR T cells with target cells (Axl- or Axl+ K562) (**Figure 2.6.3B**). Forward- and side- scatter FACS plots of the cell mixture after 24 hours co-culture of T cells with K562 tumor cell showed that Axl CAR-expressing CD8+ T cells could kill Axl+ tumor cells efficiently (**Figure 2.6.3C left**). However, Axl CAR-expressing T cells did not kill Axl negative target cells (**Figure 2.6.3C right**). Consistent with this result, live K526 cell counts, which were gated by 7-AAD-negative and fluorescent markers, decreased only in the co-culture of Axl CAR T cells with Axl+ K562 cells (**Figure 2.6.5B**). Furthermore, we tested the killing efficiency against Axl expressing Jurkat T cells, and Jurkat T cells were killed by Axl CAR-expressing CD8+ T cells in a dose-dependent manner (**Figure 2.6.5C**). Importantly, Axl CAR T cells also killed endogenous Axl-expressing tumor cells, such as SK-OV-3 an ovarian cancer cell line, demonstrating the clinical relevance of Axl CAR (**Figure 2.6.3D**). We next tested cytokine secretion and verified that Axl CAR-expressing human primary CD8+ T cells secreted a high level of IFN- γ and IL-2 only when they were co-cultured with Axl+ K562 tumor cells (**Figure 2.6.3E**).

2.2.3 Design and Characterization of the humanized Axl SynNotch

Recently, Lim and colleague demonstrated the use of synNotch receptors for cellular immunotherapy applications [39,63]. Here, we tested if the Axl scFv can be utilized to generate a functional synNotch receptor. The Axl synNotch receptor is composed of the Axl scFv as the extracellular domain and notch core region fused to

engineered transcription factor (tTA) (**Figure 2.6.4A**). Jurkat T cells were engineered to stably express Axl synNotch receptor using electroporation and piggyBac transposon-based system. The expression of the Axl SynNotch was verified by α-myc cell surface staining with flow cytometry (**Figure 2.6.4B**). A reporter construct that composes of a tTA responsive promoter followed by a gene of interest (e.g., a blue fluorescent protein (BFP) or IL-10) were also introduced into Jurkat T cells [39,63,116]. IL-10 was chosen as an output because lL-10 is an inhibitory cytokine that can be used to control inflammation (O'Garra et al., 2008: Roybal et al. 2017). When Axl synNotch expressing T cells engage with tumor cells that express Axl, the tTA transcription factor is cleaved from the synNotch and translocated into the nucleus to regulate gene expression from the reporter.

To test the functionality of the Axl synNotch receptor, Axl synNotch-expressing Jurkat T cells were stimulated with plate-bound Axl protein, and BFP expression from the synNotch transcription reporter was quantified. Interestingly, the dose-response curve of the Axl synNotch receptor displayed a Bell curve characteristic, with maximum activation occurring at ~100ng of Axl protein (**Figure 2.6.4C**). We also tested if Axl synNotch receptor could be activated with tumor cells that express Axl (**Figure 2.6.4D**). Jurkat T cells expressing the Axl synNotch were activated and produced BFP only when co-cultured with Axl+ K562 tumor cells for 24hr (**Figure 2.6.4E**), whereas cells containing tTA responsive element without the Axl SynNotch did not have high BFP expression (**Control, Figure 2.6.4E**) even when co-cultured with Axl+ tumor cells. Consistently, Jurkat T cells that were transiently transfected with tTA responsive IL-10 reporter showed a similar result, activating and secreting IL-10 only when co-cultured with Axl+ tumor cells (**Figure**

2.6.4F). Note that the basal activity of Axl synNotch is minimal when compared to Axl-K562 cell condition and no target cell condition. These results demonstrate the potential cellular immunotherapy application using Axl synNotch receptor.

2.3 Discussion

Genetic engineering of T cell for cellular immunotherapy application has become a promising cancer therapeutic approach. While multiple clinical trials against B cell malignancies have shown encouraging results, CARs that target antigens overexpressed in other cancers besides B cell tumors are still needed. In addition to CARs, the recently developed synNotch receptor have displayed novel therapeutic capabilities by enabling programmable T cell responses such as user-defined cytokine secretion, T cell differentiation, and local delivery of therapeutic antibodies. However, only anti-CD19, GFP, or Her2 synNotch receptors have been explored. In this study, we developed a humanized Axl scFv from previously reported Axl monoclonal antibody by fusing variable region of heavy and light chain via a polypeptide linker. Using this Axl scFv, we successfully created the first Axl CAR and synNotch receptor, which can be valuable therapeutic reagents since Axl is overexpressed in many cancers including colon, breast, prostate, pancreatic and lung cancers.

The anti-Axl CAR and synNotch behaved mostly as expected. To demonstrate the clinical potential of our Axl receptors, further studies in animal models will be required. Interestingly, we demonstrated that Axl synNotch receptor can be strongly activated by plate-bound Axl protein and observed that optimal activation of Axl synNotch receptor

occurred when Axl protein was plated at 100ng/well. Moreover, we showed that Axl synNotch receptor expressing Jurkat T cells could be activated by Axl+ tumor cells. Although not investigated in this study, we observed that the activation of Axl SynNotch is much stronger with plate-bound Axl than cells expressing Axl. We hypothesize that such discrepancy may be due to the suboptimal expression level of Axl on tumor cells. Furthermore, the surface stiffness (plastic vs. cell membrane) could also be a contributing factor since Notch receptor is known to be regulated by force [117–119].

2.4 Conclusion

Here we developed a humanized Axl scFv that can be exploited in the design of CAR and synNotch receptors. We validated the function of Axl CAR by demonstrating that human primary T cells expressing Axl CAR can effectively kill Axl+ tumor cells. We further showed the therapeutic potential of Axl scFv by designing a functional Axl synNotch receptor that can produce IL-10 when activated by Axl+ tumor cells. In further studies, Axl CAR and Axl synNotch expressing T cells can be tested in mouse xenograft studies to test *in vivo* efficacy.

2.5 Methods

2.5.1 *Humanized single chain variable fragment (scFv) against Axl design*

Humanized scFv against Axl was derived by fusing a variable region of an immunoglobulin heavy chain to the variable region of the light chain through a polypeptide linker (GS linker). Humanized heavy and light chain sequences were obtained from a previously

published sequence.

2.5.2 *Axl CAR/synNotch construct design*

Axl CAR was designed by fusing humanized Axl scFv to the hinge region of the human CD8α chain and transmembrane and cytoplasmic regions of the human CD28, 4-1BB, and CD3ζ signaling endodomains. They were under SFFV promoter for primary T cell experiments and under CAG promoter for Jurkat cell experiments. Axl synNotch receptor was designed by fusing humanized Axl scFv to the notch core intracellular domain fused to the tTA transcription factor. Both Axl CAR and Axl synNotch contain a myc tag for verifying surface expression. Furthermore, the Axl CAR used in human primary T cell experiments was fused to a mCherry after the CD3ζ chain for expression level quantification. The Axl CAR used in Jurkat experiments was cloned into the piggyBac vector (System Bioscience Inc.), which has been modified by replacing the CMV promoter with a CAG promoter.

2.5.3 *Primary Human T cell Isolation and Culture*

Whole peripheral blood was obtained from Boston Children's hospital, as approved by the University Institutional Review Board (IRB) approved consent forms and protocols. Primary human CD8+ T cells were isolated from anonymous healthy donor blood by negative selection (STEMCELL Technologies #15063). T cells were cultured in human T cell medium consisting of X-Vivo 15 (Lonza), 5% Human AB serum (Valley Biomedical #HP1022), 10 mM N-acetyl L-Cysteine (Sigma-Aldrich #A9165), 55uM 2-

mercaptoethanol (Thermo Scientific #31350010) supplemented with 50 units/mL IL-2 (NCI BRB Preclinical Repository). T cells were cryopreserved in 90% heat-inactivated FBS and 10% DMSO.

2.5.3 *Lentiviral Transduction of Human T cells*

Replication-incomplete lentivirus was packaged via transfection of HEK 293 FT cells (Invitrogen) with a pHR transgene expression vector and the viral packaging plasmids: pMD2.G encoding for VSV-G pseudotyping coat protein (Addgene #12259), pDelta 8.74 (Addgene#22036), and pAdv (Promega). One day after transfection, viral supernatant was harvested every day for 3 days and replenished with pre-warmed Ultraculture media (Lonza #12-725F) supplemented with 2mM L-glutamine, 100U/ml penicillin, 100ug/mL streptomycin, 1mM sodium pyruvate, and 50mM sodium butyrate. The harvested virus was purified through ultracentrifugation or Lentivirus concentrator (Takara #631232). Primary T cells were thawed 2 days before ultracentrifugation and cultured in T cell medium described above. One day before ultracentrifugation, T cells were stimulated with Human T-activator CD3/CD28 Dynabeads (Thermo Scientific #11132D) at a 1:3 cell: bead ratio and cultured for 24 hr. After viral supernatant purification, rectronectin (Clontech #T100B) was used to transduce cells. Briefly, non-TC treated 6-well plates were coated with rectronectin following the supplier's protocol. Concentrated viral supernatant was then added to each well and spun for 90 min at 1200xg. After centrifugation, viral supernatant was removed and 4ml of human T cells at 250k/ml in T cell growth media supplemented with 100U/ml of IL-2 was added to well. Cells were spun at 1200xg for 60 min and moved

to an incubator at 37 ºC.

2.5.4 *Cancer Cell Lines*

The cancer cell lines used were K562 myelogenous leukemia cells (ATCC # CCL-243) and Jurkat T cells. K562 and Jurkat T cells were cultured in RPMI-1640 (Lonza#12-702Q) with 5% (v/v) heat-inactivated FBS, 2mM L-glutamine, 100U/ml penicillin and 100ug/mL streptomycin. Jurkat and K562 were electroporated or transfected with PiggyBac Transposon system (System Biosciences) to stably express Axl CAR, Axl synNotch receptor or surface antigen: AXL. Two days after transfection, antibiotic (Puromycin (Thermo Scientific #A1113803), zeocin (Thermo Scientific # R25005), or Hygromycin B (Thermo Fisher #10687010)) was added to the medium to select for cells that express the transgenes.

2.5.5 *T cell activation by plate-bound antigen*

Recombinant human Axl protein (R&D #154-AL-100) was coated on 96 well plate (flat bottom) overnight at 4 Cº. Next day, the plate was washed with PBS three times to remove unbound Axl protein. Then, $200x10^3$ Jurkat T cells or human primary T cells engineered to express Axl CAR or Axl synNotch were added to each well. After 24hr, for Axl CAR experiment, Jurkat or primary human CD8+ T cells were stained with α-CD69-APC (BD bioscience #340560) to measure CD69 expression level. GPF expression level driven form NFAT promoter was shown as NFAT promoter activity. For Axl synNotch experiment, BFP expression was measured as a tTA promoter reporter.

2.5.6 *Co-culture experiments*

Jurkat T cells or primary T cells expressing Axl CAR (200 x 10^3 cells/well/200ul) were incubated with K562 target cells (100 x 10^3 cells/well) or with SK-OV-3 cells (100 x 10^3 cells/well) at an E:T ratio of 2:1 or 1:1. For suspension cells, effector cells and target cells were mixed at the same time as seeding. For adherent cells (SK-OV-3), SK-OV-3 cells were pre-cultured for 12hr. Then, Axl CAR T cells were added to wells. After 24 hr of co-culture, the supernatant was harvested and followed the supplier's protocol to determine IFN-γ, IL-2, IL-10 level. Cytokine release assays were carried out using IFN-γ, IL-2, or IL-10 ELISA Kit (BD Biosciences #555142, #555190, #555157). For detection of activation of T cell, expression CD69, GFP, and BFP were measured use Attune NxT flow cytometry (Thermo).

2.5.7 *Cytolysis assay*

Two hundred thousand primary T cells expressing Axl CAR and control CD8 T cells were incubated with K562 target cells or SK-OV-3 cells (100 x 10^3 cells/well). After 24 hr co-culture, the number of live K562 cells was counted by Attune NxT flow cytometry (Thermo). Live K562 cells were identified as 7-AAD-GFP+BFP+ cells. For detection of live SK-OV-3 after 24 hr co-culture, non-adherent cells were washed out, and adherent cells were stained with Calcein AM using LIVE/DEAD Viability/Cytotoxicity Kit (Thermo # L3224), following manufacturer's protocol. For detection of cell-cell contact independent cytolysis activity, Axl-expressing K562 cells were incubated with conditioned medium from K562 cytolysis experiments described above. After 24 hr, the number of live K562 cells was counted by Attune NxT flow cytometry. For Jurkat cell targeting cytolysis

assay, indicated number of Axl CAR-expressing primary T cells (0, 12.5 $x10^3$, 25 $x10^3$, 50 x 10^3, 100 x 10^3, 200 $x10^3$ cells) were cultured with 100 $x10^3$ Axl^+ $luciferase^+$ Jurkat cells for 4 hr. Culture medium was removed, and cells were resuspended with 50 ul/well of 2% FBS in PBS and lysed with 50 ul/well luciferin reagent (Promega #E2610). Lysates were transferred to 96-well plate (Corning #3904), and luminescence was measured with the SpectraMax M5 (Molecular Devices).

2.*5.8 Cell surface protein staining*

After 24 hr stimulation, engineered Jurkat cells and primary T cells were stained with anti-CD69-APC antibody (BD bioscience #340560) for 30 min at room temperature. For detection of expression of cell surface synNotch, transfected Jurkat cells were stained with anti-Myc-PE (Santa Cruz Biotechnology, sc-40) for 30 min at room temperature. Fluorescence was measured by Attune NxT flow cytometry.

2.6 Figures

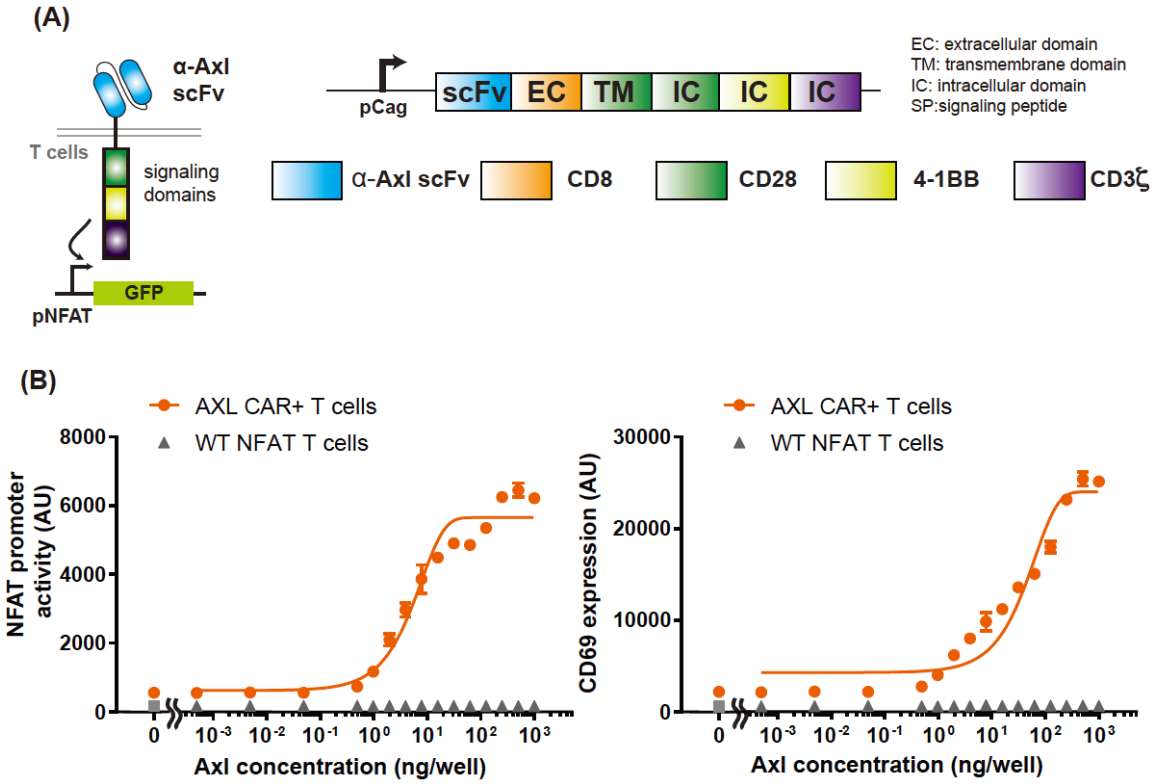

Figure 2.6.1. Design and characterization of the Axl CAR

(A) Humanized Axl CAR is composed of a humanized Axl scFv as the extracellular domain and CD28, 4-1BB, and CD3ζ signaling domain as the intracellular domain. (B) The NFAT promoter activity and CD69 expression levels of Axl CAR-expressing Jurkat T cells after 24hr of culturing with different amount of plate-bound Axl protein. WT NFAT T cells indicate Jurkat T cells harboring an NFAT reporter without the Axl CAR. Data are representative of three biological replicates and presented as the mean ± standard deviation (SD).

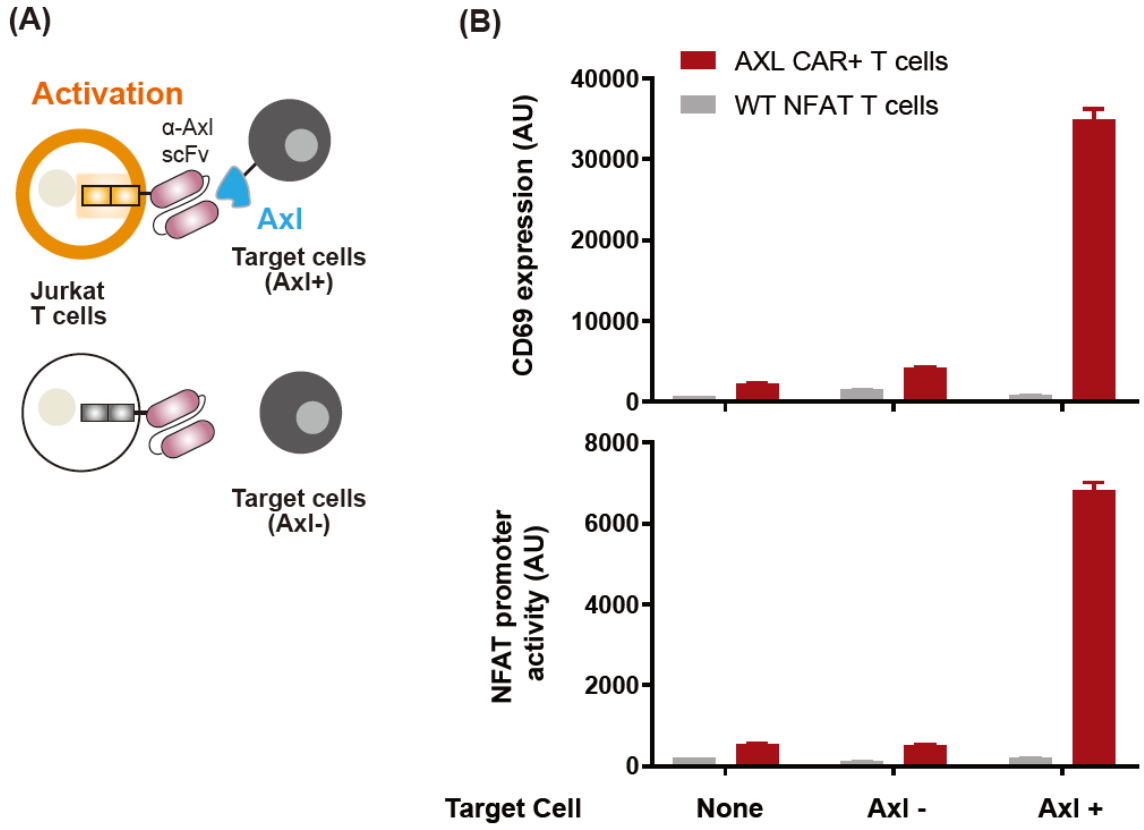

Figure 2.6.2. Axl CAR activation via cell-cell interaction

(A) Axl CAR-expressing or wild-type NFAT Jurkat T cells were co-cultured *in vitro* with Axl+ or Axl- K562 cells. (B) The NFAT promoter activity and CD69 expression level were measured after Axl CAR-expressing Jurkat T cells, and Axl+ K562 cells were co-cultured for 24 hr. Data are representative of three biological replicates and presented as the mean ± SD.

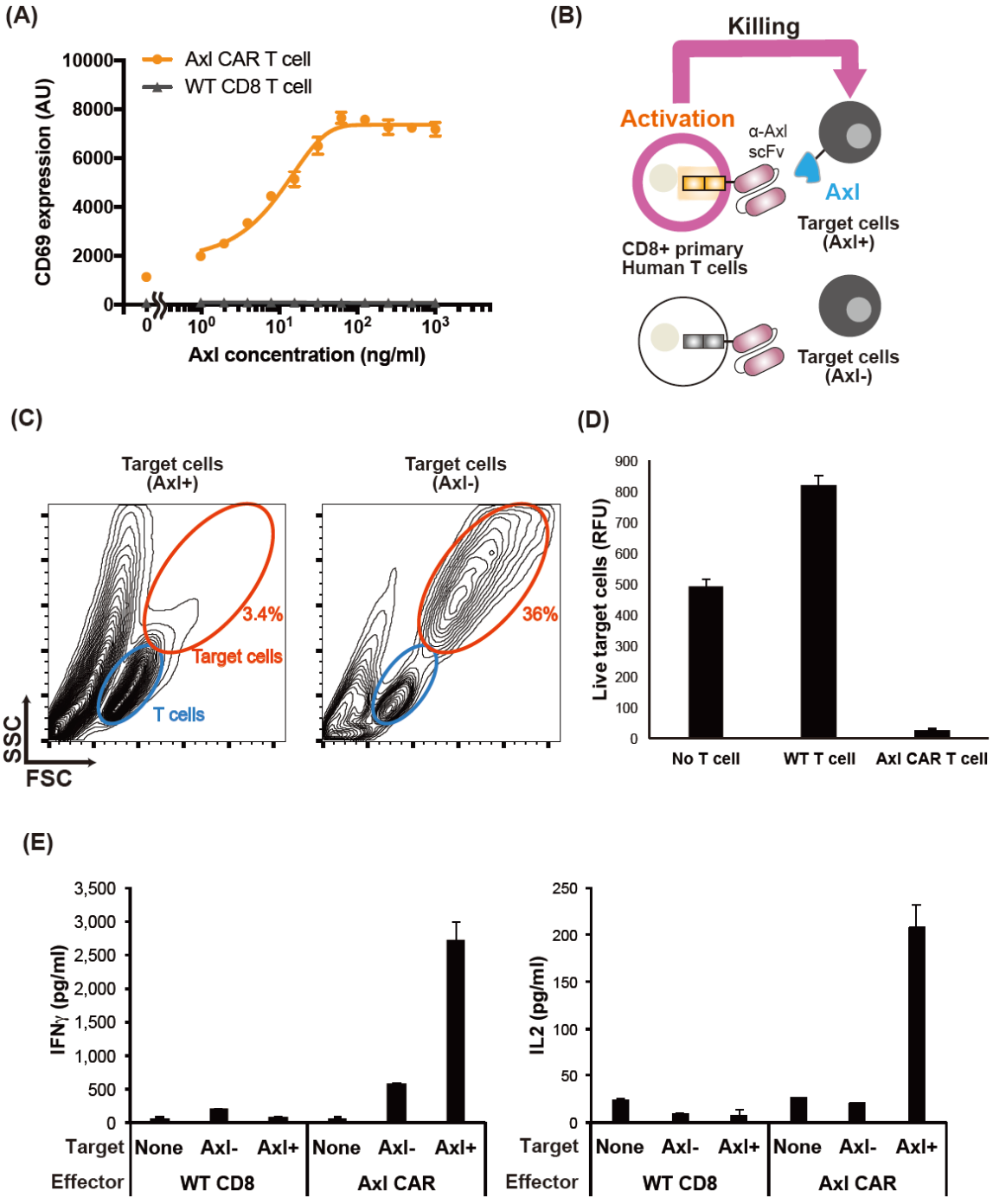
(A)
Axl CAR T cell
WT CD8 T cell
CD69 expression (AU)
Axl concentration (ng/ml)
(B)
Killing
Activation
α-Axl scFv
Axl
Target cells (Axl+)
CD8+ primary Human T cells
Target cells (Axl-)
(C)
Target cells (Axl+)
Target cells (Axl-)
3.4%
Target cells
T cells
36%
SSC
FSC
(D)
Live target cells (RFU)
No T cell
WT T cell
Axl CAR T cell
(E)
IFNγ (pg/ml)
IL2 (pg/ml)
Target
Effector
None
Axl-
Axl+
WT CD8
Axl CAR

Figure 2.6.3. Characterization of Axl CAR in human primary CD8+ T cells

(A) The CD69 expression level measured after 24hr of culturing Axl CAR-expressing CD8+ T cell with a different amount of plate-bound Axl protein. (B) Schematics of cell killing against K562 target cells by Axl CAR-expressing CD8+ T cells. (C) Forward- and side- scatter FACS plots of the cell mixture after 24hr co-culture of T cells (blue) with target cells (orange). (D) Killing assay against SK-OV-3. Fluorescence of Calcein AM was used to quantify live SK-OV3 cells after 24hr co-culture with T cells. (E) IFN- γ and IL-2 measurement after 24hr co-culture of human primary CD8+ T cells with Axl expressing target cells (K562). Data are representative of three biological replicates and presented as the mean ± SD.

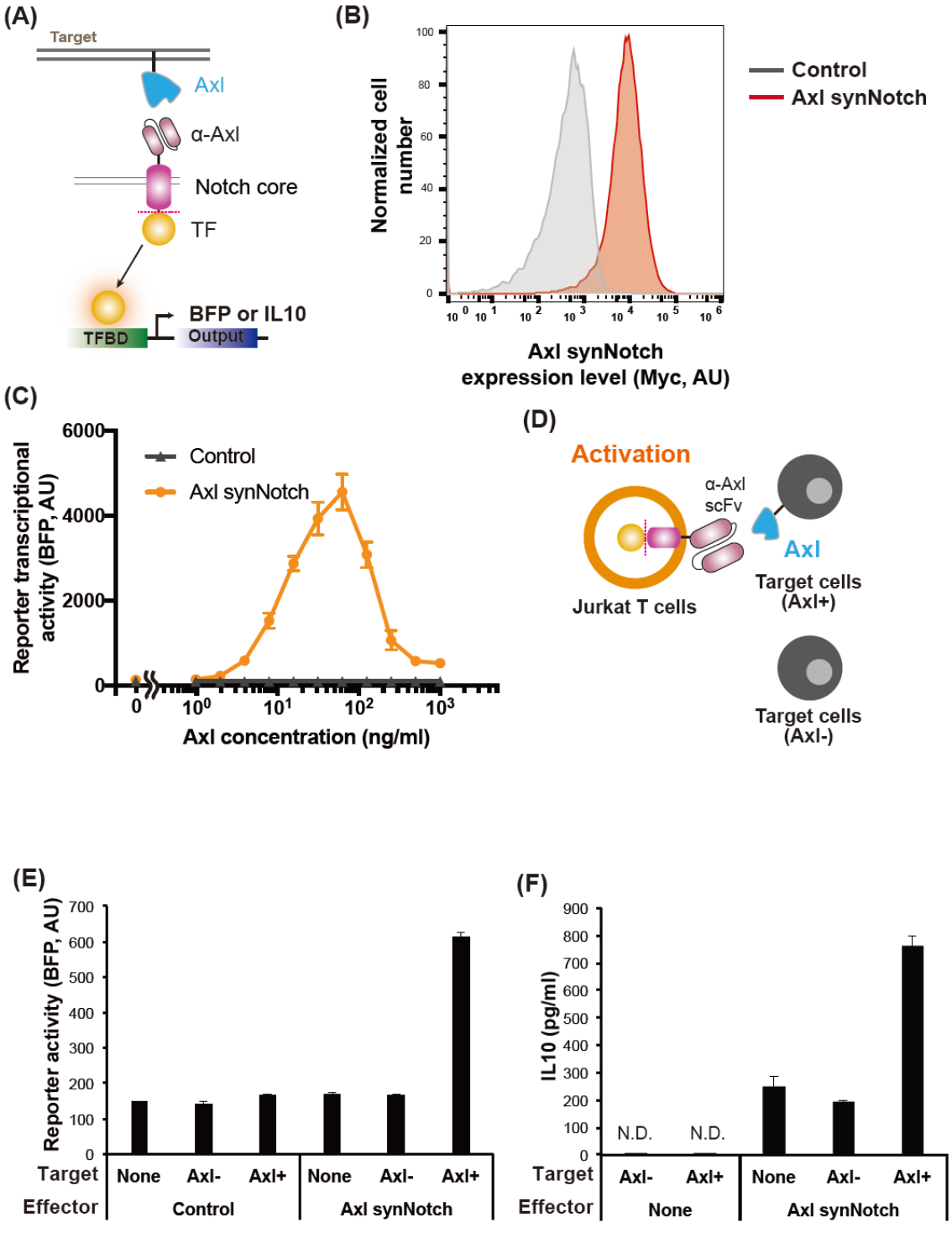
(A)
Target
Axl
α-Axl
Notch core
TF
BFP or IL10
TFBD
Output
(B)
Normalized cell number
Control
Axl synNotch
Axl synNotch expression level (Myc, AU)
(C)
Reporter transcriptional activity (BFP, AU)
Control
Axl synNotch
Axl concentration (ng/ml)
(D)
Activation
α-Axl scFv
Axl
Jurkat T cells
Target cells (Axl+)
Target cells (Axl-)
(E)
Reporter activity (BFP, AU)
Target
Effector
None
Axl-
Axl+
Control
Axl synNotch
(F)
IL10 (pg/ml)
N.D.
N.D.
Target
Effector
Axl-
Axl+
None
Axl synNotch

Figure 2.6.4. Design and characterization of Axl synNotch in human Jurkat T cells

(A) Axl synNotch design. TF, transcriptional factor (tTA); TFBD, transcriptional factor binding domain. (B) The expression level of the Axl synNotch in Jurkat T cells. The myc-tag was stained with an anti-myc antibody for the measurement of surface synNotch expression. Control indicates non-transfected Jurkat cells that containing only tTA responsive reporter. (C) Axl synNotch response from plate bound Axl protein activation. Control indicates Jurkat T cells harboring synNotch responsible BFP reporter without Axl synNotch. (D) Axl synNotch activation via co-culturing of Axl+/Axl- K562 target cells. (E) BFP fluorescence level after co-culturing of Axl synNotch expressing Jurkat T cells with target K562 cells for 24hr. Control indicates Jurkat T cells harboring only BFP reporter without Axl synNotch receptor. (F) IL-10 production level when co-cultured Jurkat T cells harboring tTA responsive IL-10 reporter cells with K562 cells for 24hr. (None, no target cell or no effector cell condition. N.D., not detected: Data are representative of three biological replicates and presented as the mean ± SD).

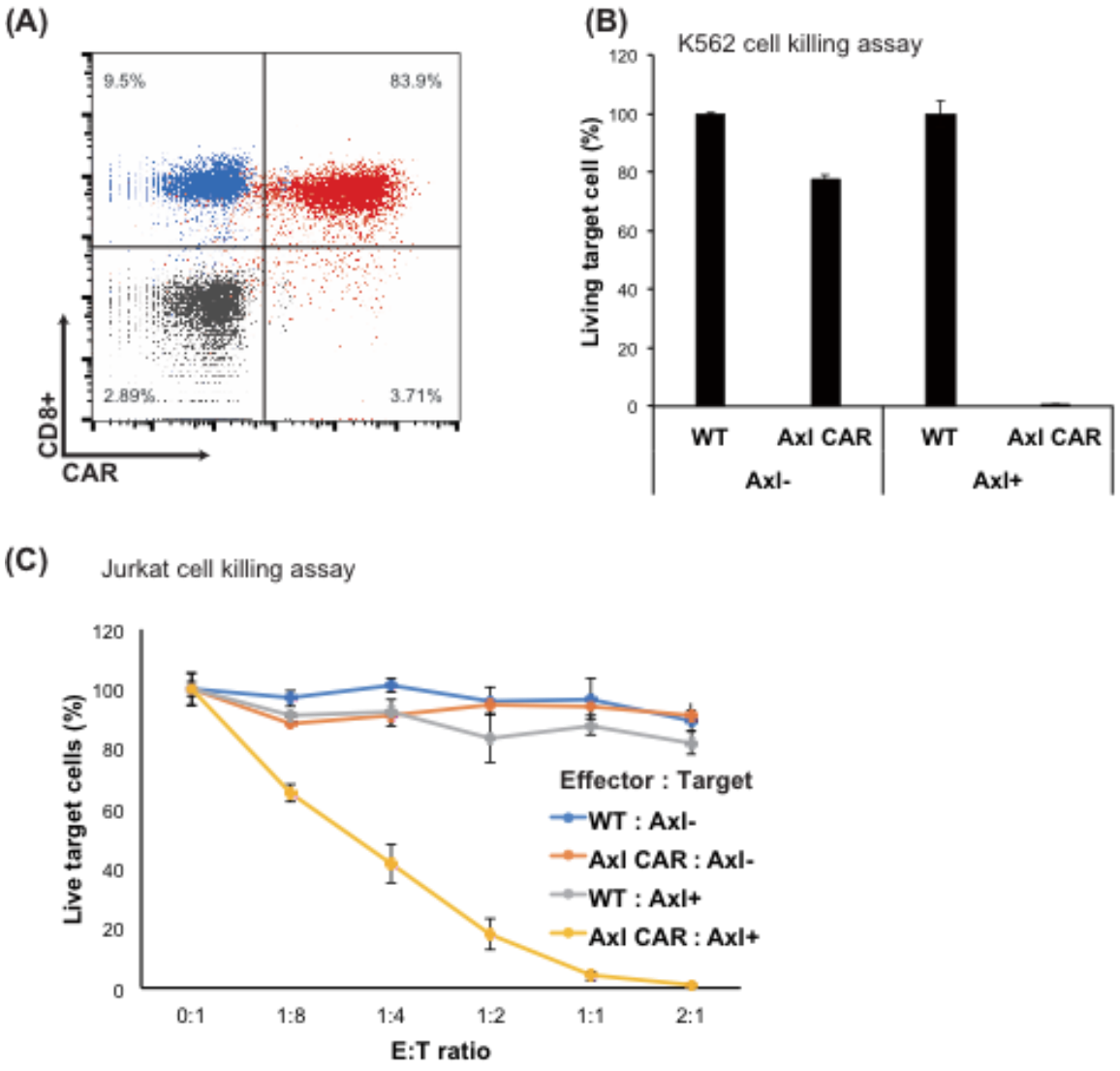

Figure 2.6.5. Human primary CD8 T cells expressing Axl-CAR show effective *in vitro* cytotoxicity against Axl+ target cancer cells.

(A) Axl CAR expression level in human primary CD8+ T cells. (B) Killing assay against K562. Live K562 cells were counted by flow cytometry analysis. The graph indicates the ratio to live K562 cells in the condition of co-culture with WT T cells. (C) Killing assay against Jurkat cells. Axl+ and Axl+ Jurkat cells express luciferase. Graph indicates the

percentage to the luminescence in no effector T cell condition. Co-culture was performed in the indicated ratio of effector and target (E:T) for 4 hr. Data are representative of three biological replicates and presented as the mean ± SD.

2.7 Acknowledgment

I want to acknowledge Dr. Atsushi Okuma and Dr. Wilson Wong for their significant contributions including editing published manuscript to complete this chapter.

CHAPTER THREE: UNIVERSAL CHIMERIC ANTIGEN RECEPTORS FOR MULTIPLEXED AND LOGICAL CONTROL OF T CELL RESPONSES

3.1 Introduction

The transfer of CAR-expressing T cells to patients is a promising approach for cancer immunotherapy [107–109,120]. Despite these encouraging results, safety and efficacy continue to be major hurdles that hinder CAR T cell therapy development [60,110,121,122]. To improve overall effectiveness and safety of CAR T cell therapy, there is an urgent need for a better system that can finely tune T cell activation, enhance tumor specificity, and independently control different signaling pathways and cell types.

The CAR T cells used in clinical trials typically have a rigid design that is difficult to alter without re-engineering the T cells. Current CAR designs are composed of a fixed antigen-specific single-chain variable fragment (scFv) and intracellular signaling domains (CD3ζ and co-stimulatory domains). When the constant antigen-specific CAR binds to the target antigen, these invariable signaling domains are activated simultaneously at a predetermined level. Due to the fixed design that limited the controllability of CAR T cell activation level, managing CAR T cell-related toxicities have proven to be challenging [58,107,110].

In addition to constraining the controllability of CAR T cell activity, this fixed CAR design also restricts the antigen specificity and affinity. High-affinity scFvs are often used in the CAR design to ensure high antigen specificity. However, CARs made with high-affinity scFvs have limited capacity in discriminating antigen density, which have led to

dangerous reactivity against healthy organs expressing a low level of antigens [59,60]. Using an scFv with lower antigen affinity allowed better antigen density discrimination [123,124], but antigen specificity may be compromised. Thus, modulation of CAR components other than scFv affinity may be needed for improving CAR T cell specificity.

Recently, several studies have demonstrated the importance of regulating CD3ζ and the different co-stimulatory pathways independently to achieve optimal T cell response [62,125,126]. Also, the activation of different co-stimulatory domains (e.g., CD28 or 4-1BB) is known to have different T cell functions and phenotypes (e.g., T cell differentiation and memory T cell formation) [127–129], demonstrating the value of CAR design that allows independent control of different signaling domains.

The composition of the T cell subsets, such as the ratio of CD4+ and CD8+ T cells, has also been shown to be an important parameter for enhancing the antitumor response of CAR T cells [130]. Given the fact that our immune system is composed of many different T cell subtypes with distinct effector functions (Golubovskaya and Wu, 2016; Vignali et al., 2008; Vivier et al., 2008), regulating the activity of T cell subtypes independently may be an attractive strategy for optimizing the efficacy of CAR T cell therapy [131]. However, current fixed CAR design limits independent and inducible activation of different signaling domains or different T cell subsets to achieve user-defined diverse T cell response.

New receptor designs have been developed to address some of the deficiencies (e.g., controllability, flexibility, and specificity) in current CAR T cell therapies. For instance, drug-inducible ON and kill switches have been developed to regulate CAR activity [15,83]. Also, to afford greater flexibility in antigen recognition, CARs have been split such that

the antigen recognition motif is dissociated from the signaling motif of the CAR. This split CAR configuration uses a universal receptor as the common basis for all interactions, allowing a large panel of antigens to be targeted without re-engineering the immune cells [78,80,81,132]. In addition, to increase tumor specificity, CARs were developed that allow combinatorial antigen sensing [62,63,126] or target two tumor-specific antigens that can reduce tumor antigen escape rate [65,76]. All of these features are arguably vital to ensure a safe and effective CAR T therapy. However, none of these advanced CARs has incorporated all of these features into one system. Additionally, the signaling pathways and cell types that can be activated are also fixed, thus limiting the diverse immune responses that can be achieved.

To enhance the specificity, safety, and programmability of CARs, we develop a split, universal, and programmable (SUPRA) CAR system composed of a universal receptor expressed on T cells and a tumor-targeting scFv adaptor molecule (**Figure 3.6.1A**). The activity of SUPRA CARs can be finely regulated via multiple mechanisms to limit overactivation. SUPRA CARs can also logically respond to multiple antigens for improving tumor specificity. We show the SUPRA CAR system is effective against two different tumor models, demonstrating the broad clinical potential of this system. In addition, we show that SUPRA components can be humanized to reduce potential immunogenicity. Furthermore, we use orthogonal SUPRA CARs to inducibly regulate multiple signaling pathways or different human T cell subtypes to increase the range of the immune responses that can be achieved. Together, the SUPRA CAR system is a feature-rich system with inducible and logical control capabilities that can improve the safety and

efficacy of current cellular cancer immunotherapy.

3.2 Results

3.2.1 *Design and characterization of the SUPRA CAR system*

The SUPRA CAR is a two-component receptor system composed of a universal receptor (zipCAR) expressed on T cells and a tumor-targeting scFv adaptor (zipFv) (**Figure 3.6.1A**). The zipCAR universal receptor is generated from the fusion of intracellular signaling domains and a leucine zipper as the extracellular domain. The zipFv adaptor molecule is generated from the fusion of a cognate leucine zipper and an scFv. The scFv of the zipFv binds to the tumor antigen, and the leucine zipper binds and activates the zipCAR on the T cells (**Figures 3.6.8A and 3.6.9**). Unlike the conventional fixed CAR design, the SUPRA CAR modular design allows targeting of multiple antigens without further genetic manipulations of a patient's immune cells (**Figure 3.6.1B, left**). To test the ability of the SUPRA CAR system targeting multiple antigens with the same batch of T cells expressing the zipCAR, we first engineered human primary CD8+ T cells to express an RR zipCAR (RR leucine zipper with CD28, 4-1BB co-stimulatory and a CD3ζ signaling domain, **Figure 3.6.8A**). Next, we designed three different zipFvs to target three common tumor antigens (α-Her2, α-Axl, and α-Mesothelin, **Figure 3.6.8A**) by fusing the corresponding scFvs to an EE leucine zipper, which binds to the RR zipCAR on T cells. The engineered CD8+ T cells were co-cultured *in vitro* with K562 myelogenous leukemia

cells that express Her2, Axl, or Mesothelin tumor antigens. The CD8+ zipCAR T cells killed the corresponding tumor cells when the matching zipFvs were added **(Figure 3.6.1B, right)**.

A unique feature of the split CAR design is that it has multiple tunable variables, such as (1) the affinity between leucine zipper pairs, (2) the affinity between tumor antigen and scFv, (3) the concentration of zipFv, and (4) the expression level of zipCAR, that can be used to modulate the T cell response (**Figure 3.6.1C**). We first characterized the effect of zipFv concentration and zipper affinity on T cell activation. We generated three zipFvs with the same α-Her2 scFv but fused to leucine zippers (SYN5, SYN 3, and EE) that have different affinity to the RR zipCAR [133,134]. The amount of zipFv required to activate T cells to half-maximal IFN-γ secretion and cytotoxicity inversely correlated with the affinity of leucine zipper pairs where α-Her2-EE zipFv showed the lowest EC_{50} and α-Her2-SYN5 zipFv showed the highest EC_{50} value (**Figures 3.6.1D and 3.6.8C**). Also, the maximum level of IFN-γ secretion or killing efficiency correlated with the affinity of leucine zipper pairs.

We next investigated the effect of scFv–tumor antigen affinity, leucine zipper affinity, and zipCAR expression levels on the IFN-γ secretion and cancer-killing efficiency by the SUPRA CAR T cells (**Figures 3.6.1E and 3.6.8D**). We created 12 different zipFvs (three different leucine zippers with different affinity and four scFvs against Her2 (G98, C65, ML39, and H3B1) with K_d ranging from 3.2×10^{-7} to 1.2×10^{-10} M) [135]. We also generated two batches of T cells with high or low RR zipCAR expression level using fluorescence-activated cell sorting (**Figure 3.6.8B**). Cells expressing higher levels of

zipCAR exhibited greater cytokine secretion when activated (**Figure 3.6.1E**). The affinity of scFv to Her2 correlated weakly with cytokine secretion or target cell lysis [135]. The affinity between leucine zippers, however, correlated well with cellular activation regarding cancer cell killing efficiency and cytokine secretion. As high-affinity scFv CARs often over-activate and show severe toxicities in clinical trials [58,59], the SUPRA platform can mitigate these toxicities by controlling other factors (e.g., zipFv concentration, the affinity between leucine zipper pairs) to regulate T cell activation level. Together, these results demonstrate the tunable and modular nature of the SUPRA CAR design.

3.2.2 *Competitive zipFvs for tuning SUPRA CAR activity*

As many patients treated with CAR T cell therapy face cytokine release syndrome which can be life-threatening [57,60], it is important to prevent CAR T cell activity when necessary. Thus, we explored the possibility of inhibiting the SUPRA CAR T cell activation through the addition of a competitive zipFv that can bind to the other zipFv, thus preventing zipCAR from being activated (**Figure 3.6.2A, left**). To test this approach, we screened several competitive zipFvs with different affinities for the EE zipFv (strong, medium and weak) (**Figures 3.6.10B and 3.6.10C**). Human CD8+ T cells were transduced with RR zipCAR and co-cultured with Her2+ K562 cells. Then EE zipFv (22.5nM, red) was subsequently added to activate the T cells. Without the competitive zipFv, the EE zipFv alone could activate T cells to destroy Her2+ cancer cells (**Figure 3.6.2A, right**).

However, when the competitive zipFv (SYN4, SYN 47, or SYN 13) was also introduced (90nM, green), it bound to the EE zipFv and prevented the EE zipFv from activating the zipCAR T cells. By utilizing this competitive approach, we were able to inhibit primary CD8+ T cell activation *in vitro* with the strong competitive zipFv (SYN4). Furthermore, we were able to tune the activation levels with weaker binding zippers (SYN 47 and SYN 13). To understand inhibition dynamics, we varied the amount of competitive zipFv and timing of its addition. The increasing amount of competitive zipFv or delaying competitive zipFv addition did not affect inhibition strength greatly (**Figure 3.6.10D**).

3.2.3 *Logical operation with the SUPRA CAR system*

Antigen escape is a major challenge for targeted cancer therapies [136], including adoptive T cell therapies [75,137]. As such, bispecific receptors that can be triggered by CD19 and Her2 or CD19 and CD20, respectively, have been developed to combat antigen escape [65,76]. Also, CD22 and CD123 CARs have been recently developed to increase tumor specificity [67,138]. However, as illustrated in a recent clinical trial with CD22 CAR T cells for patients relapsed from CD19 CAR T therapy, tumors can still evade detection by the engineered T cells by losing or down-regulating both antigens [66]. In such cases, T cells would need to be re-engineered to target another antigen. Using the SUPRA CAR platform, however, different antigens can be easily targeted without further genetic manipulation. To test if SUPRA CAR could be used to target either one of the two antigens on the cell surface, we co-cultured Her2/Axl+ K562 cancer cells with RR zipCAR

expressing CD8+ T cells. Then, different zipFv combinations were added to the cell mixture (α-Axl zipFv, α-Her2 zipFv, or both) (**Figure 3.6.2B**). As expected, the addition of zipFv targeting either Her2, Axl or both led to high killing efficiency, illustrating the potential of programming the SUPRA CAR system to combat antigen escape.

Another limitation of targeted tumor therapy is the difficulty in identifying a single tumor-specific antigen, which affects both tumor specificity and toxicity. Receptor systems that can perform combinatorial antigen detection have been developed to enhance the specificity of CAR T cell therapy [62,63]. However, these receptor systems have a fixed antigen specificity design. Here, we investigated if the SUPRA CAR system can also be used to increase tumor specificity through combinatorial antigen sensing (**Figure 3.6.2C**). In particular, we used the SUPRA CAR system to target cells that express Her2 only and spare cells that express both Her2 and Axl, where Axl served as a "safety marker". To achieve our design, we developed an α-Axl-SYN2 zipFv (green) that binds to α-Her2-EE zipFv (red) through a complementary zipper on each zipFv; this prevents the α-Her2-EE zipFv from binding to the zipCAR, thus protecting the Her2+/Axl+ cells. In contrast, since α-Axl-SYN2 zipFv cannot bind to Her2-only cells, the α-Her2-EE zipFv will not be blocked from activating the zipCAR.

To demonstrate such Her2 but NOT Axl logical operation, we first co-cultured RR zipCAR expressing CD8+ T cells with Her2+/Axl+ cells and zipFvs (**Figure 3.6.2C, left**). As expected, the addition of the α-Her2-EE zipFv alone achieved high tumor killing efficiency. However, when the α-Her2-EE zipFv was added after the α-Axl-SYN2 zipFv, the two zipFvs bound to each other and prevented the activation of the zipCAR, which led

to a significant reduction in cytotoxicity (**Figure 3.6.2C, right**). As a control, we designed an α-Axl-SYN13 zipFv that did not bind strongly to the α-Her2-EE zipFv and showed no inhibition of T cell activity (**Figure 3.6.10E**). When the same SUPRA CAR system was challenged equally with cells expressing only Her2, the presence of α-Her2-EE zipFv alone again showed a high cytotoxicity rate (**Figure 3.6.2C, right**). Moreover, the addition of α-Axl zipFvs did not affect killing efficiency. For both dual and single antigen target cells, α-Axl-SYN2 zipFv that binds strongly to α-Her2-EE zipFv or α-Axl-SYN13 zipFv that does not bind strongly to α-Her2-EE zipFv was first added to the cell mixture. After unbound α-Axl zipFvs were washed away, α-Her2-EE zipFv was added to stimulate CD8+ T cell activity (refer to the STAR Method section for further detail). As expected, RR zipCAR engineered CD8+ T cells showed high activity toward Her2+ cancer cells, regardless of zipFv combinations, thus demonstrating the potential of the SUPRA CAR system to increase tumor specificity and reduce the toxicity of CAR T cell therapy.

3.2.4 *Tumor clearance in a xenograft tumor model*

After characterizing the SUPRA CAR system *in vitro*, we next tested whether SUPRA CARs can be used to reduce the tumor burden in a mouse xenograft model. For this experiment, we injected SK-BR-3 breast cancer cells (Her2 positive) intraperitoneally into immunocompromised NOD.Cg-*Prkdc*^{scid} *Il2rg*^{tm1Wjl}/SzJ (NSG) mice. After two weeks to allow for tumor establishment, we injected primary CD8+ human T cells expressing RR

zipCAR or conventional Her2 CAR into the mice. α-Her2-EE zipFv was subsequently injected every 2 days at 5mg/kg for 2 weeks. Tumor growth was monitored by *in vivo* imaging (IVIS) of the luciferase signal from SK-BR-3 cancer cells in each mouse over the course of 41 days. RR zipCAR with α-Her2-EE zipFv showed robust tumor burden clearance, comparable to the conventional Her2 CAR. However, T cells expressing RR zipCAR alone without zipFvs were not able to reduce tumor burden (**Figure 3.6.3A**).

To verify that the decrease in tumor burden was due to binding between zipCAR and zipFv, we also tested an α-Her2-RR zipFv, which does not bind to the RR zipCAR (**Figures 3.6.3B and 3.6.11A**). We set up a similar tumor model with SK-BR-3 breast cancer cells and injected RR zipCAR expressing CD8+ T cells at day 38 (**Figures 3.6.11A and 3.6.11B**). Both zipFvs (α-Her2-RR or α-Her2-EE) were dosed every two days for two weeks at 8mg/kg. Representative IVIS images and quantified luminescence from each mouse at day 57 demonstrated a decrease in tumor burden only when the α-Her2-EE zipFv that binds to zipCAR was injected (**Figure 3.6.3B and 3.6.3C**). We also measured the cytokine release *in vivo* to verify that cytokine production is specific to the binding between zipFv and zipCAR. As expected, the injection of α -Her2-RR zipFv did not increase IFN-γ level *in vivo*. However, the administration of the α-Her2-EE zipFv showed a significant increase in IFN- γ after 24 hours of CD8+ T cells and zipFv injection (**Figure 3.6.3D**).

Intraperitoneal xenograft tumor models are frequently used to evaluate immunotherapy against human ovarian cancers [139–142], but demonstrating the efficacy of the SUPRA system with a blood tumor model could further validate the applicability of this system against different tumors (e.g., T cell cancers). As such, we also tested the

SUPRA system against a blood tumor model. We injected modified Jurkat T cancer cells (engineered to be Her2 positive) intravenously into immunocompromised NSG mice. After three days, we injected primary CD8+ human T cells expressing RR zipCAR or conventional Her2 CAR into the mice. α-Her2-EE zipFv was subsequently injected every day at 3mg/kg for six days. Tumor growth was monitored by *in vivo* imaging (IVIS) of the luciferase signal from Jurkat cancer cells in each mouse over the course of 21 days. RR zipCAR with α-Her2-EE zipFv showed robust tumor burden clearance, comparable to the conventional Her2 CAR. However, T cells expressing RR zipCAR alone without zipFvs were not able to reduce tumor burden (**Figure 3.6.3E**). Moreover, the long-term survival rate was observed for the group that received both RR zipCAR with α-Her2-EE zipFv (**Figure 3.6.12A**). We further characterized our SUPRA CAR system in this blood tumor model by modulating T cell numbers (from $10x10^6$ per mice to $2.5x10^6$ per mice) and lowering zipFv dose to 1mg/kg (**Figures 3.6.12B and 3.6.12C**). At these reduced T cell numbers and zipFv doses, robust reduction of tumor burden was still observed. The observed robust activity of the SUPRA system against different xenograft tumor models demonstrates the potential of the SUPRA CAR system to combat many different cancers.

3.2.5 *Characterization of the humanized SUPRA CAR system in vitro and in vivo*

To mitigate the potential immunogenicity against synthetic leucine zippers, we created a new zipCAR and zipFv pair using zipper domains derived from human FOS and JUN transcription factors, respectively [133,143]. Human primary CD8+ T cells were

engineered to express a FOS zipCAR. An α-Her2-JUN zipFv was used to activate the FOS zipCAR (**Figure 3.6.13A**). FOS zipCAR and RR zipCAR engineered CD8+ T cells have comparable *in vivo* killing efficiencies against Jurkat T cells that express Her2 (**Figure 3.6.13A**). In addition, FOS zipCAR can be activated only when α-Her2-JUN zipFv and Her2 expressing tumor cells are present as measured by CD69 expression and IFN-γ secretion (**Figures 3.6.13B and 3.6.13C**). FOS zipCAR with α-Her2-JUN zipFv can efficiently eliminate leukemia *in vivo* as demonstrated in a blood tumor model (**Figure 3.6.13D**). Together, these results illustrate that the SUPRA components can be humanized to reduce potential immunogenicity and they are as effective as the ones derived from synthetic zippers.

3.2.6 *Controlling SUPRA CAR activity in vivo*

Strategies that enable controlled cytokine production by CAR T cells *in vivo* are critical to preventing cytokine release syndrome [57,60]. As such, we explored *in vivo* cytokine production by SUPRA CAR T cells in a zipFv dose-dependent manner. We first injected SK-BR-3 breast cancer cells and allowed the tumor to be established (**Figure 3.6.4C**). After verifying tumor establishment, RR-zipCAR expressing CD8+ T cells were injected and mice were dosed with 8, 4, 2, or 0.5 mg/kg of the α-Her2-EE zipFv every other day for 2 weeks (**Figure 3.6.11BC**). Again, the tumor burden was monitored by *in vivo* imaging (IVIS) of the luciferase signal from SK-BR-3 cancer cells in each mouse. Increasing zipFv dose beyond 2mg/kg (e.g., 4mg/kg or 8mg/kg) resulted in the faster and

more efficient killing of cancer cells. There were no significant differences between groups that received 0.5mg/kg and 2mg/kg or between groups that received 4mg/kg and 8mg/kg (**Figure 3.6.11D**). However, zipFv dosage correlated with cytokine release *in vivo* in a step-wise fashion, which demonstrates the possibility of using the SUPRA CAR to finely regulate cytokine release *in vivo* (**Figure 3.6.4A**).

We also examined if *in vivo* cytokine production could be modulated with different leucine zippers (SYN3, SYN5, and EE) or α-Her scFv (G98, ML39, and H3B1) affinity on the zipFv (4mg/kg) (**Figures 3.6.4B and 3.6.11E**). Indeed, *in vivo* IFN-γ release correlated with the affinity between leucine zippers (**Figure 3.6.4B**). The cytokine release also increased as the scFv changed from low (G98, $K_d = 3.2 \times 10^{-7}$) to medium-high affinity (ML39, H3B1, $K_d < 1 \times 10^{-8}$). However, as shown in the *in vitro* results, zipFvs with medium-high binding domains affinity (ML39, H3B1, $K_d < 1 \times 10^{-8}$) did not increase IFN-γ secretion (**Figures 3.6.11E**).

Lastly, we investigated if the SUPRA CAR could be inhibited *in vivo* with a competitive zipFv to reduce cytokine production (**Figures 3.6.4C**). As expected, the group that only received α-Her2-EE zipFv (4mg/kg) secreted a high level of IFN-γ. Moreover, when a competitive zipFv (8mg/kg) that can bind to the activating zipFv was added (SYN4), the IFN-γ level reduced significantly, similar to that of the no-zipFv control. However, the addition of a control zipFv, which does not bind to the activating EE zipFv, did not decrease cytokine release *in vivo* (SYN13). We did not observe a significant effect of competitive zipFvs on the anti-tumor cytotoxicity *in vivo*. However, *in vivo* cytokine production results demonstrate that the SUPRA CAR platform affords multiple approaches

to control cytokine production, providing the tools needed to manage severe cytokine release syndrome and other potential toxicities that arise from conventional CAR T cell therapies.

3.2.7 *Controlling different signaling domains using orthogonal SUPRA CARs*

Currently, only a small number of signaling domains are being utilized in CAR T cell therapy to regulate T cell responses. Moreover, we lack independent control of different signaling domains as they are activated simultaneously. However, the repertoire of co-signaling domains – both co-stimulatory and co-inhibitory domains – are highly diverse, and it is the activation of different co-signaling domains that sculpts ultimate T cell function [144–146]. One of the key attributes of the SUPRA CAR design is that multiple orthogonal SUPRA CARs can be designed to control distinct signaling pathways in the same cell, which provides highly customizable tuning of T cell signaling and response. To identify orthogonal SUPRA CARs, Jurkat T cells expressing different zipCARs were co-cultured with Her2+ K562 target cells and different zipFvs. (**Figures 3.6.13A and 3.6.13B**). From the screen, we identified several pairs of orthogonal SUPRA CARs (**Figures 3.6.13C**). We then engineered two orthogonal SUPRA CARs to regulate separate signaling pathways in primary CD4+ T cells – FOS zipCAR (binds to α-Her2-SYN9 zipFv) that contains only a CD3ζ domain and RR zipCAR (binds to α-Axl-EE zipFv) that contains CD28 and 4-1BB co-stimulatory domains (**Figures 3.6.5A**). We chose these signaling domains because they have been used previously for demonstrating

combinatorial antigen detection ("AND" logic) *in vivo* [62]. To trigger each zipCAR independently, we co-cultured engineered CD4+ T cells and K562 target cells that express Her2 and Axl. We then added two different zipFvs at varying concentrations and measured CD69 expression, which can be triggered by CD28 activation [147]. Triggering CD3ζ alone increased CD69 expression. Activating the CD28/4-1BB and CD3ζ domain, however, led to a further increase in CD69 expression (**Figures 3.6.5B and 3.6.14F**). To confirm this dual antigen sensing functionality, we also measured different cytokine (IFN-γ, IL-2, and IL-4) levels that are known to be regulated by CD28 and 4-1BB signaling [148–150]. For all cytokines tested, we observed similar synergistic AND logic effects of these two receptors (**Figures 3.6.5B, 3.6.14D, 3.6.14E, and 3.6.14F**). Surprisingly, the effect of the CD28 and 4-1BB co-stimulatory signaling was much higher when we increased the α-Her2-SYN9 zipFv concentration (as CD3ζ signaling strength increased) (**Figures 3.6.14F**).

3.2.8 *Controlling different cell types using orthogonal SUPRA CARs*

We recognized that orthogonal SUPRA CARs can also be used to control different T cell subtypes, such as CD4+ and CD8+ T cells (**Figures 3.6.6A**). CD4+ T cells are helper T cells that secrete a variety of cytokines and regulate the immune responses such as activation, growth, and memory formation of CD8+ T cells [151]. CD8+ T cells are cytotoxic T cells that can directly kill cancer cells. As the use of both CD4+ and CD8+ T cells has been shown to enhance the antitumor response of CAR T cells [130], independent

control of both cell types to induce different T cell responses could further improve the effectiveness of CAR T cell therapy. To demonstrate orthogonal control of both T cell types, we introduced an RR zipCAR into CD4+ T cells (binds to α-Axl-EE zipFv) and an orthogonal FOS zipCAR (binds to the α-Her2-SYN9 zipFv) into CD8+ T cells. All zipCARs here contain CD3ζ, CD28, and 4-1BB signaling domains. To trigger each cell type independently, we co-cultured both engineered CD4+ and CD8+ T cells with K562 cells that express Axl and Her2 (**Figures 3.6.6A**). CD69 expression level was upregulated in CD4+ or CD8+ T cells only in response to the addition of α-Axl zipFv or α-Her2 zipFv, respectively. When both zipFvs were added simultaneously, the CD69 level was upregulated for both cell types (**Figures 3.6.6B**). Furthermore, activating both cell types simultaneously achieved IFN- γ secretion levels similar to the sum of cytokine secretion levels from two subsets of T cells activated individually (**Figures 3.6.6C**). Finally, 24-hour co-culture of CD4+ and CD8+ T cells with Axl+/Her2+ K562 cells led to cytotoxicity against tumor cells (as measured by K562 population percentage through flow cytometry) when CD8+ T cells were activated, but minimally for CD4+ T cells [152] (**Figures 3.6.6D**).

3.3 Discussion

3.3.1 *SUPRA CAR: The Swiss Army knife of CAR*

There is a great need for a flexible platform that can control T cell activation with improved precision and tunability to make CAR T cell therapy safer and more effective.

Here we have developed a split CAR system with enhanced flexibility, specificity, and controllability. We demonstrated that our SUPRA CAR system can target different antigens without having to re-engineer the T cells. The activity of the SUPRA CAR system can also be flexibly modulated through multiple mechanisms. In addition, the SUPRA CAR can be easily designed for combinatorial logic antigen detection and regulate different signaling pathways in the same cell as well as different cell types independently. Together, the SUPRA CAR represents a feature-rich receptor system for adoptive T cell therapy.

While several split systems have been introduced with biomolecule-labeled antibodies [78–81,153] to redirect the specificity of CARs, none of these systems have demonstrated the same level of flexibility and functionality as our SUPRA CAR system. Furthermore, some of the systems require extensive and non-intuitive optimization of the receptor design. The modular design approach of our SUPRA CAR platform, however, allows convenient redirection of target specificity and adjustment to T cell activity. Several structural parameters, such as the location of the scFv binding to the antigen, scFv affinity, and extracellular spacing [65,78,154] are important to the CAR signaling. Given that the leucine zipper design constraints some of the structure parameters (e.g. the extracellular spacing) of the zipCAR, further investigation would be needed to determine the effect of these parameters on the SUPRA CAR system activity.

We were able to generate zipFvs targeting three different targets without having to individually optimize each zipFv. Moreover, we showed that SUPRA CAR components can be humanized by using leucine zipper domains derived from human transcription factors to reduce potential immunogenicity. Because these endogenous leucine zippers are

localized inside the cells, we do not expect crosstalk to occur between humanized SUPRA CAR components and human transcription factors. In addition, although not investigated here, we anticipate that each zipFv will have a short pharmacokinetic half-life *in vivo*, similar to an scFv [155], which could allow increased temporal control, and we expect that its small size will lead to increased tumor penetration [156]. However, the short serum half-life could also be problematic as the SUPRA system requires zipFvs to maintain *in vivo* T cell activity. Nonetheless, SUPRA CAR T cells were able to clear tumor burden *in vivo* with a zipFv dose comparable to other FDA approved protein drugs. Moreover, several well-developed protein engineering approaches are available (e.g., PEGylation, Fc/Albumin fusion, Glyco-engineering) to increase the half-life of scFv, which can be employed to modulate zipFv stability *in vivo* if necessary *[157–160]*.

3.3.2 *SUPRA CAR could enhance the safety of T cell therapy*

Controlling cytokine secretion is critical to limiting cytokine release syndrome in patients. We were able to titrate cytokine secretion and cytotoxicity with different zipFv doses and configurations, demonstrating the tunability of the SUPRA system *in vivo*. Furthermore, we showed through the use of competitive leucine zippers for OFF switch function, that one can significantly reduce cytokine secretion both *in vitro* and *in vivo*. Moreover, this competition-based strategy can improve target specificity by directing the competitive zipFv toward a surface marker for "normal" cells, thus safeguarding them from being targeted by the zipCAR. We anticipate that to efficiently block the accessibility of

zipCAR, the expression level of the cancer cell marker and the normal cell marker will need to be comparable.

3.3.3 *Toward the synthesis of a prosthetic immune system*

A central feature of the SUPRA CAR system is the availability of orthogonal zippers with the varying affinity [133], thus providing a valuable resource for engineering facile and complex control of T cell signaling. Most CARs have been designed as a single receptor controlling all the necessary signaling domains at the same time at a preset (but undefined) level. In contrast, we have shown that multiple orthogonal SUPRA CARs can be utilized to control different signaling domains (e.g., CD3ζ, CD28, 4-1BB), which enable independent and tunable control of different signaling pathways. Moreover, each CAR can be paired with zipFvs that target different tumor antigens or with a different affinity of the leucine zipper, thus allowing regulatable combinatorial antigen sensing, a useful feature that has not been achieved in other CAR or receptor systems (**Figures 3.6.7A**). Furthermore, previous designs for combinatorial antigen sensing using two CARs often require precise control of the expression level of each receptor or careful choice of scFv affinity to achieve an optimal balance of signaling strength [62]. While useful and novel, such designs lack the flexibility to combat tumor relapse due to antigen escape, which will require the extensive design of a different dual CAR system. However, with the SUPRA system, the zipFv composition can be simply changed and the signaling strength from each receptor can be easily tuned by the amount of zipFv, rather than re-engineering T cells, to

meet the challenge of antigen escape.

In addition to regulating different signaling pathways, multiple orthogonal SUPRA CAR can also be used to control different subsets of immune cells. Current CAR-based therapy is typically implemented in a cell mixture (e.g., peripheral blood mononuclear cells) or single subsets of immune cell types (e.g., CD4+, CD8+, Treg, or NK cells [161–164]). Even when two defined T cell subsets (CD4+ and CD8+) were utilized, they were not regulated independently. Given that our immune system is composed of many different cell types with unique effector functions and behaviors *in vivo*, a platform that enables independent control of different cell types could greatly increase the range of responses that can be achieved by the engineered cells (**Figures 3.6.7B**). As a proof of concept, we engineered two different T cells subtypes (CD4+ and CD8+) and demonstrated that two orthogonal SUPRA receptors can independently regulate two cell types. While it is possible to engineer two cell types with conventional fixed CARs that target different antigens, our SUPRA system enables the first orthogonal inducible control of two cell types simultaneously. We anticipate that the SUPRA system can also be applied to regulatory T cells and NK cells along with CD4+ and CD8+ T cells to form a ***prosthetic immune system*** that allows unparalleled control for cell-based immunotherapy (**Figures 3.6.7B**).

3.4 Conclusion

T cells expressing chimeric antigen receptors (CARs) are promising cancer therapeutic agents, with the prospect of becoming the ultimate smart cancer therapeutics. To expand

the capability of CAR T cells, here we present a *s*plit, *u*niversal, and *pr*ogramm*a*ble (SUPRA) CAR system that simultaneously encompasses multiple critical "upgrades", such as the ability to switch targets without re-engineering the T cells, finely tune T cell activation strength, and sense and logically respond to multiple antigens. These features are useful to combat relapse, mitigate over-activation, and enhance specificity. We test our SUPRA system against two different tumor models to demonstrate its broad utility and humanize its components to minimize potential immunogenicity concerns. Furthermore, we extend the orthogonal SUPRA CAR system to regulate different T cell subsets independently, demonstrating a dually inducible CAR system. Together, these SUPRA CARs illustrate that multiple advanced logic and control features can be implemented into a single, integrated system.

3.5 Methods

3.5.1 *zipCAR Receptor Construct Design*

zipCARs were designed by fusing different leucine zippers [133,134] to the hinge region of the human CD8α chain and transmembrane and cytoplasmic regions of the human CD28, 4-1BB, and CD3ζ signaling endodomains. They were under SFFV promoter for all primary T cell experiments and under CAG promoter for all Jurkat cell experiments. All zipCARs contain myc tag to verify surface expression. Furthermore, zipCARs used in primary T cell experiments were fused to mCherry after CD3ζ chain to visualize expression. ZipCARs used in Jurkat experiments were cloned into the piggyback vector

(System Bioscience Inc.), which has been modified by replacing CMV promoter to CAG promoter.

3.5.2 *ZipFv Construct Design*

The general design of zipFv is as follows. scFv (α-HER2, α-Axl or α-MESO) is linked by a 35-aa glycine/serine linker to a leucine zipper. Constructs were cloned into pSecTag2A vectors (Thermo Fisher) for transient expression. These vectors contain the CMV promoter, murine Ig-k-chain leader sequence, C-terminal c-myc epitope, and a 6X His tag for purification.

3.5.3 *Expression and Purification of zipFv*

For transient expression of the protein, Freestyle 293-F cells (Thermo Scientific #R79007) were transfected with pSecTag2A plasmid according to the supplier's protocol. After 4 days of culture, cells were pelleted by centrifugation at 300 × g for 5 minutes, and supernatant protein expression was confirmed by Coomassie gel stain (Thermo Scientific #24592) and western blot (Abcam #ab62928). Proteins derived from transient transfection were purified as follows. The supernatant was passed through columns containing ProBond nickel chelating resin (Thermo Scientific #R80101). Then, each column was washed four times with native purification buffer (50 mM NaH2PO4 and 0.5 M NaCl pH 8.0) plus 20 mM imidazole (Sigma Aldrich # I5513) and eluted three times with native purification buffer plus 250mM imidazole concentrations. Eluted proteins were concentrated to ~2ml and dialyzed into 1× PBS (Thermo Scientific #AM9625). After dialysis, the protein was

verified by western blot and SDS-PAGE gel electrophoresis and protein concentration was quantified by the Pierce BCA Protein Assay Kit (Thermo Scientific # 23227).

3.5.4 *Western Blot and SDS-PAGE Gel Electrophoresis*

SDS-PAGE gel electrophoresis was performed via a standard protocol. Briefly, protein samples were mixed with NuPAGE LDS sample buffer (Thermo Scientific #NP0008) and NuPAGE reducing agent (Thermo Scientific). Samples were heated at 90ºC for 20 minutes and run in NuPAGE MOPS SDS running buffer (Thermo Scientific #NP0001). SDS-PAGE gel was stained with GelCode Blue stain (Thermo Scientific #24590) and images were taken using Gel Doc EZ imager (Biorad). Western blot was performed using iBlot2 gel transfer device (Thermo Scientific #NP0009), following the manufacturer's protocol. For detection, α-C-Myc-HRP antibody (Abcam #ab62928) was used.

3.5.5 *Primary Human T cells Isolation and Culture*

Normal whole peripheral blood was obtained from Boston Children’s hospital, as approved by the University Institutional Review Board (IRB) approved consent forms and protocols. Primary human CD4+ and CD8+ T cells were isolated from anonymous healthy donor blood by negative selection (STEMCELL Technologies #15062 and #15063). T cells were cultured in human T cell medium consisting of X-Vivo 15 (Lonza), 5% Human AB serum (Valley Biomedical #HP1022), 10 mM N-acetyl L-Cysteine (Sigma-Aldrich

#A9165), 55uM 2-mercaptoethanol (Thermo Scientific #31350010) supplemented with 50 units/mL IL-2 (NCI BRB Preclinical Repository). T cells were cryopreserved in 90% heat-inactivated FBS and 10% DMSO.

3.5.6 *Lentiviral Transduction of Human T cells*

Replication-incomplete lentivirus was packaged via transfection of HEK 293 FT cells (Invitrogen) with a pHR transgene expression vector and the viral packaging plasmids: pMD2.G encoding for VSV-G pseudotyping coat protein (Addgene #12259), pDelta 8.74 (Addgene#22036), and pAdv (Promega). One day after transfection, viral supernatant was harvested every day for 3 days and replenished with pre-warmed Ultraculture media (Lonza #12-725F) with 2mM L-glutamine, 100U/ml penicillin, 100ug/mL streptomycin, 1mM sodium pyruvate, and 5mM sodium butyrate. Then, the harvested virus was purified through ultracentrifugation or Lentivirus concentrator (Takara #631232). Primary T cells were thawed 2 days before ultracentrifugation and cultured in T cell medium described above. One day before ultracentrifugation, T cells were stimulated with Human T-activator CD3/CD28 Dynabeads (Thermo Scientific #11132D) at a 1:3 cell:bead ratio and cultured for 24 hr. After viral supernatant purification, rectronectin (Clontech #T100B) was used to transduce cells. Briefly, non-TC treated 6-well plates were coated with rectronectin following the supplier's protocol. Then, concentrated viral supernatant was added to each well and spun for 90 min at 1200xg. After centrifugation, viral supernatant was removed and 4ml of human T cells at 250k/ml in T cell growth media supplemented with 100U/ml of IL-2 was added to well. Cells were spun at 1200xg for 60

min and moved to an incubator at 37 ºC.

3.5.7 *Cancer Cell Lines*

The cancer cell lines used were K562 myelogenous leukemia cells (ATCC # CCL-243), Jurkat T cells, and SK-BR-3 (ATCC #HTB-30). K562 and Jurkat cells were cultured in RPMI-1640(Lonza#12-702Q) with 5% (v/v) heat-inactivated FBS, 2mM L-glutamine, 100U/ml penicillin and 100ug/mL streptomycin. SK-BR-3 cells were cultured in DMEM(Corning #10-013) supplemented with 10% (v/v) heat-inactivated FBS, 2mM L-glutamine, 100U/ml penicillin and 100ug/mL streptomycin. Jurkat, K562, and SK-BR-3 were electroporated or transfected with PiggyBac Transposon system (System Biosciences) to stably express zipCAR or surface antigens: Mesothelin, AXL, and/or HER-2. Two days after transfection, antibiotic (Puromycin (Thermo Scientific #A1113803), Zeocin (Thermo Scientific # R25005), or Hygromycin B (Thermo Fisher #10687010)) was added to the medium to select for cells that express the transgenes.

3.5.8 *Cytokine Release Assays*

Cytokine release assays were carried out using IFN-γ or IL-2 ELISA Kit (BD Biosciences #555142, #555190). Primary T cells expressing zipCAR were incubated with K562 target cells (10 x 10^4 cells/well) at an E:T ratio of 2:1 with corresponding zipFvs (amount of zipFvs were titrated to give a maximum response). After 24 hr, the supernatant was harvested and followed the supplier's protocol to determine IFN-γ or IL-2 level. In order to determine *in vivo* cytokine release level, murine blood was drawn submandibular

after 24hr of the initial injection of engineered CD8+ T cells and zipFv. Blood plasma was harvested by centrifuging collected blood for 10 minutes at 3000 x g. *In vivo* IFN-γ release was measured by Luminex Magpix at BUMC (Boston University Medical Campus) core facility.

3.5.9 *Luciferase Cytotoxic T Lymphocyte Assay*

Cytotoxicity assays were carried out using bioluminescence previously described [165]. Briefly, CAR-T cells were incubated with zipFv and target cells (K562 cells) that were engineered to express luciferase at varying effector to target ratio (e.g., E:T=8:1, 4:1, 2:1, or 1:1) for 4hr at 37 ºC. Initially, target cells were seeded at 75,000 or 100,000 cells per well (96-well plate) and zipFv at varying concentrations were added (amount of zipFvs were titrated to give a maximum response). Then, engineered T cells were added (unless otherwise noted, T cells used in the experiment were not sorted based on the SUPRA CAR expression level). After ~4hr incubation, the culture medium was removed to leave 50ul per well, then 50ul of prepared luciferase reagent (Promega #E2610) was added to each well of the 96-well plate (Corning #3904). Measurements were performed with the SpectraMax M5 (Molecular Devices). Target cell cytotoxicity was calculated using the following formula: Cytotoxicity = 100 x [(Total Target cell luminescence – luminescence of remaining cells after lysis) / (Total Target cell luminescence)].

For *in vitro* cytotoxicity assay shown in **Figures 3.6.2CB**, single or dual expressing target cells was first added into each well. In both of the cases, both cells were equally treated by adding α-Axl zipFv. After ~20 minutes of incubation to allow α-Axl zipFv to

bind to target cells, cells were spun down and washed to remove unbound α-Axl zipFv. Subsequently, α-Her2 zipFv and SUPRA CAR T cells were added to the washed target cells sequentially. After ~4hr incubation, luminescence from each well was measured as described above.

3.5.10 *Xenograft Mouse Models*

Female NSG mice, 4-6 weeks of age, were purchased from Jackson Laboratories (#005557) and maintained in the BUMC Animal Science Center (ASC). All protocols were approved by the Institutional Animal Care and Use Committee at BUMC. In order to carry out the intraperitoneal xenograft models, NSG mice were initially injected with 7.5 X 10^6 luciferized SK-BR-3 intraperitoneally. After 2 weeks or after tumor burden reached ~10^{10} luminescence (photons/sec), 35 x 10^6-CD8+ CAR-T cells were infused intraperitoneally along with zipFv. ZipFvs were added every two days for 2 weeks (total of 8 times) at specified doses. For blood tumor model, NSG mice were initially injected with 5 X 10^6 luciferized Jurkat tumor cells intravenously. After 3 or 5 days, 2.5 to 10 x 10^6-CD8+ CAR-T cells were infused intravenously along with zipFv. ZipFvs were added every day for 6 or 9 days at specified doses. Tumor burden was measured by IVIS Spectrum (Xenogen) and was quantified as total flux (photons per sec) in the region of interest. Images were acquired within 30 minutes following intraperitoneal injection of 150mg/kg of D-luciferin (PerkinElmer #122799).

3.5.11 *QUANTIFICATION AND STATISTICAL ANALYSIS*

Statistical significance was determined by student's T test (two tailed) unless otherwise noted. All curve fitting was performed with Prism 7 (Graphpad) and *p* values are reported (not significant = $p > 0.05$, * = $p \leq 0.05$, ** = $p \leq 0.01$, *** ≤ 0.001). All error bars are represented either SEM or SD.

3.6 Figures

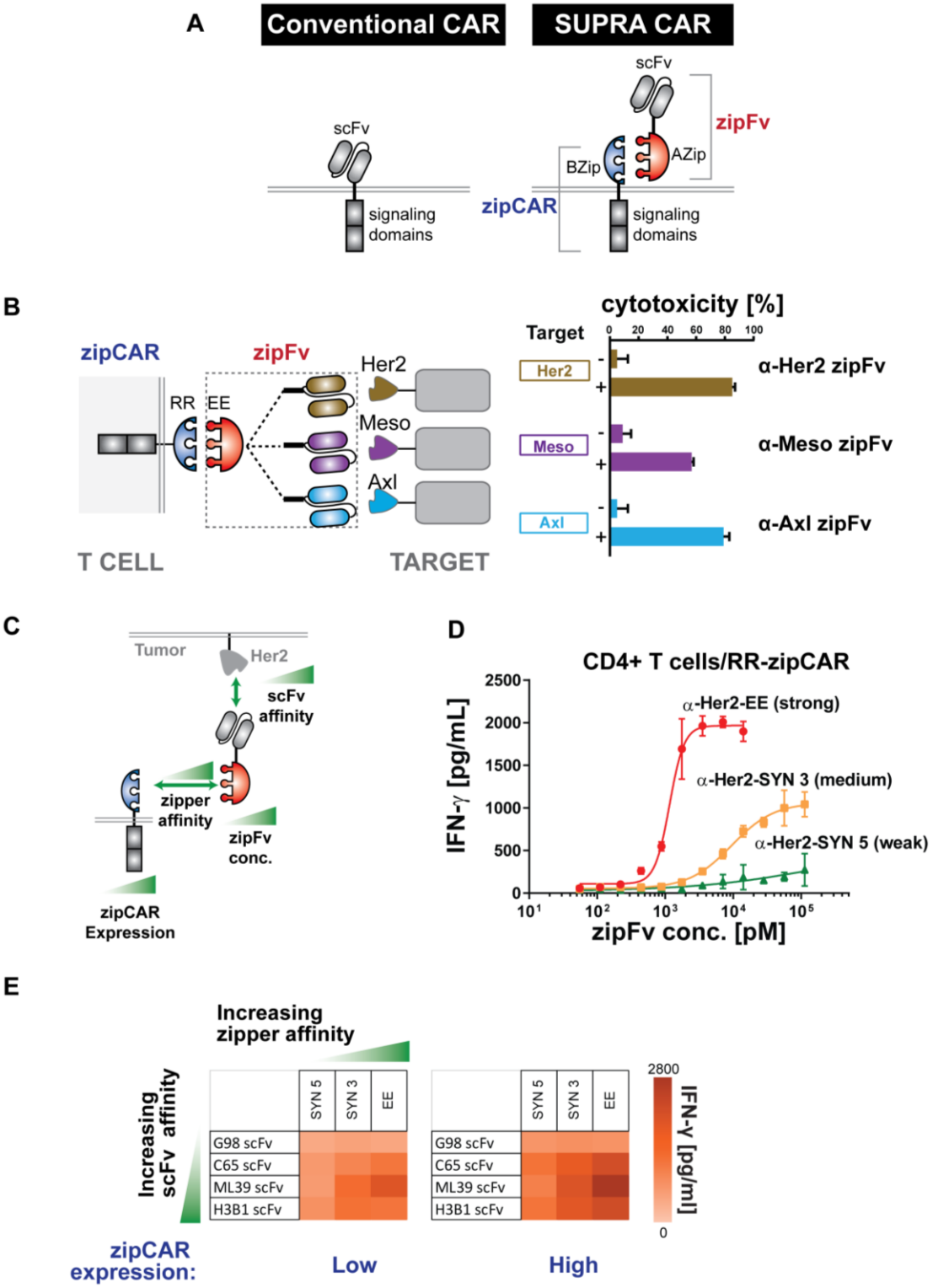
A
Conventional CAR
SUPRA CAR
scFv
signaling domains
scFv
zipFv
BZip
AZip
zipCAR
signaling domains
B
zipCAR
zipFv
RR
EE
Her2
Meso
Axl
T CELL
TARGET
cytotoxicity [%]
Target
0 20 40 60 80 100
Her2
Meso
Axl
α-Her2 zipFv
α-Meso zipFv
α-Axl zipFv
C
Tumor
Her2
scFv affinity
zipper affinity
zipFv conc.
zipCAR Expression
D
CD4+ T cells/RR-zipCAR
IFN-γ [pg/mL]
2500
2000
1500
1000
500
0
α-Her2-EE (strong)
α-Her2-SYN 3 (medium)
α-Her2-SYN 5 (weak)
10¹ 10² 10³ 10⁴ 10⁵
zipFv conc. [pM]
E
Increasing zipper affinity
Increasing scFv affinity
SYN 5
SYN 3
EE
G98 scFv
C65 scFv
ML39 scFv
H3B1 scFv
2800
IFN-γ [pg/ml]
0
zipCAR expression:
Low
High

Figure 3.6.1. Design and characterization of the SUPRA CAR system.

(A) Comparison between the conventional CAR and SUPRA CAR design. A SUPRA CAR system is composed of a zipCAR and zipFv. A zipCAR has a leucine zipper as the extracellular portion of the CAR and zipFv has scFv fused to a cognate leucine zipper that can bind to a leucine zipper on zipCAR.

(B) A SUPRA CAR system targeting multiple tumor antigens using different zipFvs. K562 cells expressing Her2, Mesothelin, or Axl were co-cultured *in vitro* with RR zipCAR expressing CD8+ human primary T cells (n=3, data are represented as mean ± SD).

(C) Variables explored for characterization of the SUPRA CAR system: (1) the affinity between leucine zipper pairs, (2) the affinity between tumor antigen and scFv, (3) the concentration of zipFv, and (4) the expression level of zipCAR.

(D) Effect of concentration of three zipFvs with leucine zippers (SYN 3, SYN5, and EE) that have different affinity to RR zipCAR on IFN- γ production by primary CD4+ T cells (n=3, data are represented as mean ± SD).

(E) Effect of the zipper affinity, scFv-tumor affinity, and zipCAR expression level on IFN-ιφν production by primary CD4+ T cells expressing RR zipCAR (n=3, data are represented as mean).

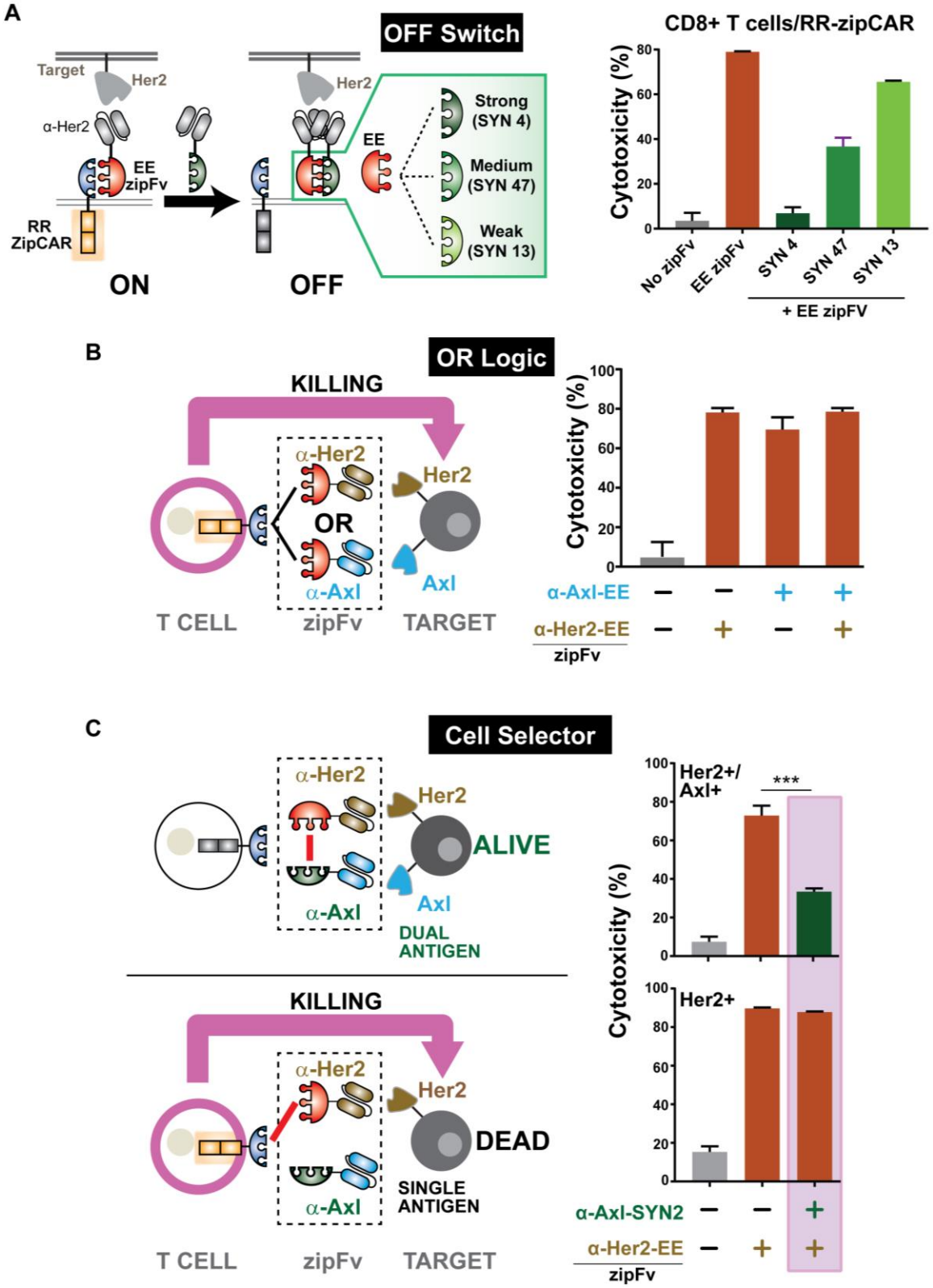
A
OFF Switch
Target
Her2
α-Her2
EE zipFv
RR ZipCAR
ON
OFF
EE
Strong (SYN 4)
Medium (SYN 47)
Weak (SYN 13)
CD8+ T cells/RR-zipCAR
Cytotoxicity (%)
No zipFv
EE zipFv
SYN 4
SYN 47
SYN 13
+ EE zipFV
B
OR Logic
KILLING
α-Her2
OR
α-Axl
Her2
Axl
T CELL
zipFv
TARGET
Cytotoxicity (%)
α-Axl-EE
α-Her2-EE
zipFv
C
Cell Selector
ALIVE
DUAL ANTIGEN
DEAD
SINGLE ANTIGEN
Her2+/ Axl+
Her2+
***
α-Axl-SYN2

Figure 3.6.2. Utilizing SUPRA CAR for OFF switch function and combinatorial antigens targeting.

(A) (Left) Schematic diagram of the SUPRA CAR with an OFF switch zipFv. Three competitive leucine zippers that can bind to the EE leucine zipper with different affinities are used to tune the T cell activation level. (Right) Cytotoxicity plot demonstrating the effect of the competitive zipFvs (n=3, data are represented as mean ± SD).

(B) Cytotoxicity plot of "OR" gate implementation of the SUPRA CAR system. Her2+/Axl+ K562 tumor cells were co-cultured with RR zipCAR expressing CD8+ T cells with different zipFv combinations (n=3, data are represented as mean ± SD).

(C) Using SUPRA CAR system as cell selector. Cells either expressed Her2 or Her2 and Axl. Axl acted as a "safe marker" that can inhibit SUPRA CAR T cell activity (data are represented as mean ± SD, statistical significance was determined by Student's t-test, *** = $p \leq 0.001$).

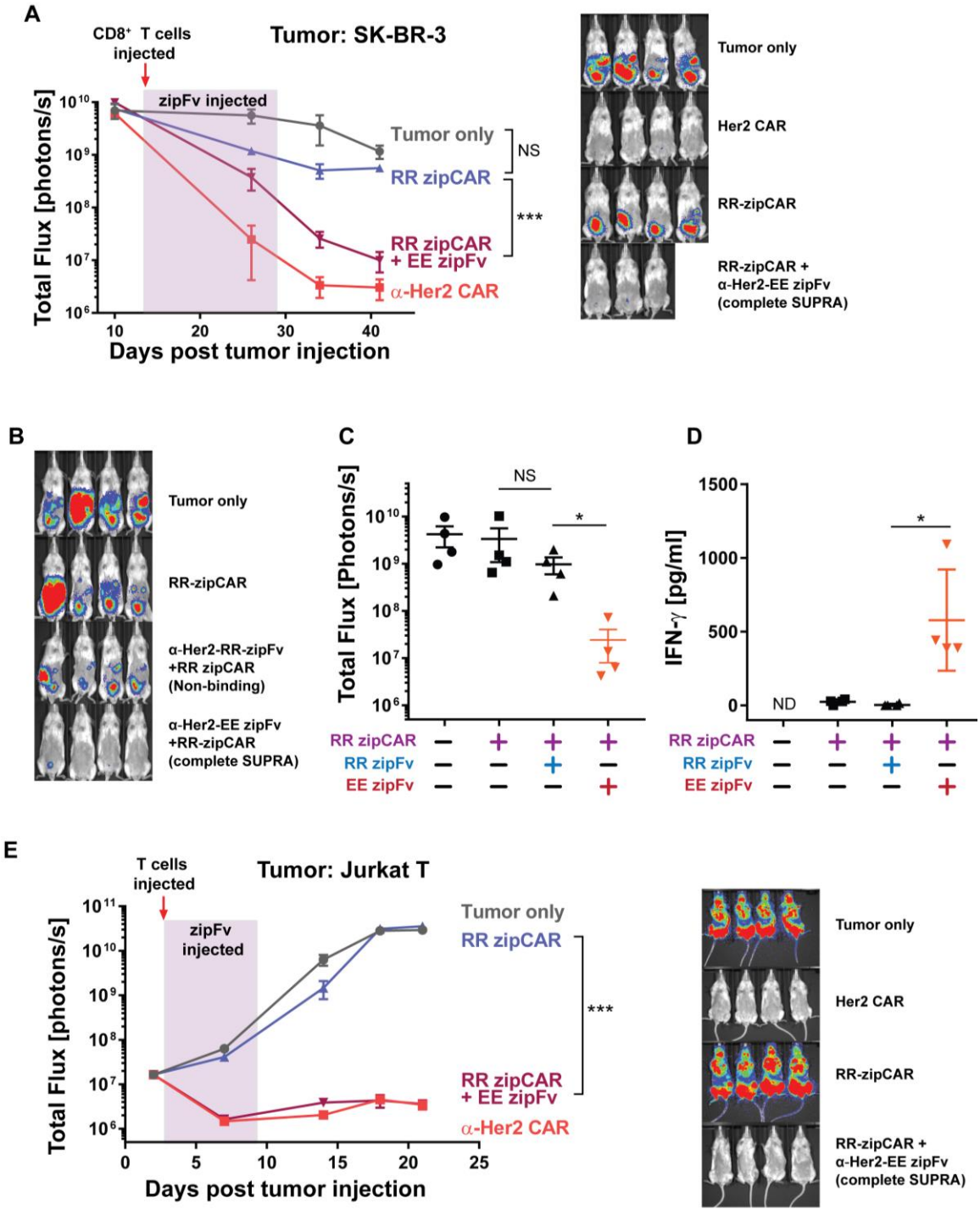
A
CD8+ T cells injected
Tumor: SK-BR-3
zipFv injected
Total Flux [photons/s]
Days post tumor injection
Tumor only
RR zipCAR
RR zipCAR + EE zipFv
α-Her2 CAR
NS
***
Tumor only
Her2 CAR
RR-zipCAR
RR-zipCAR + α-Her2-EE zipFv (complete SUPRA)
B
Tumor only
RR-zipCAR
α-Her2-RR-zipFv +RR zipCAR (Non-binding)
α-Her2-EE zipFv +RR-zipCAR (complete SUPRA)
C
Total Flux [Photons/s]
NS
*
RR zipCAR
RR zipFv
EE zipFv
D
IFN-γ [pg/ml]
ND
*
RR zipCAR
RR zipFv
EE zipFv
E
T cells injected
Tumor: Jurkat T
zipFv injected
Total Flux [photons/s]
Days post tumor injection
Tumor only
RR zipCAR
RR zipCAR + EE zipFv
α-Her2 CAR
***
Tumor only
Her2 CAR
RR-zipCAR
RR-zipCAR + α-Her2-EE zipFv (complete SUPRA)

Figure 3.6.3. *In vivo* activity of SUPRA CAR in SK-BR-3 and Jurkat xenograft models.

(A) (Left) The tumor burden was quantified as the total flux (photons/sec) from the luciferase activity of each mouse using IVIS imaging. Compared to RR zipCAR or tumor only control groups, the RR zipCAR + EE zipFv group showed significantly reduced tumor burden, comparable to conventional Her2 CAR (red arrow indicates injection of engineered CD8+ T cells and highlighted region indicates injection of zipFv (every 2 days at 5mg/kg for 2 weeks)). (Right) Representative IVIS images of groups treated with (1) no T cells, (2) conventional Her2 CAR, (3) RR zipCAR, and (4) RR zipCAR with EE zipFv at day 41 (n=4, data are represented as mean ± SEM).

(B) Representative IVIS images of groups treated with (1) no T cells, (2) RR zipCAR, (3) α-Her2 RR zipFv with RR zipCAR (non-binding), and (4) α-Her2 EE zipFv with RR zipCAR (complete SUPRA) (day 57, Figure S4B).

(C) Tumor burden as total flux (photons per sec) of each mouse shown in Figure 3B (n=4, data are represented as mean ± SEM).

(D) *In vivo* IFN-γ cytokine level after 24 hours of initial CD8+ T cells and zipFv injection (n=4, data are represented as mean ± SD).

(E) (Left) Jurkat tumor cells were injected intravenously at day 0 to immune-compromised NSG mice. At day 3, primary human CD8+ T cells expressing RR zipCAR were injected once (red arrow) with α-Her2-EE zipFv which was dosed every day for 6 days at 3mg/kg (highlighted). The tumor burden was quantified as the total flux (photons/sec) from the luciferase activity of each mouse using IVIS imaging. (Right) Representative IVIS images

of groups treated with (1) no T cells, (2) conventional Her2 CAR, (3) RR zipCAR, and (4) RR zipCAR with EE zipFv at day 21 (n=4, data are represented as mean ± SEM, statistical significance was determined by Student's t-test, *= $p \leq 0.05$, ***= $p \leq 0.001$).

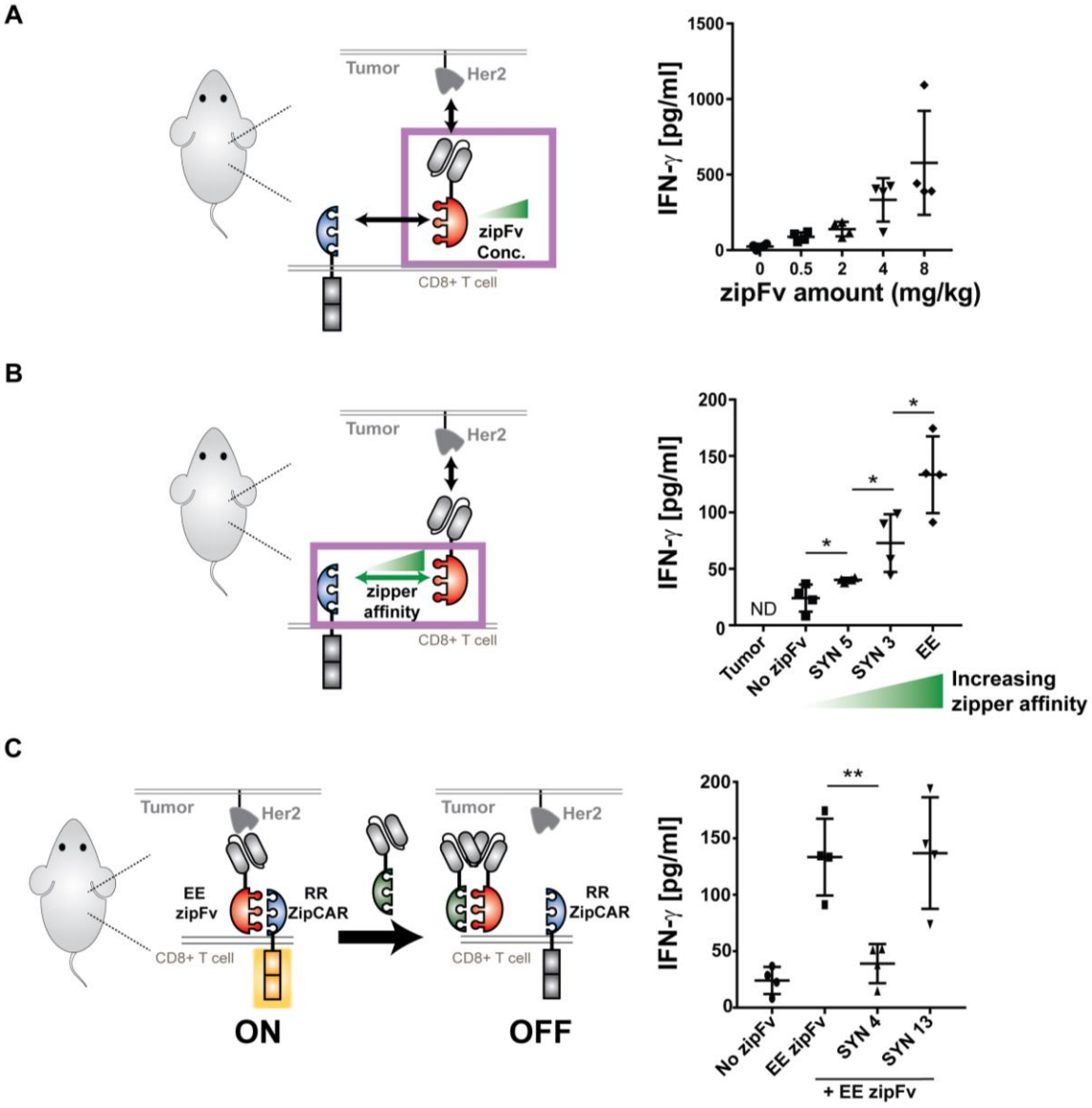
A
Tumor
Her2
zipFv
Conc.
CD8+ T cell
IFN-γ [pg/ml]
1500
1000
500
0
0
0.5
2
4
8
zipFv amount (mg/kg)
B
Tumor
Her2
zipper
affinity
CD8+ T cell
IFN-γ [pg/ml]
200
150
100
50
0
ND
*
*
*
Tumor
No zipFv
SYN 5
SYN 3
EE
Increasing
zipper affinity
C
Tumor
Her2
EE
zipFv
RR
ZipCAR
CD8+ T cell
ON
Tumor
Her2
RR
ZipCAR
CD8+ T cell
OFF
IFN-γ [pg/ml]
200
150
100
50
0
**
No zipFv
EE zipFv
SYN 4
SYN 13
+ EE zipFv

Figure 3.6.4. *In vivo* control of cytokine production by the SUPRA CAR.

(A) *In vivo* IFN-γ cytokine level at 24 hr. *In vivo* cytokine level increased in a dose-dependent manner (n=4, data are represented as mean ± SD).

(B) *In vivo* IFN-γ cytokine level at 24hr, demonstrating leucine zipper affinity-dependent increase of *in vivo* IFN-γ cytokine (n=4 mice, data are represented as mean ± SD).

(C) *In vivo* IFN-γ cytokine level demonstrating the effect of competitive zipFv (n=4 mice, data are represented as mean ± SD, the statistical significance was determined by Student's t-test, * = $p \leq 0.05$, *** = $p \leq 0.001$).

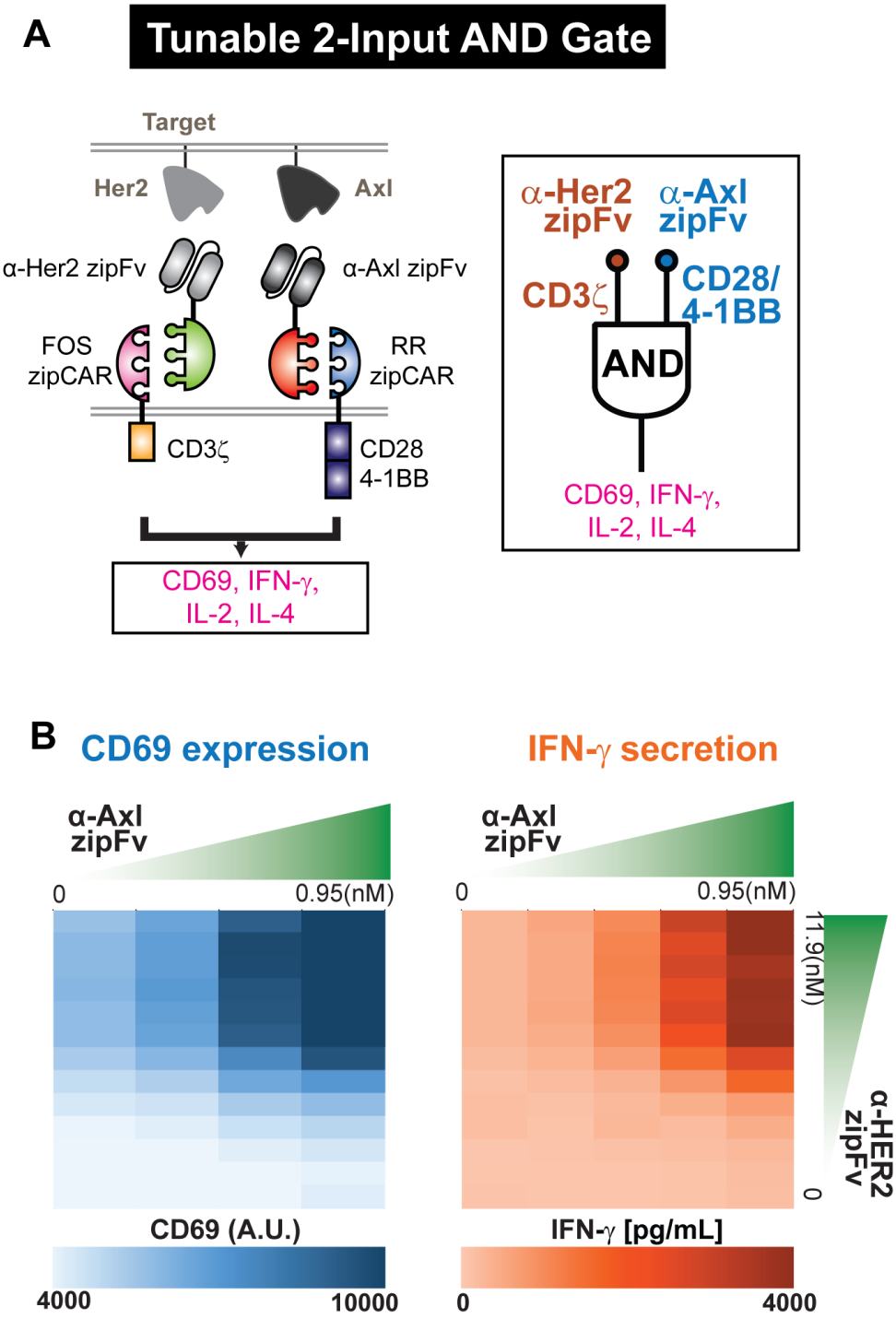
A
Tunable 2-Input AND Gate
Target
Her2
Axl
α-Her2 zipFv
α-Axl zipFv
FOS zipCAR
RR zipCAR
CD3ζ
CD28
4-1BB
CD69, IFN-γ, IL-2, IL-4
α-Her2 zipFv
α-Axl zipFv
CD3ζ
CD28/ 4-1BB
AND
CD69, IFN-γ, IL-2, IL-4
B
CD69 expression
IFN-γ secretion
α-Axl zipFv
0
0.95(nM)
α-Axl zipFv
0
0.95(nM)
11.9(nM)
0
α-HER2 zipFv
CD69 (A.U.)
4000
10000
IFN-γ [pg/mL]
0
4000

Figure 3.6.5. Controlling different signaling domains with orthogonal SUPRA CARs.

(A) Design of orthogonal SUPRA CARs that control either CD3ζ or CD28/4-1BB signaling domains. The RR zipCAR and FOS zipCAR contain CD28/4-1BB co-stimulatory and CD3ζ signaling domain, respectively. α-Her2 zipFv binds to the FOS zipCAR and activates the CD3ζ domain, whereas the α-Axl zipFv binds to the RR zipCAR and activates CD28/4-1BB co-stimulatory domains. CD69 expression, IFN-γ, IL-2, and IL-4 secretion were measured as outputs.

(B) Amount of each zipFv was varied to define signaling strength from each receptor. CD69 expression (left) and IFN-γ secretion (right) were measured (n=3, data are represented as mean).

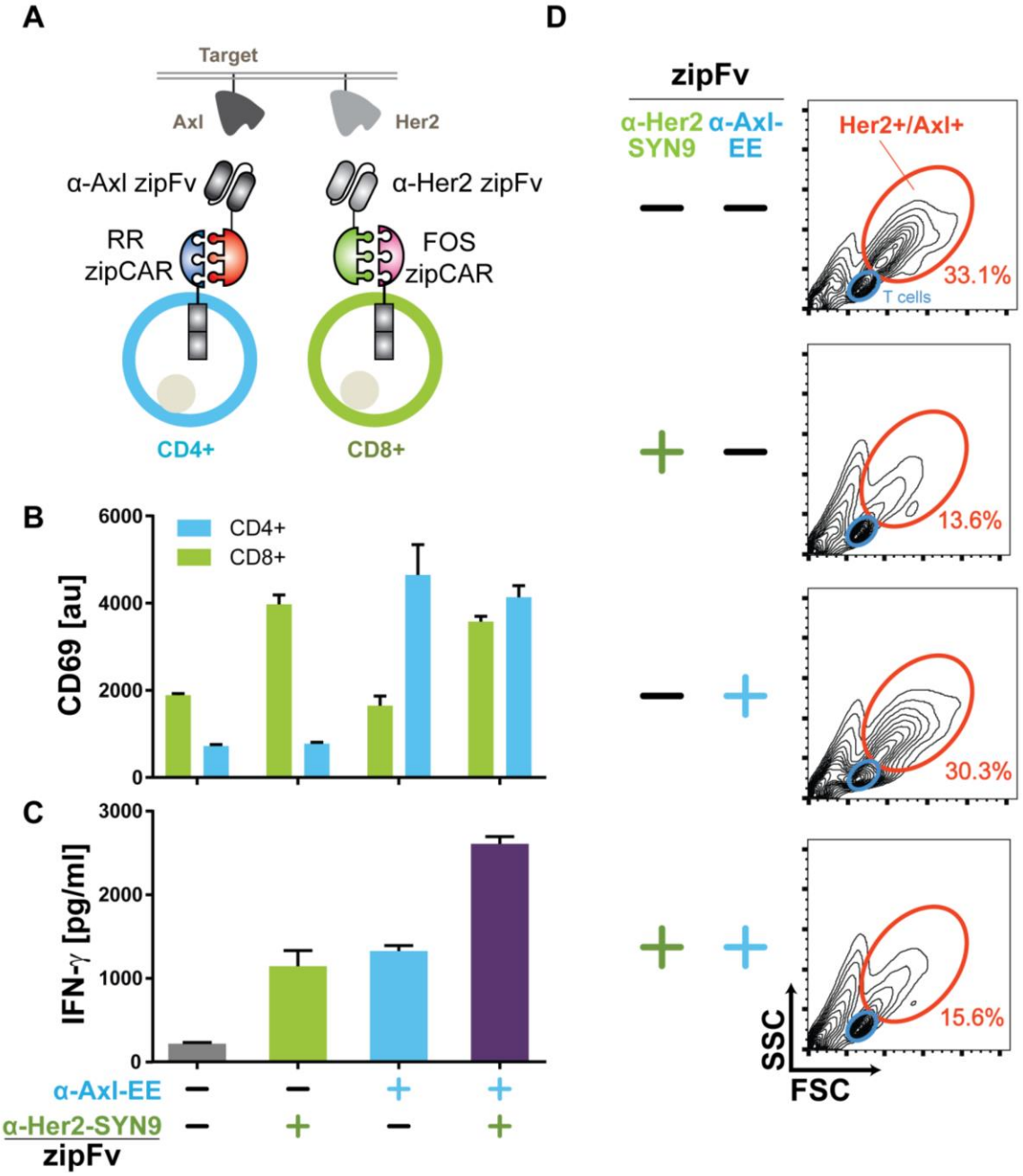
A
Target
Axl
Her2
α-Axl zipFv
α-Her2 zipFv
RR zipCAR
FOS zipCAR
CD4+
CD8+
B
CD69 [au]
6000
4000
2000
0
CD4+
CD8+
C
IFN-γ [pg/ml]
3000
2000
1000
0
α-Axl-EE
α-Her2-SYN9
zipFv
D
zipFv
α-Her2 SYN9
α-Axl-EE
Her2+/Axl+
33.1%
T cells
13.6%
30.3%
15.6%
SSC
FSC

Figure 3.6.6. Controlling different cell types with orthogonal SUPRA CARs.

(A) Design of orthogonal SUPRA CARs that control either CD4+ or CD8+ human primary T cells. The RR zipCAR and FOS zipCAR control CD4+ and CD8+ T cells activity, respectively. α-Axl zipFv binds to RR zipCAR and activates CD4+ T cells. α-Her2 zipFv binds to the FOS zipCAR and activates CD8+ T cells.

(B, C) The CD69 expression and IFN-γ measurements showing independent control of CD4+ and CD8+ T cells with orthogonal SUPRA CARs (n=3, data are represented as mean ± SD).

(D) Forward- and side-scatter FACS plots of the cell mixture after 24 hours co-culture of T cells (both CD4+ and CD8+, blue) with Her2+/Axl+ K562 tumor cells (orange). Tumor cells are killed efficiently when CD8+ cytotoxic T cells were activated by the α-HER2 zipFv (representative of three biological replicates).

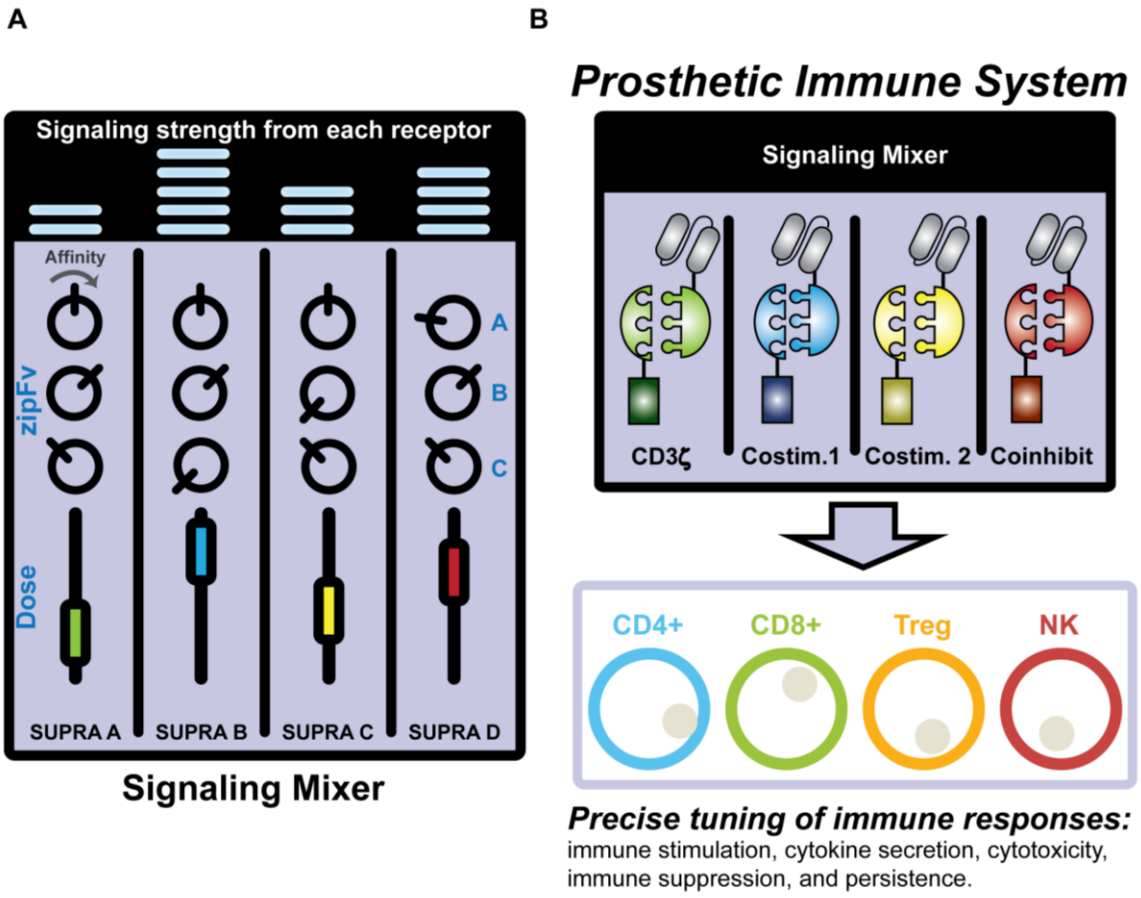
A
Signaling strength from each receptor
Affinity
zipFv
Dose
A
B
C
SUPRA A
SUPRA B
SUPRA C
SUPRA D
Signaling Mixer
B
Prosthetic Immune System
Signaling Mixer
CD3ζ
Costim.1
Costim. 2
Coinhibit
CD4+
CD8+
Treg
NK
Precise tuning of immune responses:
immune stimulation, cytokine secretion, cytotoxicity,
immune suppression, and persistence.

Figure 3.6.7. Engineering a prosthetic immune system with SUPRA CARs.

(A) The SUPRA CAR system enables the flexible and advanced control of signaling in T cells, reminiscent of an audio mixing console for controlling audio signals. The affinity and dosage of each zipFv are like knobs and dials on the mixing console, which can be varied to achieve user-defined T cell activation levels. Different orthogonal pairs of SUPRA CARs are like different channels, which can be utilized to control different signaling pathways in the same cells. (B) The SUPRA CAR system can also be implemented in other cell types, thus setting the foundation for creating a prosthetic immune system.

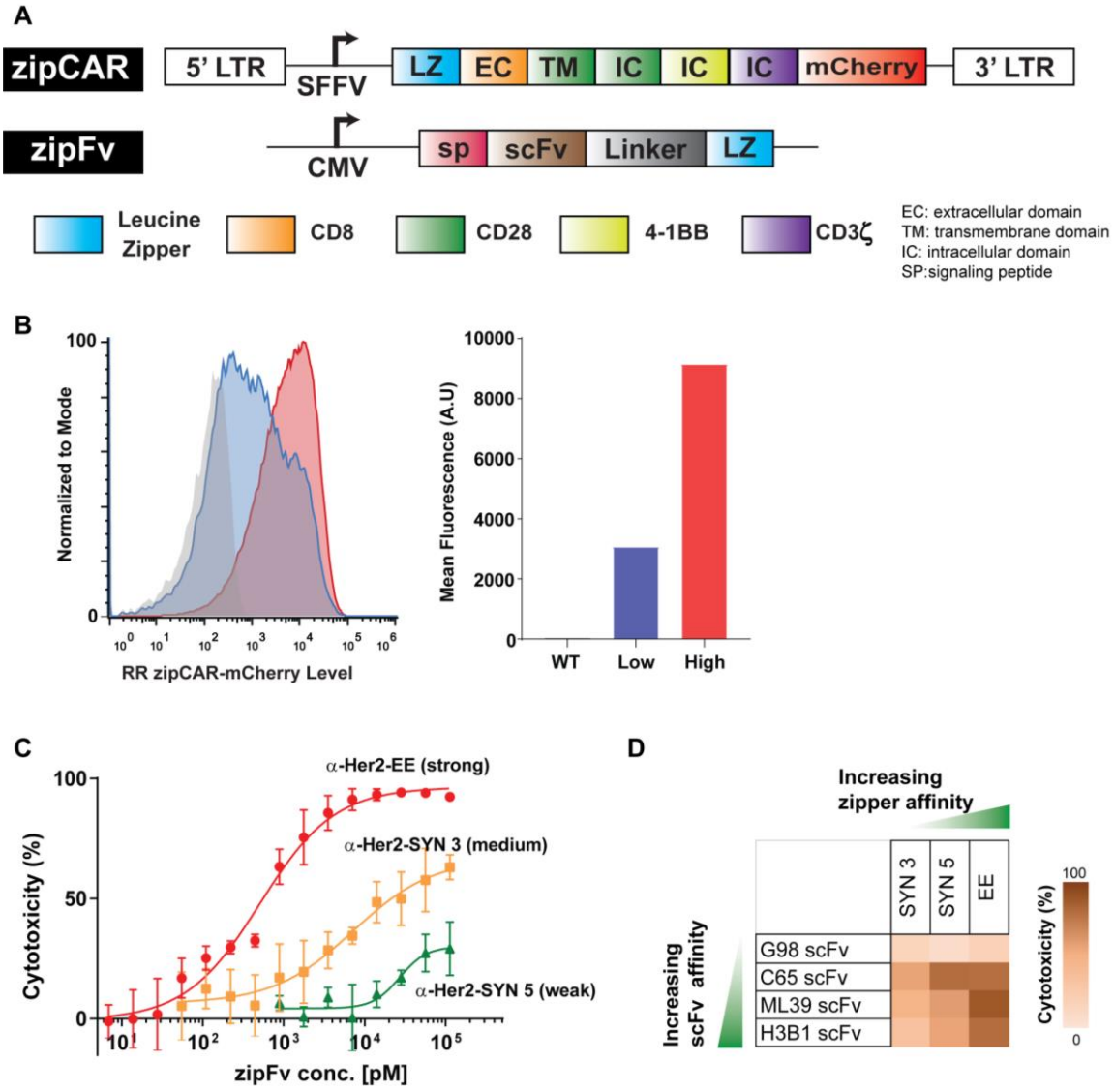
A
zipCAR
5' LTR
SFFV
LZ
EC
TM
IC
IC
IC
mCherry
3' LTR
zipFv
CMV
sp
scFv
Linker
LZ
Leucine Zipper
CD8
CD28
4-1BB
CD3ζ
EC: extracellular domain
TM: transmembrane domain
IC: intracellular domain
SP:signaling peptide
B
Normalized to Mode
RR zipCAR-mCherry Level
Mean Fluorescence (A.U)
WT
Low
High
C
α-Her2-EE (strong)
α-Her2-SYN 3 (medium)
α-Her2-SYN 5 (weak)
Cytotoxicity (%)
zipFv conc. [pM]
D
Increasing zipper affinity
Increasing scFv affinity
SYN 3
SYN 5
EE
G98 scFv
C65 scFv
ML39 scFv
H3B1 scFv
Cytotoxicity (%)

Figure 3.6.8. Schematic of SUPRA CAR and effect of different parameters on cytotoxicity, Related to Figure 3.6.1.

(A) Schematic of zipCAR and zipFv construct designs. ZipCAR composes of leucine zipper on the extracellular domain and intracellular signaling domains which contain two co-stimulatory signaling domains (CD28 and 4-1BB), and CD3ζ. zipCAR is fused to mCherry for visualization.

(B) (Left) FACS histogram that shows different CAR expression level of CD4+ T cells used in Figure 1E

(Right) Quantified fluorescence value. WT is represented as gray, high CAR expressing cells as red and low CAR expressing cells as blue (n=1).

(C) Effect of concentration of three zipFvs with leucine zippers (SYN3, SYN5, and EE) that have different affinity to RR zipCAR on cytotoxicity (n=3, data are represented as mean ± SD).

(D) Effect of zipper affinity and scFv affinity on cytotoxicity (n=3, data are represented as mean).

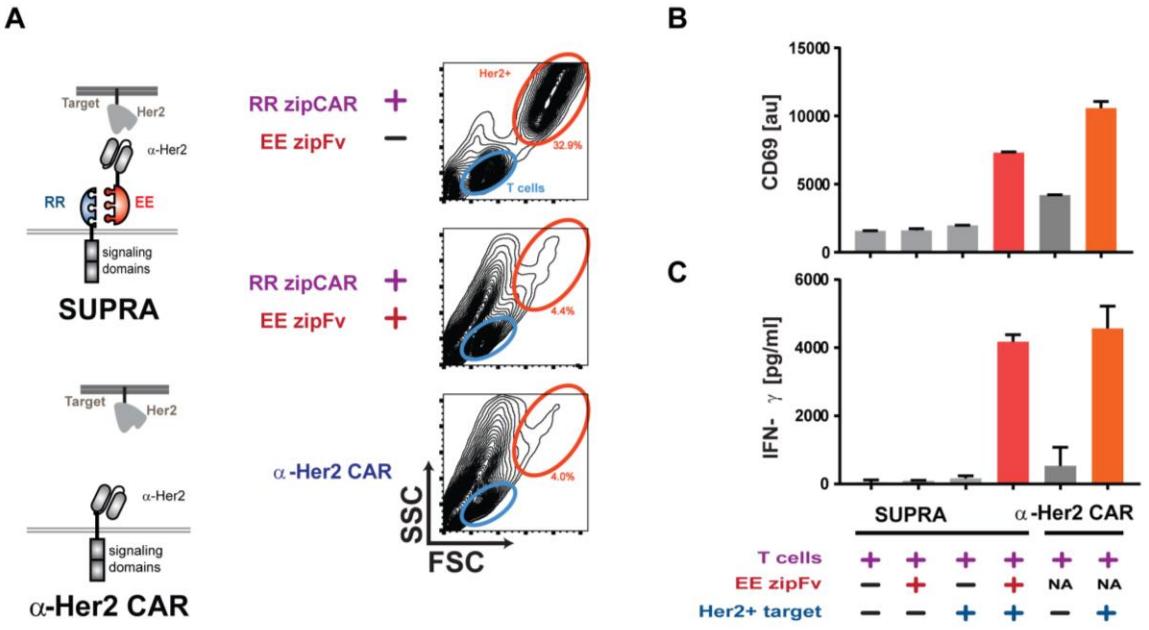

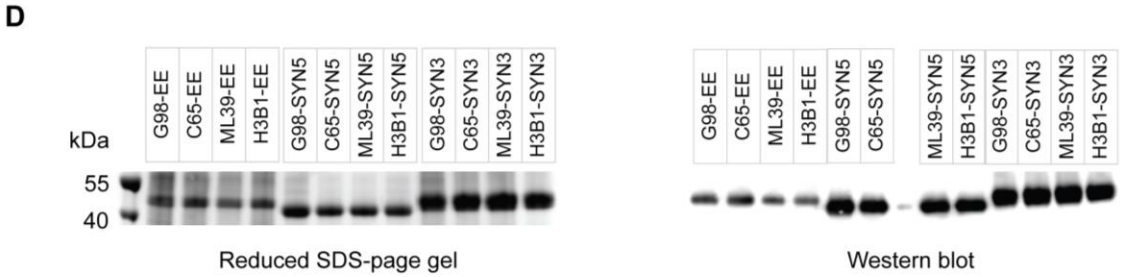

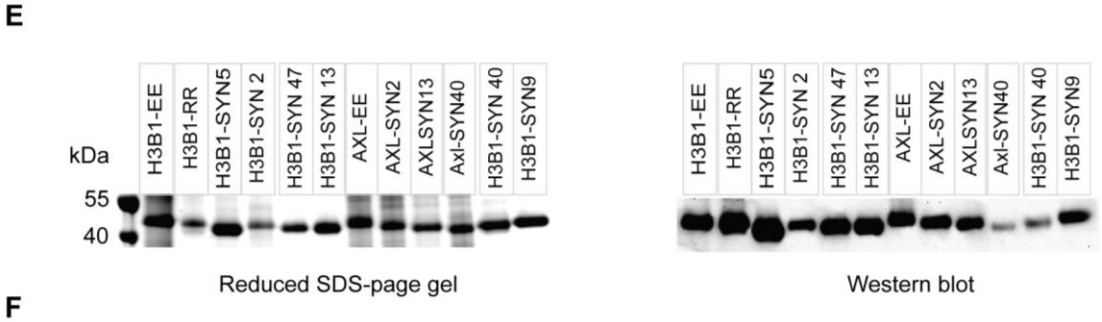

F

	Expected Protein Mass(Da)			Expected Protein Mass(Da)
G98-EE	39681.72		H3B1-RR	39819.79
C65-EE	39667.68		H3B1-SYN 2	39898.99
ML39-EE	39803.83		H3B1-SYN 47	38835.79
H3B1-EE	39901.98		H3B1-SYN 13	39130.14
G98-SYN5	39007.96		AXL-EE	35979.35
C65-SYN5	38993.92		AXL-SYN2	35976.36
ML39-SYN5	39130.07		AXLSYN13	35207.51
H3B1-SYN5	39228.22		Axl-SYN40	35156.44
G98-SYN3	38632.52		H3B1-SYN 40	39079.07
C65-SYN3	38618.48		H3B1-SYN9	38170.04
ML39-SYN3	38754.63			
H3B1-SYN3	38852.78			

Figure 3.6.9. Comparison of SUPRA CAR with conventional α-Her2 CAR and characterization of zipFvs, Related to Figures 3.6.1., 3.6.2. and 3.6.5.

(A) (Left) Schematic of SUPRA CAR (EE-RR pair) and a-Her2 CAR. (Right) Forward- and side-scatter FACS plots of the cell mixture after 24 hours co-culture of T cells (blue) with Her2+ K562 tumor cells (orange) (representative of three biological replicates).

(B, C) The CD69 expression and IFN-γ measurement after 24hr of co-culturing with RR zipCAR / α- Her2 CAR and Her2+ K562 target cells (n=3, data are represented as mean ± SD).

(D, E) Denaturing SDS-PAGE and western blot images of the different zipFvs used in the paper

(F) Table of expected protein mass (Da) of different zipFvs

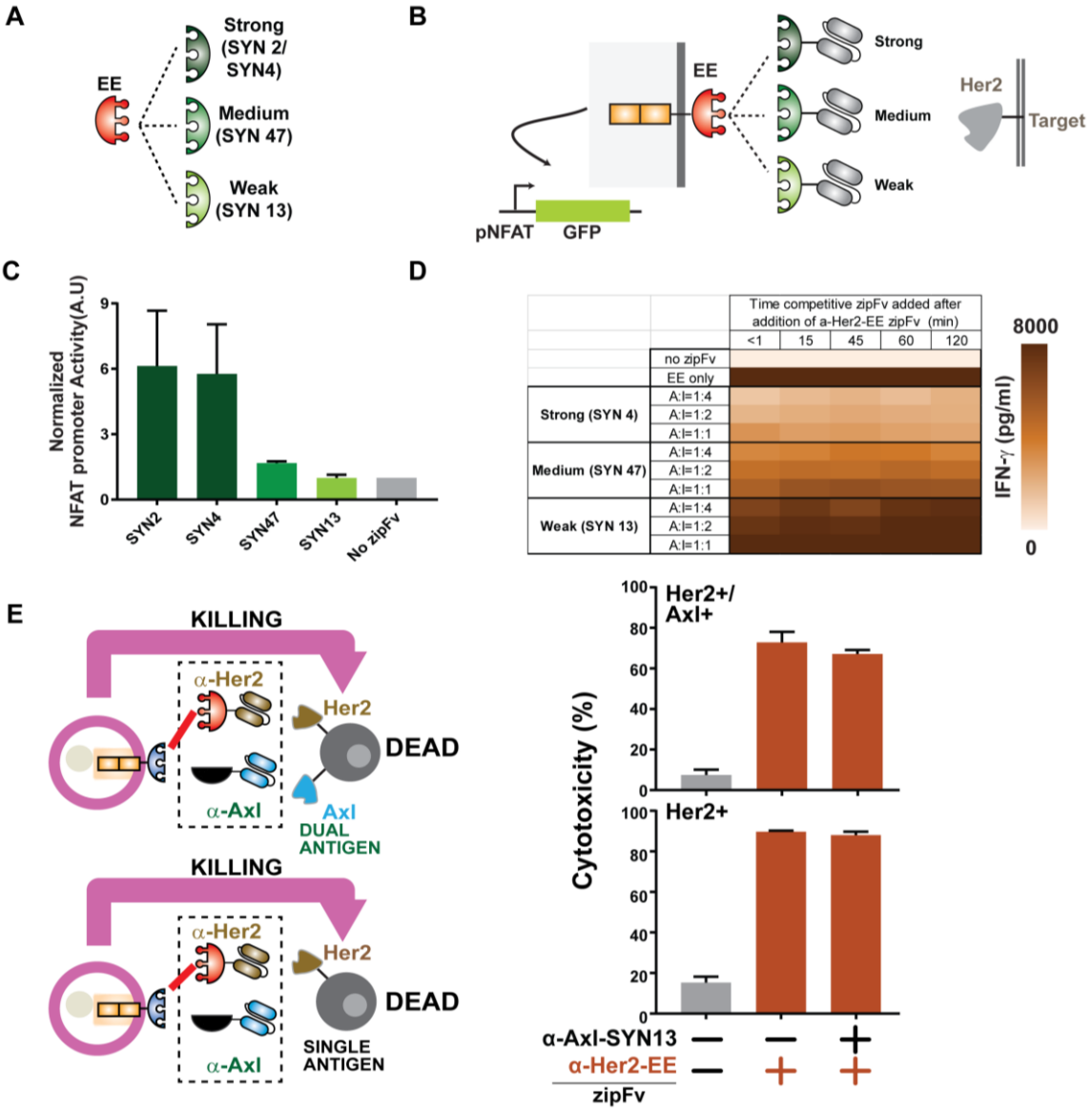
A
EE
Strong (SYN 2/ SYN4)
Medium (SYN 47)
Weak (SYN 13)
B
EE
Strong
Medium
Weak
Her2
Target
pNFAT
GFP
C
Normalized NFAT promoter Activity(A.U)
9
6
3
0
SYN2
SYN4
SYN47
SYN13
No zipFv
D
Time competitive zipFv added after addition of a-Her2-EE zipFv (min)
<1
15
45
60
120
no zipFv
EE only
Strong (SYN 4)
A:I=1:4
A:I=1:2
A:I=1:1
Medium (SYN 47)
A:I=1:4
A:I=1:2
A:I=1:1
Weak (SYN 13)
A:I=1:4
A:I=1:2
A:I=1:1
8000
IFN-γ (pg/ml)
0
E
KILLING
α-Her2
Her2
DEAD
α-Axl
Axl
DUAL ANTIGEN
KILLING
α-Her2
Her2
DEAD
α-Axl
SINGLE ANTIGEN
Cytotoxicity (%)
Her2+/ Axl+
Her2+
100
80
60
40
20
0
α-Axl-SYN13
α-Her2-EE
zipFv

Figure 3.6.10. Competitive zipFv screen to tune SUPRA CAR activity and using SUPRA as a Cell Selector, Related to Figure 3.6.2.

(A) Leucine zippers with different affinities to EE leucine zipper.

(B) EE zipCAR expressing Jurkat T cells were co-cultured with Her2 expressing K562. Then, different zipFvs (α-Her2-SYN2, α-Her2-SYN4, α-Her2-SYN47, or α-Her2-SYN13) were added. GFP expression was measured after 24 hours to quantify NFAT promoter activity.

(C) Normalized NFAT promoter activity measured by GFP expression of different zipFvs (n=2, data are represented as mean ± SD).

(D) RR zipCAR expressing CD8+ T cells were co-cultured with Her2 expressing K562. α-Her2-EE zipFv (22.5nM) was added to activate T cells. Then, a different amount of competitive zipFv (90nM, 45nM, and 22.5nM) was added at a different time after EE zipFv was added (n=3, data are represented as mean).

(E) Cell selector with zipFv (α-Axl-SYN13) that does not bind strongly to α-Her2-EE zipFv.

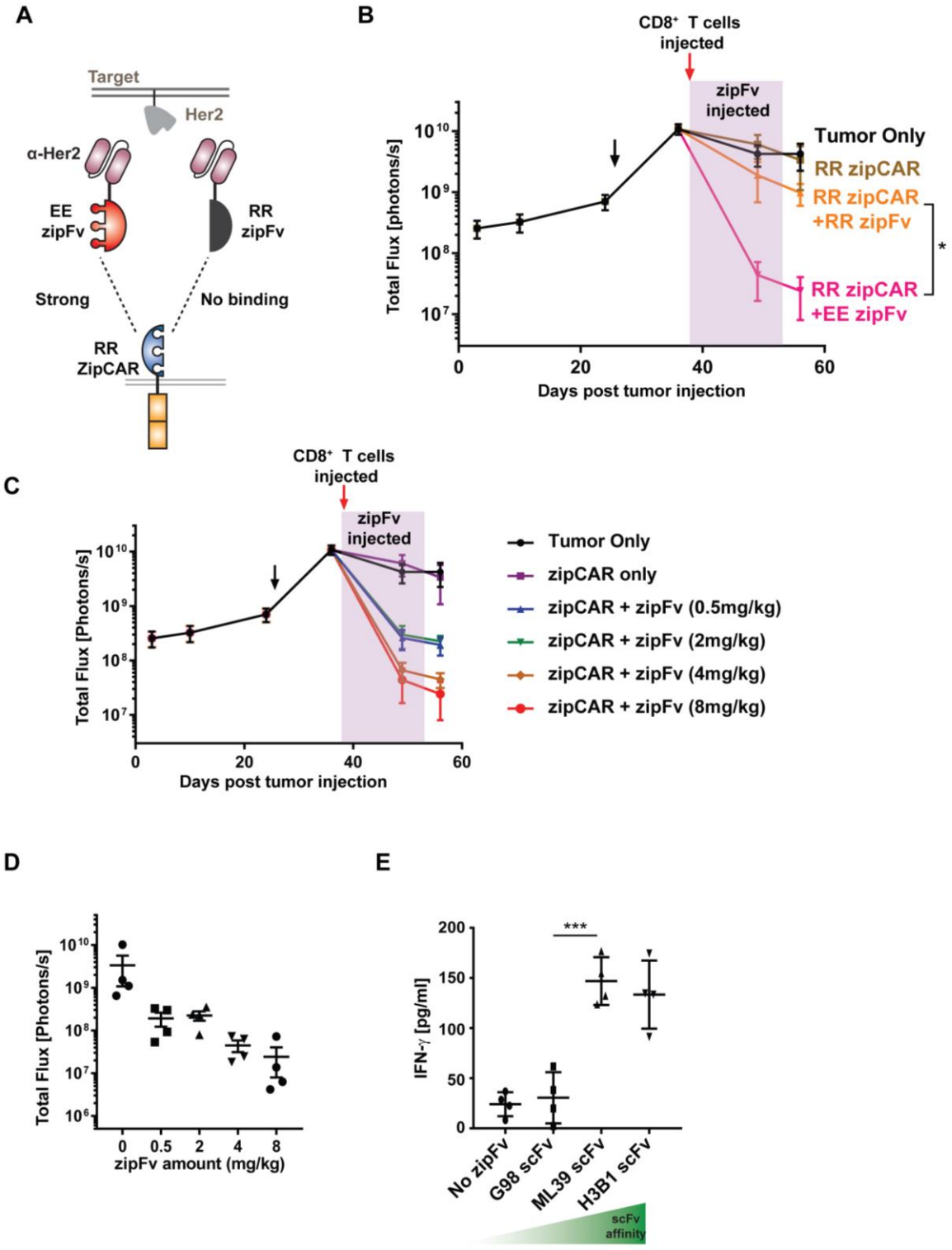
A
Target
Her2
α-Her2
EE zipFv
RR zipFv
Strong
No binding
RR ZipCAR
B
CD8⁺ T cells injected
zipFv injected
Total Flux [photons/s]
Tumor Only
RR zipCAR
RR zipCAR +RR zipFv
RR zipCAR +EE zipFv
*
Days post tumor injection
C
CD8⁺ T cells injected
zipFv injected
Total Flux [Photons/s]
Tumor Only
zipCAR only
zipCAR + zipFv (0.5mg/kg)
zipCAR + zipFv (2mg/kg)
zipCAR + zipFv (4mg/kg)
zipCAR + zipFv (8mg/kg)
Days post tumor injection
D
Total Flux [Photons/s]
zipFv amount (mg/kg)
E
IFN-γ [pg/ml]
***
No zipFv
G98 scFv
ML39 scFv
H3B1 scFv
scFv affinity

Figure 3.6.11. Binding between zipFv and zipCAR is required to clear the tumor *in vivo*. Effect of zipFv dose and scFv affinity on tumor burden and *in vivo* cytokine production, Related to Figures 3.6.3. and 3.6.4.

(A) Diagram showing the xenograft study described in Figure 3B. Two different zipFvs were used; α-Her2-EE zipFv that binds to RR zipCAR strongly and α-Her2-RR zipFv that does not bind to RR zipCAR strongly.

(B) SK-BR-3 breast cancer cells were injected intraperitoneally at day 0 and at day 26 (black arrow) to immune compromised NSG mice. After verifying tumor establishment, RR zipCAR expressing CD8+ T cells (red arrow) were injected along with α-Her2 EE zipFv or α-Her2 RR zipFv (dosed every 2 days for 2 weeks at 8mg/kg, highlighted). Tumor burden was quantified as total flux (photons/sec) of luciferase activity from each mouse using IVIS imaging (n= 4 mice, data are represented as mean ± SEM, statistical significance was determined by two-tailed Student t-test, * = $p \leq 0.05$).

(C) SK-BR-3 breast cancer cells were injected intraperitoneally at day 0 and at day 26 (black arrow) to NSG mice. Primary human CD8+ T cells expressing the RR zipCAR were injected (red arrow) with the α-Her2-EE zipFv (injected every 2 days for 2 weeks at varying concentrations, highlighted). Tumor burden was quantified as total flux (photons/sec) from luciferase activity of each mouse using IVIS imaging (n=4, data are represented as mean ± SEM).

(D) Tumor burden as total flux (photons per sec) of each mouse shown in Figure S4C at day 57 (n=4, data are represented as mean ± SEM)

(E) *In vivo* IFN- γ release as scFv affinity changes from low (G98) to medium-high affinity (ML39, H3B1) (n= 4 mice, data are represented as mean ± SD, statistical significance was determined by two-tailed Student t-test, *** = $p \leq 0.001$).

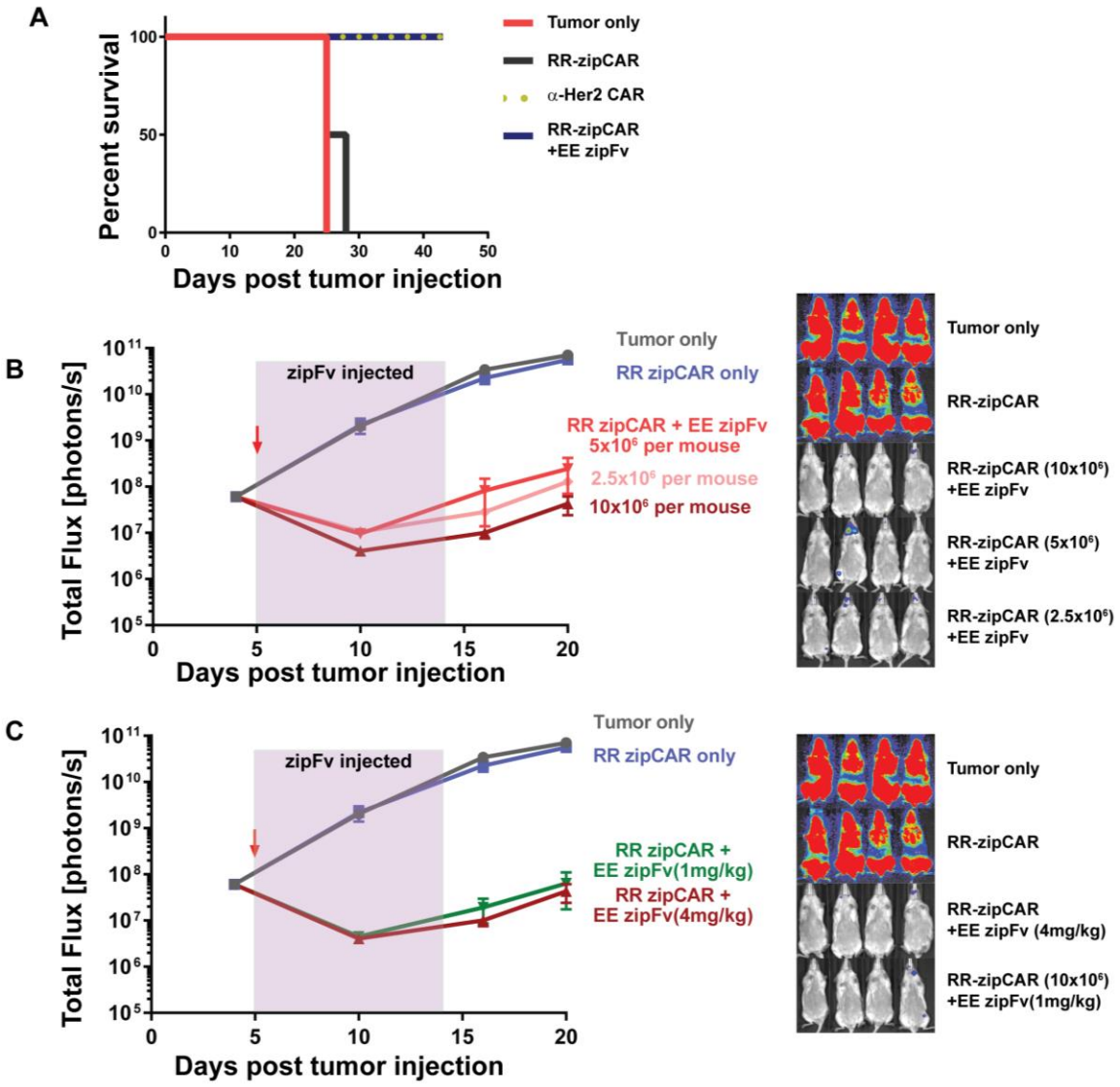
A
Percent survival
100
50
0
0
10
20
30
40
50
Days post tumor injection
Tumor only
RR-zipCAR
α-Her2 CAR
RR-zipCAR
+EE zipFv
B
Total Flux [photons/s]
zipFv injected
Days post tumor injection
Tumor only
RR zipCAR only
RR zipCAR + EE zipFv
5x10⁶ per mouse
2.5x10⁶ per mouse
10x10⁶ per mouse
Tumor only
RR-zipCAR
RR-zipCAR (10x10⁶)
+EE zipFv
RR-zipCAR (5x10⁶)
+EE zipFv
RR-zipCAR (2.5x10⁶)
+EE zipFv
C
Total Flux [photons/s]
zipFv injected
Days post tumor injection
Tumor only
RR zipCAR only
RR zipCAR +
EE zipFv(1mg/kg)
RR zipCAR +
EE zipFv(4mg/kg)
Tumor only
RR-zipCAR
RR-zipCAR
+EE zipFv (4mg/kg)
RR-zipCAR (10x10⁶)
+EE zipFv(1mg/kg)

Figure 3.6.12. Tumor clearance of SUPRA CAR in vivo using Jurkat xenograft model, Related to Figure 3.6.3.

(A) Kaplan-Meier survival curves of various groups shown in Figure 3E

(B) Effect of different T cell dose on tumor burden. (Left) The tumor burden was quantified as the total flux (photons/sec) from the luciferase activity of each mouse using IVIS imaging (red arrow indicates injection of T cells (day 5) and zipFv was dosed daily for 9 days at 4mg/kg). (Right) Representative IVIS images of different groups at day 20 (n=4, data are represented as mean ± SEM).

(C) Effect of zipFv dose on tumor burden. (Left) The tumor burden was quantified as the total flux (photons/sec) from the luciferase activity of each mouse using IVIS imaging (red arrow indicates injection of T cells (day 5) and zipFv was dosed daily for 9 days). (Right) Representative IVIS images of different groups at day 20 (n=4, data are represented as mean ± SEM).

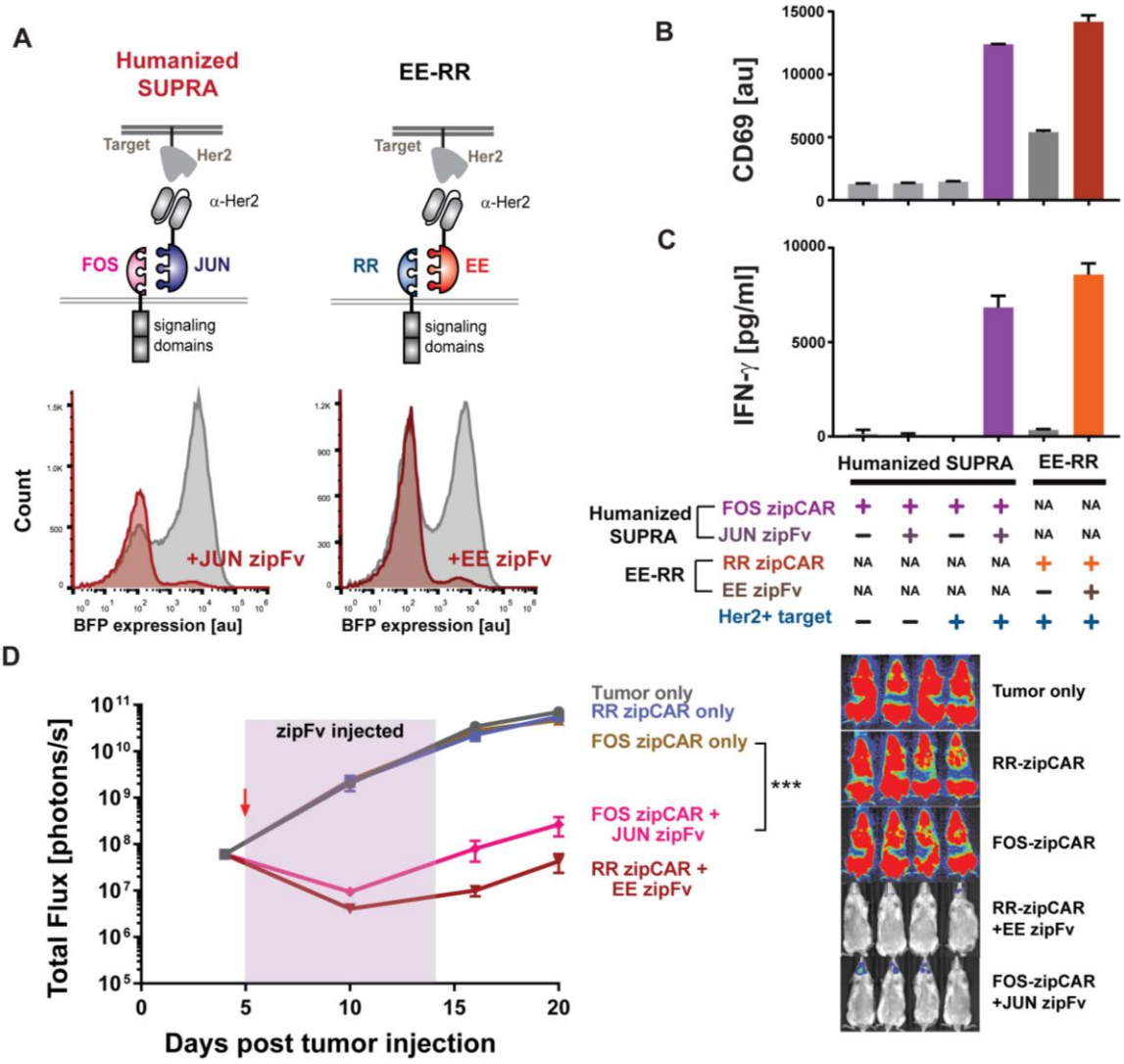
A
Humanized SUPRA
EE-RR
Target
Her2
α-Her2
FOS
JUN
RR
EE
signaling domains
Count
+JUN zipFv
+EE zipFv
BFP expression [au]
B
CD69 [au]
C
IFN-γ [pg/ml]
Humanized SUPRA
EE-RR
Humanized SUPRA
FOS zipCAR
JUN zipFv
EE-RR
RR zipCAR
EE zipFv
Her2+ target
D
Total Flux [photons/s]
zipFv injected
Days post tumor injection
Tumor only
RR zipCAR only
FOS zipCAR only
FOS zipCAR + JUN zipFv
RR zipCAR + EE zipFv
***
Tumor only
RR-zipCAR
FOS-zipCAR
RR-zipCAR +EE zipFv
FOS-zipCAR +JUN zipFv

Figure 3.6.13. Comparison of Humanized SUPRA CAR with EE-RR SUPRA pair

(A) Schematic of Humanized SUPRA CAR (FOS-JUN pair) and RR-EE SUPRA CAR. FACS plots of the cell mixture after 24 hours co-culture of SUPRA CAR T cells with Her2+ Jurkat tumor cells. Jurkat tumor cells express blue fluoresce protein (BFP) (representative of three biological replicates).

(B, C) The CD69 expression and IFN-γ measurements after 24hr of co-culturing with FOS / RR zipCAR and Her2+ Jurkat target cells (n=3, data are represented as mean ± SD).

(D) (Left) The tumor burden was quantified as the total flux (photons/sec) from the luciferase activity of each mouse using IVIS imaging (red arrow indicates injection of T cells (day 5) and zipFv was dosed daily for 9 days at 4mg/kg). (Right) Representative IVIS images of groups treated with (1) no T cells, (2) RR zipCAR ($10x10^6$ T cells per mouse), (3) FOS zipCAR ($10x10^6$ T cells per mouse), (4) RR zipCAR with α-Her2 EE zipFv (4mg/kg), and (5) FOS zipCAR with α-Her2 JUN zipFv (4mg/kg) at day 20 (n=4, data are represented as mean ± SEM).

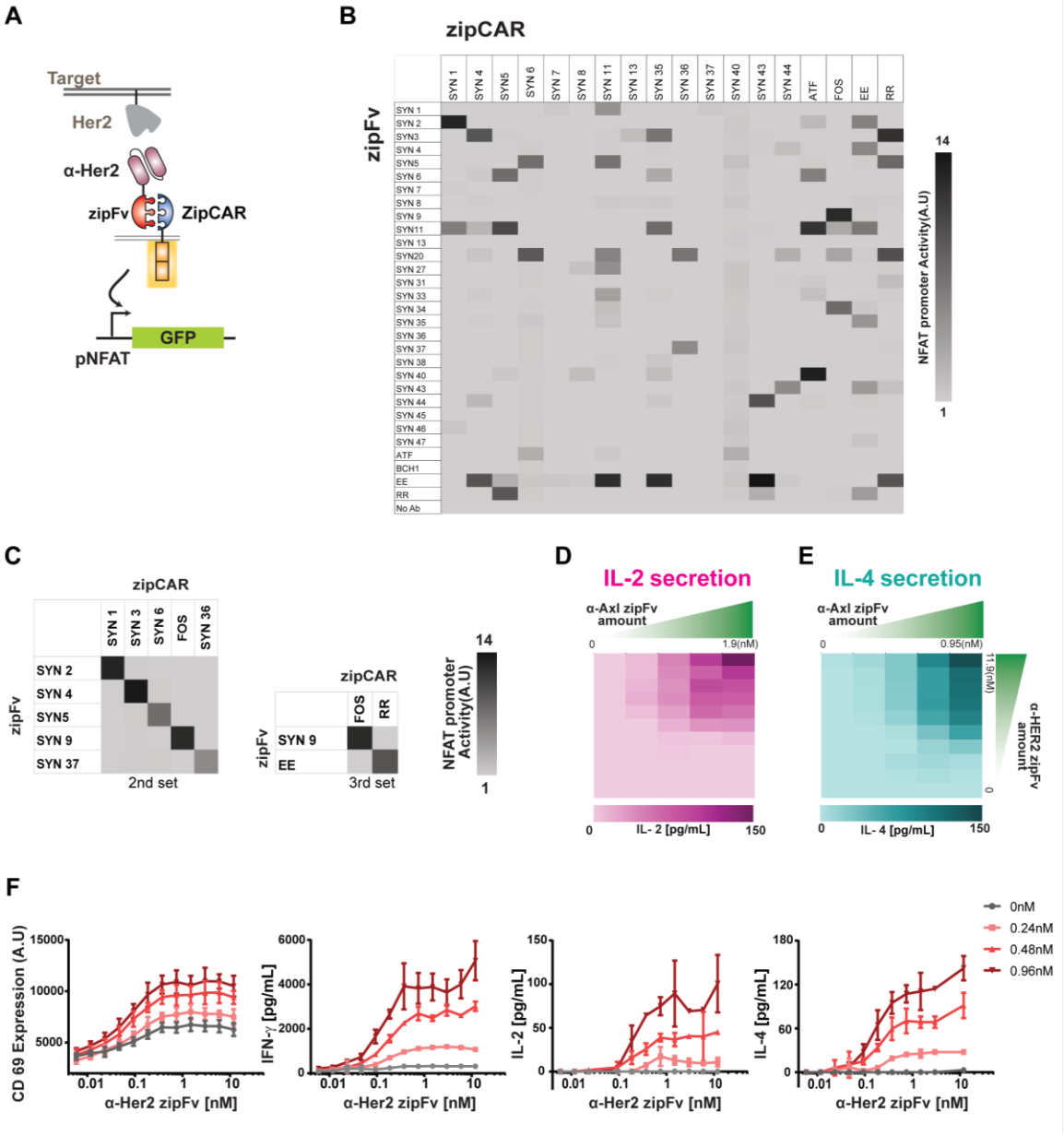
A
Target
Her2
α-Her2
zipFv
ZipCAR
GFP
pNFAT
B
zipCAR
zipFv
SYN 1
SYN 4
SYN5
SYN 6
SYN 7
SYN 8
SYN 11
SYN 13
SYN 35
SYN 36
SYN 37
SYN 40
SYN 43
SYN 44
ATF
FOS
EE
RR
SYN 2
SYN3
SYN 9
SYN11
SYN20
SYN 27
SYN 31
SYN 33
SYN 34
SYN 45
SYN 46
SYN 47
BCH1
No Ab
14
NFAT promoter Activity(A.U)
1
C
zipCAR
SYN 1
SYN 3
SYN 6
FOS
SYN 36
zipFv
SYN 2
SYN 4
SYN5
SYN 9
SYN 37
2nd set
zipCAR
FOS
RR
zipFv
SYN 9
EE
3rd set
14
NFAT promoter Activity(A.U)
1
D
IL-2 secretion
α-Axl zipFv amount
0
1.9(nM)
0
IL- 2 [pg/mL]
150
E
IL-4 secretion
α-Axl zipFv amount
0
0.95(nM)
1.9(nM)
0
α-HER2 zipFv amount
0
IL- 4 [pg/mL]
150
F
CD 69 Expression (A.U)
15000
10000
5000
IFN-γ [pg/mL]
6000
4000
2000
0
IL-2 [pg/mL]
150
100
50
0
IL-4 [pg/mL]
180
120
60
0
0.01
0.1
1
10
α-Her2 zipFv [nM]
0nM
0.24nM
0.48nM
0.96nM

Figure 3.6.14. Orthogonal SUPRA CAR screen and controlling different signaling domains using orthogonal SUPRA CARs, Related to Figures 3.6.5. and 3.6.6.

(A) Jurkat T cells expressing different zipCARs were co-cultured with Her2 expressing K562 target cells and different zipFvs. GFP expression was used to measure the interaction between two leucine zippers.

(B) In order to identify several pairs of orthogonal SUPRA CARs, we chose 18 zipCARs and 30 zipFvs and quantified NFAT promoter activity (n= 2, data are represented as mean).

(C) Sets of orthogonal SUPRA CARs (n= 2, data are represented as mean).

(D, E) Quantified IL-2 and IL-4 production when dual orthogonal CARs were activated with varying concentration of two zipFvs (n=2 for IL-2 and n=3 for IL-4, data are represented as mean, Related to Figure 5A).

(F) Comparison of quantified CD69 expression, IFN- γ, IL-2, and IL-4 production when the varying concentration of two zipFvs was added as shown in Figures 5B, S7D, and S7E.

3.7 Acknowledgment

I want to acknowledge Dr. James Collins and Dr. Wilson Wong for their significant contributions including editing published manuscript to complete this chapter.

CHAPTER FOUR: ENGINEERING IMMUNE CELL CONSORTIA WITH ADVANCED LOGIC COMPUTATION USING UNIVERSAL CHIMERIC ANTIGEN RECEPTORS

4.1 Introduction

The human immune system composes of a variety of cell types that constantly sense and integrate multiple environmental inputs to defend against disease. Recent findings on immune cell-cell interactions led to achieve many novel drug discoveries. For instance, Sipuleucel-T (also known as Provenge) has been developed to treat metastatic prostate cancer [48]. This treatment utilizes antigen presenting cells (APCs) to stimulate CD4+ helper T cells and CD8+ cytotoxic T cells. Furthermore, different checkpoint blocker therapies (e.g., CTLA-4 blockade, PD-1 inhibitors, PD-L1 inhibitors) that block interactions between immune cells and cancer cells, have shown to be very effective cancer immunotherapy [50,166–168]. Despite these successes, responses of checkpoint inhibitor treatment are restricted only to subsets of cancer patients [169–171]. Thus, we still need better tools to program cell-cell interactions with advanced logic and control capabilities to enhance the efficacy of cancer immunotherapy.

Recently, chimeric antigen receptors (CARs) are utilized as a prominent genetic tool for cancer immunotherapy by redirecting the native T cell responses against B cell malignancies [110,122,172,173]. CARs are composed of the single-chain variable fragment (scFv) fused to T cell signaling domains. When scFv binds to a tumor antigen,

CAR T cells activate and eliminate B cell cancers. After demonstrating its efficacy as an effective cancer immunotherapy agent, CAR T therapy is now being applied to treat many other diseases such as autoimmune diseases by utilizing different types of immune cells [52,174]. Although very promising, most of the current CAR T cell therapy has been implemented in single subsets of immune cell type. As our immune system is composed of many different immune cell types that constantly interact with each other with varying *in vivo* phenotypes, genetic tools that endow inducible control of different immune cell types can have a profound impact in designing more effective therapy.

Current CAR design utilizes fixed sFv design that lacks specificity and flexibility in controlling T cell responses, thereby leading to CAR T toxicities [58,59,107]. To enhance the target specificity of CARs, combinatorial antigen sensing CAR designs that allow increased target specificity were introduced [62,63]. However, the main limitation of these combinatorial receptors is that these approaches still utilize fixed scFvs that require re-engineering of T cells to switch target specificities. Also, these receptors have been shown to incorporate two distinct tumor targets, but more stringent target specificity may be needed [175].

There have been several studies demonstrating the importance of host immune environment on tumor immunity [72,176]. For instance, compositions of innate dendritic cells and natural killer cells in tumor microenvironment have been demonstrated to improve the efficacy of cancer immunotherapy [177,178]. Furthermore, several immune cell populations have been demonstrated to increase cancer progressions and reduce immunotherapy responses. For instance, it is now well characterized that tumor-associated

macrophages (TAMs) have suppressive function and blocking TAM suppression improves the response of adoptive T cell therapy [179,180]. Also, the increase in a number of tumor-infiltrating neutrophils and monocyte has been associated with poor patient survival [181]. These results imply the importance of manipulating the host immune system to enhance the efficacy of immunotherapy.

Recently, we developed split, universal, and programmable (SUPRA) CAR that enables fine control of immune cell responses [64]. SUPRA CAR is composed of zipFv and zipCAR, where zipFv is composed of scFv fused to leucine zipper and zipCAR is composed of extracellular leucine zipper domain fused to intracellular T cell signaling domains. Thus, zipFv mediates binding between zipCAR and tumor antigens. With SUPRA CAR, we previously demonstrated regulating ON/OFF switch, fine-tuning of T cell activation, and controlling two orthogonal inputs in human primary T cells.

To generate synthetic cell-cell interactions with advance logical capabilities, we engineer seven innate and adaptive immune cells with SUPRA CAR and illustrate that we can successfully redirect the activity of different immune cells. Next, we build logic gates in different immune cell types and further expand the multi-input logic gate by integrating three inputs in a single cell using orthogonal SUPRA CARs. These logic gates perform as basic tools for constructing synthetic immune cell consortia and also improve the specificity of CAR T cell therapy. We also show regulatory T cell-mediated immune suppression and intercellular logic gate by engineering immune cell-cell interaction. Lastly, we also demonstrate endogenous immune cell polarization using SUPRA CARs. Thus, these wide-range SUPRA CAR applications imply its versatility as a platform for

engineering cell-cell interactions with advanced logical functions.

4.2 Results

4.2.1 SUPRA CARs Can Activate Diverse Adaptive and Innate Immune Cell Types

To expand cell types that SUPRA CARs can redirect, we first tested various T cell subtypes, NK cell, and macrophage. These cell types were transduced to express SUPRA CARs and co-cultured with or without α-Her2 zipFvs in the presence of the Her2-expressing NALM6 target cells. Consistent with our previous report [64], SUPRA CAR can efficiently induce target cell killing by CD8+ T cells (**Figure 4.6.1A**). As subtypes of CD4+ T cells are highly diverse, and cytokines released by each subtype regulate the direction of the immune responses [182], we wanted to illustrate a possibility of SUPRA CAR controlling different subsets of CD4+ T cells. Here, we differentiated naive CD4+ T cells to Th1 and Th2 cells. Then, we demonstrated that SUPRA CAR-containing *in vitro* differentiated Th1 and Th2 cells were activated by the corresponding zipFvs and secreted IFN- γ and IL-4 respectively (**Figures 4.6.1B, 1C, and 4.6.7A)**. Additionally, regulatory T (Treg) cells are a unique subtype of CD4+ T cells that show various antigen-dependent immunosuppressive phenotypes such as secretion of IL-10 and expression of CTLA-4 [183] and have been demonstrated to be effective to treat the autoimmune disorder [184]. A pan-T cell activation marker, CD69, was upregulated in SUPRA CAR-containing Treg cells when corresponding zipFv was added (**Figures 4.6.1D and 4.6.7B**). In order to increase Treg stability, the Foxp3 transcription factor was overexpressed with RR zipCAR

(**Figure 4.6.7C**). Another T cell subtype, gamma delta T cells (γδ T cells) express a unique T-cell receptor (TCR) composed of a γ-chain and a δ-chain. γδ T cells are low abundance in the body but are anticipated to be a remarkable cell type for solid tumor therapy because of their specific tissue homing ability [185]. Here, we demonstrated that SUPRA CAR γδ T cells were activated and secreted IFN-γ after the corresponding zipFv was added **(Figures 4.6.1E, 4.6.7D, and 4.6.7E)**. Natural killer (NK) cell is a type of lymphoid cells and is known to mediate anti-cancer effects without the risk of inducing graft-versus-host disease (GvHD) [186]. In addition to donor-derived primary NK cells, NK-92, the established NK cell line, is also being developed for adoptive immunotherapy as the safety of infusion of irradiated NK-92 cells has been demonstrated in phase I clinical trials [187–189]. We utilized IL-2-producing NK-92 line, NK-92MI, and demonstrated that SUPRA CAR can induce antigen-specific cytolysis of the NK cell (**Figure 4.6.1F**). Finally, the macrophage is a type of innate immune cells and performs phagocytosis of opsonized pathogens and apoptotic cells. Through antigen presentation and release cytokines, macrophage controls activation and differentiation of CD4+ helper T cells and immune responses. It has been reported that CD3ζ domain-containing conventional CAR induced macrophages to phagocyte antigen-expressing cells [190]. SUPRA CAR also re-directed macrophage phagocytosis in a zipFv-dependent manner (**Figure 4.6.1G**). Together, we can control diverse phenotypes of immune cells with the single integrated SUPRA CAR system.

4.2.2 SUPRA CARs Can Logically Respond to Combinatorial Antigen

Lack of target specificity is one of the main challenges in CAR-T cell therapy. As many of the antigens overexpressed on cancer cells are also expressed on normal cells [60,191,192], to enhance tumor specificity, combinatorial CAR systems have been previously reported [62,82]. However, this function largely depends on the affinity between scFv and a tumor antigen, and thus fixed scFv CAR designs are not ideal for controlling the combinatorial CARs. To overcome this deficiency, we previously developed tunable combinatorial AND logic using orthogonal SUPRA CARs [64]. However, it was simply a proof-of-concept illustration as combinatorial logic was only demonstrated in conventional CD4+ T cells. Here, to expand SUPRA AND-gate in more clinically relevant T cell types, we first engineered primary CD8+ T cell to express two orthogonal SUPRA CARs to regulate different signaling pathways (**Figures 4.6.2A and 4.6.8.A**). FOS zipCAR (binds to α-Her2-SYN9 zipFv) has an only CD3ζ domain, whereas RR zipCAR (binds to α-Axl-EE zipFv) has CD28 or 4-1BB co-stimulatory domains, which are being used in clinical CAR T cell therapy [193,194]. Both types of engineered T cells showed synergistic upregulation of target cell killing with the addition of two zipFvs, demonstrating their clinical utility (**Figures 4.6.2B and 4.6.2C)**. Compared to CD28, 4-1BB expressing CAR showed higher basal activity when the 4-1BB signaling domain was activated and CD28 expressing cells performed AND logic in the wide range of zipFv concentration than those of 4-1BB.

Regulatory T (Treg) cells are a unique subset of CD4+ T cells that are becoming promising therapeutic agents to treat many different diseases including autoimmune

disorders [184,195,196]. Even though multiple clinical trials are ongoing using polyclonal Treg cells, the use of polyclonal Treg cells with a variety of specificity can bring systemic immunosuppression [197]. For instance, there has been a clinical trial where the adoptive transfer of umbilical cord-derived polyclonal Treg cells increased viral reactivation [198]. In order to enhance the specificity of Treg cells, we engineered Treg cells to express SYN6 zipCAR (binds to α-Axl-SYN5) containing CD3ζ domain and SYN1 zipCAR (binds to α-Her2-SYN2) containing CD28 co-stimulatory domain. We measured CTLA-4 expression which is an activation marker and plays an important role in immunosuppression [199] and demonstrated that this CD3ζ /CD28 AND logic was functional in Treg cells (**Figures 4.6.2D and 4.6.8B**). Together, the combination of CD3ζ and CD28 signaling domains acts as a fine-tunable intracellular AND-gate in clinically relevant cell types.

4.2.3 BTLA-derived Co-inhibitory Signaling Domain Performs NOT Logic

We also developed NOT gate in CAR T cells (**Figure 4.6.3A**). Previous studies have demonstrated the use of inhibitory domains such as PD-1 and CTLA-4 in CAR design [82], but there are other various co-inhibitory domains that can be utilized to inhibit T cell responses [144]). Here, we utilized different co-inhibitory signaling domains (PD-1, LAG3, TIM3, BTLA, CTLA-4) and validated their functions in SUPRA CAR design (**Figure 4.6.9A**). Initially, CD4+ T cells and CD8+ T cells were transduced with dual SUPRA CARs: 1) FOS zipCAR with CD28 and CD3ζ signaling domains and 2) RR zipCAR with different inhibitory domains. For dual SUPRA CAR expressing CD4+ T

cells, activation of B and T lymphocyte associated (BTLA) strongly inhibited IFN-γ production in CD4+ T cells (**Figure 4.6.3B**). However, the effect of BTLA stimulation was not as high in CD8+ T cells compared to that of CD4+ T cells measured by IFN-γ level (**Figure 4.6.9C**). Also, BLTA activation did not inhibit killing efficiency, as previously reported [200] (**Figure 4.6.9D**). Next, we changed the immune cell type from T cells to NK cells in order to develop NOT logic that can inhibit target killing efficiency. We initially screened several activation domains (CD3ζ, CD28- CD3ζ, NKG2D, 2B4, DAP12, CD28, and ICOS) that can upregulate NK cell response and selected 4 domains (CD3ζ, CD28- CD3ζ, 2B4, and DAP12) that induced high killing efficiencies (**Figures 4.6.3C and 4.6.10A**). Then, we tested whether activation of BTLA in NK cell can suppress target cell cytolysis when also stimulated by activation domain (**Figure 4.6.10B**). Surprisingly, the simulation of BTLA significantly reduced the killing efficiency of CARs containing CD3ζ alone or 2B4 (**Figure 4.6.3D**). Next, we varied the α-Her2-SYN9 and α-Axl-EE zipFvs to detect ranges of zipFv concentration that endow NOT logic function in NK cells (**Figure 4.6.3E**). These results indicate that not only the choice co-inhibitory domain but also the selection of the activating domain and the immune cell type are important for developing NOT logic gates.

4.2.4 SUPRA CARs Can Organize Multi-logic Gate in Single Cell

In order to enhance logical programmability of engineered immune cells, we tested

if we can combine AND logic and NOT logic in the single cell. Based on previous screening in Jurkat T cells, we decided to use three orthogonal SUPRA CARs to handle 3 orthogonal inputs [64]. As expected, three orthogonal SUPRA CARS in primary human T cells showed minimum cross-reactivity (**Figure 4.6.11A**). We expressed three zipCARs in T cells by using two vectors where one vector contains P2A ribosomal skipping sequence to express both zipCARs and the other vector contains puromycin resistant gene to express third zipCAR (**Figure 4.6.11B**). We transduced T cells with these two virus vectors and selected with puromycin at 2ug/ml concentration. As expected, activation of CD28 and CD3ζ significantly increased IFN- γ production compared to activation of CD28 or CD3ζ alone. (**Figure 4.6.4A**). Also, activation of BTLA significantly reduced IFN-γ production . In order to demonstrate its generalizability in different cell types and to identify the range of zipFv concentration that confers logic capability, we also transduced CD4+ T cells with three zipCARs (**Figure 4.6.4B**). As expected, it shows synergistic IFN-γ upregulation (X-Y plane). Furthermore, BTLA inhibited IFN-γ production in zipFv does dependent manner (Z axis). These data demonstrate the first three input multi-logic gates in a single T cell that can be used to enhance target specificity.

4.2.5 Engineering Cell-Cell Communication with SUPRA CARs to Achieve Intercellular NOT Logic

Here, we engineered intercellular communication using different types of T cells to demonstrate diverse logic capability. Regulatory T (Treg) cells suppress inflammatory

immune responses in the antigen-dependent manner [183]. Based on this phenotype, several types of CAR-expressing Treg cells are being developed to treat various inflammatory disorders [161,162,201]. Thus, we utilized SUPRA CAR-equipped Treg cells to demonstrate engineering of a simple synthetic cell-cell communication in an inducible manner. We co-cultured FOS zipCAR expressing conventional CD4+ T (Tconv) cells with RR zipCAR-expressing Treg cells in the presence of target cells that express Her2 and Axl (**Figure 4.6.5A**). When we added α-Her2-SYN9 zipFv which activates FOS zipCAR expressed on Tconv cells, 40% of Tconv cells proliferated (**Figures 4.6.5B and 4.6.5C**). However, activating RR zipCAR expressing Treg cell activation by α-Axl-EE zipFv inhibited proliferation of Tconv cells to the same proliferation level as no zipFv conditions (**Figures 4.6.5B and 4.6.5C**). This demonstrates that we can now use orthogonal SUPRA CARs in different immune cell types to achieve intercellular NOT logic.

4.2.6 Controlling Endogenous Immune System with SUPRA CARs

Many of the CAR treated patients undergo symptom called cytokine release syndrome (CRS). Recently, it has been demonstrated that endogenous immune cells, especially macrophages, to be a key player in the development of CRS [202,203]. This illustrates that tools to engineer interaction between engineered immune cells and the endogenous immune system can be important to enhance the safety of current CAR-T cell therapy. Since SUPRA CARs can engineer Th1 and Th2 cells (**Figures 4.6.1B and 4.6.1C**), we

tried to demonstrate if we can control the endogenous immune system indirectly by manipulating SUPRA CAR-expressing Th1 and Th2 cells. Th1 cells rely on Th1 cytokines (e.g., IFN-γ) and Th2 cells rely on Th2 cytokines (e.g., IL-4) to regulate innate and adaptive cellular immunity. As a proof of concept to demonstrate engineering endogenous immune system, we utilized a monocyte/macrophage cell line THP-1 because macrophages polarize to pro-inflammatory M1 or anti-inflammatory M2 after receiving IFN-γ and IL-4, respectively (**Figure 4.6.12A**). We co-cultured four cell types including 1) antigens-expressing Nalm-6, 2) RR zipCAR expressing Th1 cells, 3) FOS zipCAR expressing Th2 cells, and 4) THP-1-derived macrophages *in vitro* (**Figure 4.6.6A**). RR zipCAR containing Th1 cells secreted IFN-γ and macrophage polarized to M1 state measured by M1 surface markers (e.g., HLA-DR and CCR7) when α-Axl-EE zipFv was added (**Figure 4.6.6B and 4.12B**). FOS expressing Th2 cells secreted IL-4 and macrophage polarized to M2 state measured by M2 surface marker (e.g., CD206) (**Figure 4.6.6B and 4.6.12B**). These data demonstrate that SUPRA CAR platform can be implemented in diverse cell types to engineer the endogenous immune system for different therapeutic purposes.

4.3 Discussion

4.3.1 SUPRA CAR can redirect the activity of both innate and adaptive immune cells

Many of current cellular immunotherapy is utilizing a single subset of immune cell

type, limiting the therapeutic potential of cell-based therapy. Even when the mixture of cells is used, we lack independent and inducible control over different cell types. Here, we demonstrate that SUPRA CAR can redirect immune responses of both innate and adaptive immune cell types, thereby showing that single SUPRA CAR system can harness different phenotypes from a variety of immune cell types, including cytolysis and phagocytosis of tumor cells, secretion of various cytokines, and suppression of other immune cells. By utilizing orthogonal SUPRA CARs, different immune cell types can now be independently regulated which can form the basis of constructing synthetic immune cell consortia.

4.3.2 Engineering Intercellular Communication with SUPRA CARs

Engineering intercellular communication with the novel genetic tool is intriguing and has potential use in clinical settings. As many clinical trials are ongoing using Treg cells to treat GVHD or tissue rejection during transplantation and autoimmune diseases [161,197,201]**,** here we demonstrate inducible and independent control of conventional T cells and regulatory T cells using orthogonal SUPRA CARs. This approach can be useful in managing symptoms during transplantation and autoimmune diseases. For instance, in an autoimmune disease setting, we can use convention T cells to target autoimmune B cells [174] or even autoreactive CD4+ T cells and use SUPRA CAR engineered Treg to protect the tissue/cell of our interest at the same time to enhance the efficacy of Treg implemented treatment.

We also demonstrate how we can use engineered cells to manipulate the

endogenous immune system. Recent studies have demonstrated the importance of endogenous immune system on the efficacy of immunotherapies [72,176,177]. Furthermore, many patients who received CAR T therapy undergo cytokine release symptom [57,58] and recently it has been demonstrated that macrophages play a crucial role in inducing CRS [202,203]. Thus, genetic tools that enable engineering host immune cells could accelerate the efficacy and safety of CAR T cell therapy. As a proof of concept, we engineered Th1 and Th2 cells to express orthogonal SUPRA CARs and induced these cells to direct polarization of macrophages, demonstrating that SUPRA CAR is an advanced genetic tool that can manipulate host immune system.

4.3.3 Orthogonal SUPRA CARs Enable Advanced Logical Function in Different Immune Cell Types

Here, we demonstrate that SUPRA CAR can perform complicated logic in different types of immune cells. First, we show AND logic in clinically relevant cell types: both CD8+ T cells and Treg cells to enhance target specificity. Unlike previously reported combinatorial CAR [62], SUPRA CAR allows inducible control of each SUPRA CAR to regulate signaling strength from each receptor. Furthermore, by implementing the BTLA co-inhibitory signaling domain, we implement NOT logic in both CD4+ and CD8+ T cells, and NK cells. We screened for different activation domains of NK cells and identified that BTLA can downregulate both CD3ζ and 2B4 activation domains. We also verified that activation of BTLA significantly decreases cytokine secretion, demonstrating its potential

utility in the clinic to prevent cytokine release syndrome. Also, to further advance logic capability, we implemented three-input logic gate in CD4+ and CD8+ T cells and demonstrate “a AND b NOT c” logic that can greatly enhance target specificity. Diverse SUPRA CAR features demonstrate the utility of this platform as a general approach to engineer immune cells with advanced logic capabilities and to engineer immune cell-cell interaction that can improve the efficacy of cell-based immunotherapy.

4.4 Conclusion

Chimeric antigen receptors (CARs) expressing T cells have demonstrated to be very effective anti-cancer therapy. However, current CAR T cell therapy only utilizes a single subset of immune cell type. In addition, we lack genetic tools to regulate different cell types in an inducible manner that could transform the efficacy of CAR T cell therapy. Furthermore, we still need to enhance target specificity of CAR T cell to enhance its safety. Here, we significantly expanded the previously reported SUPRA CAR platform. We first show that SUPRA CAR can redirect immune responses of both innate and adaptive immune cell types, thereby illustrating that single SUPRA CAR can be used to control different phenotypes of various immune cells. Using different cell types, we also engineered intercellular communication between two different immune cells and demonstrated regulatory T cell-mediated immune suppression. In addition, inducible control of different cell types can be used to manipulate the endogenous immune system using SUPRA CAR T cells, a capability that has not been achieved before. Lastly, we expanded SUPRA CARs with advanced logic and control features using a co-inhibitory

signaling domain which can be used to increase target specificity. Overall, diverse SUPRA CAR features illustrate the versatility of this platform as a general approach to engineer immune cell phenotypes to improve safety and efficacy of cellular immunotherapy.

4.5 Methods

4.5.1 zipCAR Receptor Construct Design

zipCARs were designed by fusing different leucine zippers (Reinke et al., 2010; Thompson et al., 2012) to the hinge region of the human CD8α chain and transmembrane and cytoplasmic regions of the signaling domains including co-stimulatory domains (CD28, 4-1BB, ICOS, OX40, CD27, GITR); co-inhibitory domains (PD-1, LAG3, TIM3, BTLA, CTLA-4); and NK activating domains (2B4, DAP12, and NKG2D). They were under SFFV promoter for all primary T cells and NK cells experiments. All zipCARs contain surface tags and fused to fluorescent proteins or puromycin resistant gene to verify their expression.

4.5.2 zipFv Construct Design

The general design of zipFv is as follows. scFv (α-HER2, α-Axl, α-CD19, α-MESO, and α-CD5) is linked by a 35-aa glycine/serine linker to a leucine zipper. Constructs were cloned into pSecTag2A vectors (Thermo Fisher) for transient expression. These vectors contain the CMV promoter, murine Ig-k-chain leader sequence, C-terminal c-myc epitope, and a 6X His tag for purification.

4.5.3 Expression and Purification of zipFv

For transient expression of the protein, Freestyle 293-F cells (Thermo Scientific #R79007) were transfected with pSecTag2A plasmid according to the supplier's protocol. After 4 days of culture, cells were pelleted by centrifugation at 300 × g for 5 minutes, and supernatant protein expression was confirmed by Coomassie gel stain (Thermo Scientific #24592) and western blot (abcam #ab62928). Proteins derived from transient transfection were purified as follows. The supernatant was passed through columns containing ProBond nickel chelating resin (Thermo Scientific #R80101). Then, each column was washed four times with native purification buffer (50 mM NaH2PO4 and 0.5 M NaCl pH 8.0) plus 20 mM imidazole (Sigma Aldrich # I5513) and eluted three times with native purification buffer plus 250mM imidazole concentrations. Eluted proteins were concentrated to ~2ml and dialyzed into 1× PBS (Thermo Scientific #AM9625). After dialysis, the protein was verified by western blot and SDS-PAGE gel electrophoresis and protein concentration was quantified by the Pierce BCA Protein Assay Kit (Thermo Scientific # 23227).

4.5.4 Primary Human T cells Isolation and Culture

Normal whole peripheral blood was obtained from Boston Children's hospital, as approved by the University Institutional Review Board (IRB) approved consent forms and protocols. Primary human CD4+ and CD8+ T cells were isolated from anonymous healthy donor blood by negative selection (STEMCELL Technologies #15062 and #15063). T cells were cultured in human T cell medium consisting of X-Vivo 15 (Lonza), 5% Human AB serum (Valley Biomedical #HP1022), 10 mM N-acetyl L-Cysteine (Sigma-Aldrich #A9165),

55uM 2-mercaptoethanol (Thermo Scientific #31350010) supplemented with 50 units/mL IL-2 (NCI BRB Preclinical Repository). T cells were cryopreserved in 90% heat-inactivated FBS and 10% DMSO.

Regulatory T cells (Tregs) were isolated from whole blood using immunomagnetic cell isolation kit (STEMCELL Technologies cat# 18063 or cat#17861) and were cultured initially in human T cell medium consisting of X-Vivo 15 (Lonza), 5% Human AB serum (Valley Biomedical #HP1022), 10 mM N-acetyl L-Cysteine (Sigma-Aldrich #A9165), 55 uM 2-mercaptoethanol (Thermo Scientific #31350010) supplemented with 200 units/mL IL-2 (NCI BRB Preclinical Repository). N-acetyl L-Cysteine and 2-mercaptoethanol were removed during the Treg suppression experiment. Gamma delta (γδ) T cells were isolated from whole blood using immunomagnetic negative selection cell isolation kit (STEMCELL Technologies cat# 19255) and were activated with Zoledronic acid 3 ug/ml (Sigma-Aldrich #1724827). After 5 days of activation, γδ T cells were transduced with lentivirus as shown below.

4.5.5 Lentiviral Transduction of Human T cells and NK cells

Replication-incomplete lentivirus was packaged via transfection of HEK293FT cells (Invitrogen) with a pHR transgene expression vector and the viral packaging plasmids: pMD2.G encoding for VSV-G pseudotyping coat protein (Addgene #12259), pDelta 8.74 (Addgene#22036), and pAdv (promega). One day after transfection, viral supernatant was harvested every day for 3 days and replenished with pre-warmed Ultraculture media (Lonza #12-725F) with 2mM L-glutamine, 100 U/ml penicillin, 100 ug/mL streptomycin,

1 mM sodium pyruvate, and 5 mM sodium butyrate. Then, the harvested virus was purified through ultracentrifugation or concentrated with Lentivirus concentrator (Takara #631232). One day before transduction, T cells were stimulated with Human T-activator CD3/CD28 Dynabeads (Thermo Scientific #11132D) at a 1:2 cell:bead ratio and cultured for 24 hr. After viral supernatant purification or concentration, rectronectin (Clontech #T100B) was used to transduce cells. Briefly, non-TC treated 6-well plates were coated with rectronectin following the supplier's protocol. Then, concentrated viral supernatant was added to each well and spun for 90 min at 1200xg. After centrifugation, viral supernatant was removed and 4 ml of previously activated human T cells or NK-92MI cells were added. Cells were spun at 1200g for 60 min and moved to an incubator at 37 ºC.

4.5.6 Primary human Th1 and Th2 cells differentiation

Normal whole peripheral blood was obtained from Boston Children's hospital, as approved by the University Institutional Review Board (IRB) approved consent forms and protocols. Primary human naïve CD4+ were isolated from anonymous healthy donor blood (STEMCELL Technologies #19555). After naïve CD4+ T cell isolation, Th1 and Th2 cells were differentiated using the supplier's protocol (R&D cat. #CDK001 and #CDK002). Briefly, naïve CD4+ T cells were activated with Dynabeads (Thermo Scientific #11132D) at a 1:2 cell:bead ratio and cultured for 24 hr with Th1/Th2 differentiation media. One day after T cell activation, primary human T cells were transduced with the methods mentioned above. During culture, T cells were cultured in T cell differentiation media (Th1 or Th2 depending on the experiment) for at least 14 days.

4.5.7 Cancer Cell Lines

The cancer cell lines used were K562 myelogenous leukemia cells (ATCC # CCL-243), Jurkat T cells, NALM-6 (ATCC #CRL-3273), THP-1, and NK92-MI (ATCC # CRL-2408). K562, Jurkat, NALM-6 and THP-1 cells were cultured in RPMI-1640 (Lonza#12-702Q) with 5% (v/v) heat-inactivated FBS, 2mM L-glutamine, 100 U/ml penicillin and 100 ug/mL streptomycin. NK92-MI cells were cultured in human T cell medium consisting of X-Vivo 10 (Lonza), 5% Human AB serum (Valley Biomedical #HP1022), 2 mM L-glutamine, 100 U/ml penicillin and 100 ug/mL streptomycin. Jurkat, K562, and NALM-6 cells were electroporated with the PiggyBac Transposon system (System biosciences) to stably express surface antigens. Two days after transfection or transduction, antibiotic (Puromycin (Thermo Scientific #A1113803), zeocin (Thermo Scientific # R25005), or Hygromycin B (Thermo Fisher #10687010)) was added to the medium or FACS sorted to select for cells that express the transgenes. THP-1 cells were transduced using lentivirus to stably express zipCAR.

4.5.8 Cytokine Release Assays

Primary T cells expressing zipCAR were incubated with target cells (10 x 104 cells/well) at an E:T ratio of 2:1 or 1:1 with corresponding zipFvs. After 24 hr, the supernatant was harvested and followed the supplier's protocol to determine cytokine release level. In order to determine in vivo cytokine release level, murine blood was drawn submandibular after 24 hr of the initial injection of engineered immune cells and zipFv. Blood plasma was harvested by centrifuging collected blood for 10 minutes at 3000 x g. In vivo IFN-γ release

was measured by Luminex Magpix at BUMC (Boston University Medical Campus) core facility.

4.5.9 Cytotoxicity Assays

Cytotoxicity assays were carried out using bioluminescence as previously described (Fu et al., 2010) or using Flow cytometry (FACS). Briefly, for bioluminescence assay, CAR-T cells were incubated with zipFv and target cells that were engineered to express luciferase for 4hr at 37 ºC. Culture medium was removed to leave 50ul per well, then 50ul of prepared luciferase reagent (Promega #E2610) was added to each well of the 96-well plate (Corning #3904). Measurements were performed with the SpectraMax M5 (Molecular Devices). Target cell cytotoxicity was calculated using the following formula: Cytotoxicity = 100 x [(Total Target cell luminescence – luminescence of remaining cells after lysis) / (Total Target cell luminescence)]. For cytotoxic assay using flow cytometry, CAR-T cells or CAR-NK cells were incubated with zipFv and target cells for 24hr at 37 ºC. Prior to flow cytometry, control samples containing only the target cells were used to set a flow cytometry gate for intact target cells based on forward and side scatter patterns that had been previously confirmed to exclude apoptotic cells. Also, fluorescence markers were used to further identify the target cells. This gate was applied to all other samples. Live target cell number was calculated and target cell cytotoxicity was calculated using the following formula: Cytotoxicity = 100 x [(Total live target cell number – the number of remaining live cells after lysis) / (Total live target cell number)].

4.5.10 Treg suppression assay

Effector T cells were stained with CellTrace dye (Thermo Fisher Scientific cat# C34557) following the manufacturer's instructions. NALM-6 target cells expressing HER2 ligand were treated with 3ug/mL mitomycin C (Sigma-Aldrich cat#M4287) to make target cells replication-incompetent. Treg cells and Teff cells were mixed at 1:1 or 2:1 ratio with target cells. zipFvs were also added to final concentrations. Cells were collected for flow cytometry analysis after incubation for 4 days.

4.5.11 Phagocytosis Assays

Two days before phagocytosis assays, zipCAR containing human THP-1 cells were activated with Phorbol 12-Myristate 13-Acetate (PMA; Fisher Scientific) with 25 ng/ml and seeded into TC-treated 96 well plate (15 x 104 cells/well). One day after activation, media in every 96 wells was replaced with new media without PMA and incubated at 37 ºC. After 24 hr, NALM-6 target cells were stained with CellTrace dye (Thermo Fisher Scientific cat# C34557) following manufacturer's instructions and added into each well (15 x 104 cells/well) with the corresponding zipFv. Cells were spun down by centrifugation at 400 × g for 1 minute. X minute after co-culture, cells were treated with 5 mM EDTA (Fisher Scientific) in PBS for 15 minutes at 4 ºC and stained with CD44 antibody (Biolegend #338806) to label THP-1 macrophages and cells were collected for flow cytometry analysis. Prior to flow cytometry, control samples containing only the target cells were used to set a flow cytometry gate for intact target cells based on forward and side scatter patterns that had been previously confirmed to exclude apoptotic cells.

Also, fluorescence markers were used to further identify the target cells. Number of phagocytosed cells were calculated by dual positive cells (APC+ [anti-human CD44] and violet+ [CellTrace]). This gate was applied to all other samples. Target cell phagocytosis was calculated using the following formula: % phagocytosis = 100 x [(Number of THP-1 macrophage that are dual positive after co-culture) / (Total live THP-1 macrophage cell number)].

4.5.12 M1 and M2 Polarization Assay

In TC-treated 96 well plate, THP-1 cells were treated with 25 ng/mL PMA for 6 hr to differentiate macrophages and then cultured for 2 days in new media without PMA. Antigens-expressing Nalm-6 (1 x105 cells/well), RR-CAR-expressing Th1 cells (1 x104 cells/well), and FOS-CAR-expressing Th2 cells (2.5 x104 cells/well) were added to THP-1 with or without corresponding 4 nM zipFvs. THP-1 cells were detached with 5 mM EDTA in PBS 24 hr after starting co-culture. THP-1 cells were stained with antibodies against M1 and M1 markers and analyzed by flow cytometry (Attune NxT; Thermo Fisher Scientific).

4.5.13 Quantification and Statistical Analysis

Statistical significance was determined by student's T-test (two-tailed) unless otherwise noted. All curve fitting was performed with Prism 7 GraphPad) and *p* values are reported (not significant = $p > 0.05$, * = $p \leq 0.05$, ** = $p \leq 0.01$, *** ≤ 0.001). All error bars represent either SEM or SD.

4.6 Figures

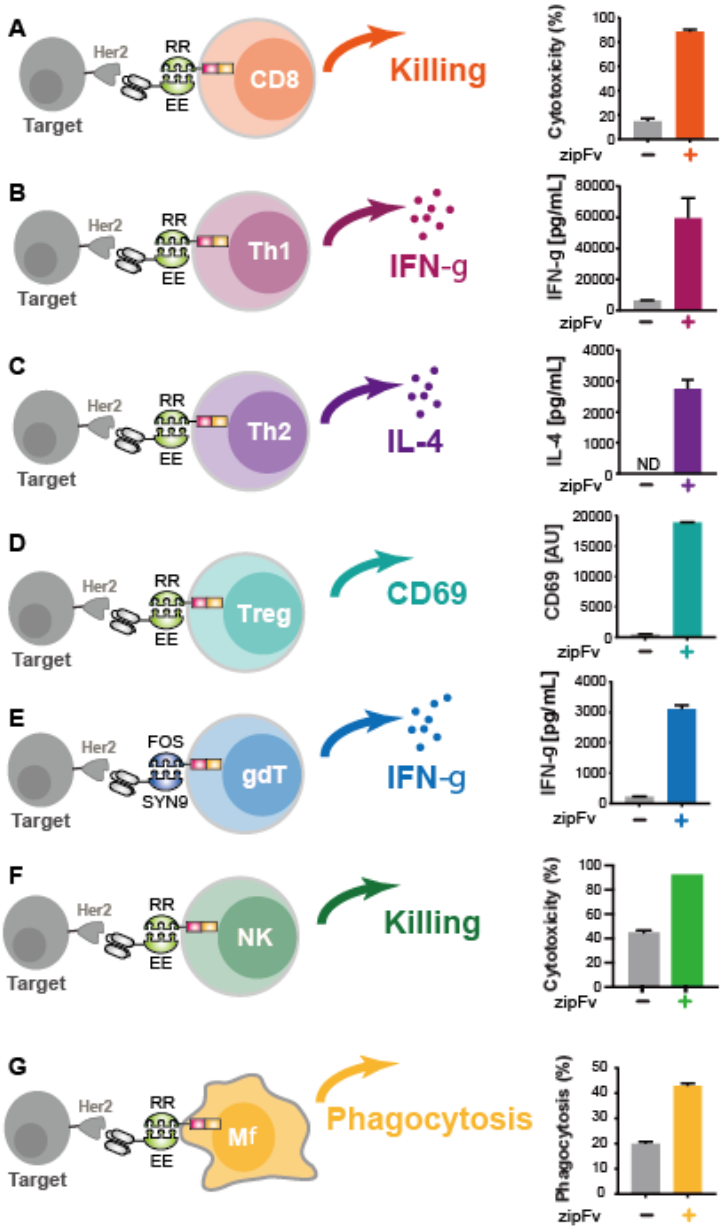

Figure 4.6.1. The Intracellular AND Logic with different signaling domains.

(A) Cytotoxicity by RR zipCAR expressing CD8+ T cells. NALM6 cells expressing Her2 were co-cultured in vitro with RR zipCAR expressing CD8+ human primary T cells with and without α-Her2-EE zipFv (n=3, data are represented as mean ± SD).

(B) IFN- γ cytokine level from RR zipCAR expressing in vitro differentiated Th1 cells. NALM6 cells expressing Her2 were co-cultured with RR zipCAR expressing Th1 cells with and without α-Her2-EE zipFv (n=3, data are represented as mean ± SD).

(C) IL-4 cytokine level from RR zipCAR expressing in vitro differentiated Th2 cells. NALM6 cells expressing Her2 were co-cultured with RR zipCAR expressing Th2 cells with and without α-Her2-EE zipFv (n=3, data are represented as mean ± SD).

(D) CD69 expression level from RR zipCAR-FoxP3 expressing isolated Treg cells (CD4+CD25hiCD127low). NALM6 cells expressing Her2 were co-cultured with RR zipCAR expressing Treg cells with and without α-Her2-EE zipFv (n=3, data are represented as mean ± SD).

(E) IFN- γ cytokine level from FOS zipCAR expressing isolated γδ T cells. NALM6 cells expressing Her2 were co-cultured with FOS zipCAR expressing γδ T cells with and without α-Her2-SYN9 zipFv (n=3, data are represented as mean ± SD).

(F) Cytotoxicity by RR zipCAR expressing NK-92MI cells. NALM6 cells expressing Her2 were co-cultured in vitro with RR zipCAR expressing NK cells with and without α-Her2-EE zipFv (n=3, data are represented as mean ± SD).

(G) Phagocytosis by RR zipCAR expressing THP-1 macrophages. NALM6 cells expressing Her2 were co-cultured in vitro with RR zipCAR expressing THP-1 macrophages with and without α-Her2-EE zipFv (n=3, data are represented as mean ± SD).

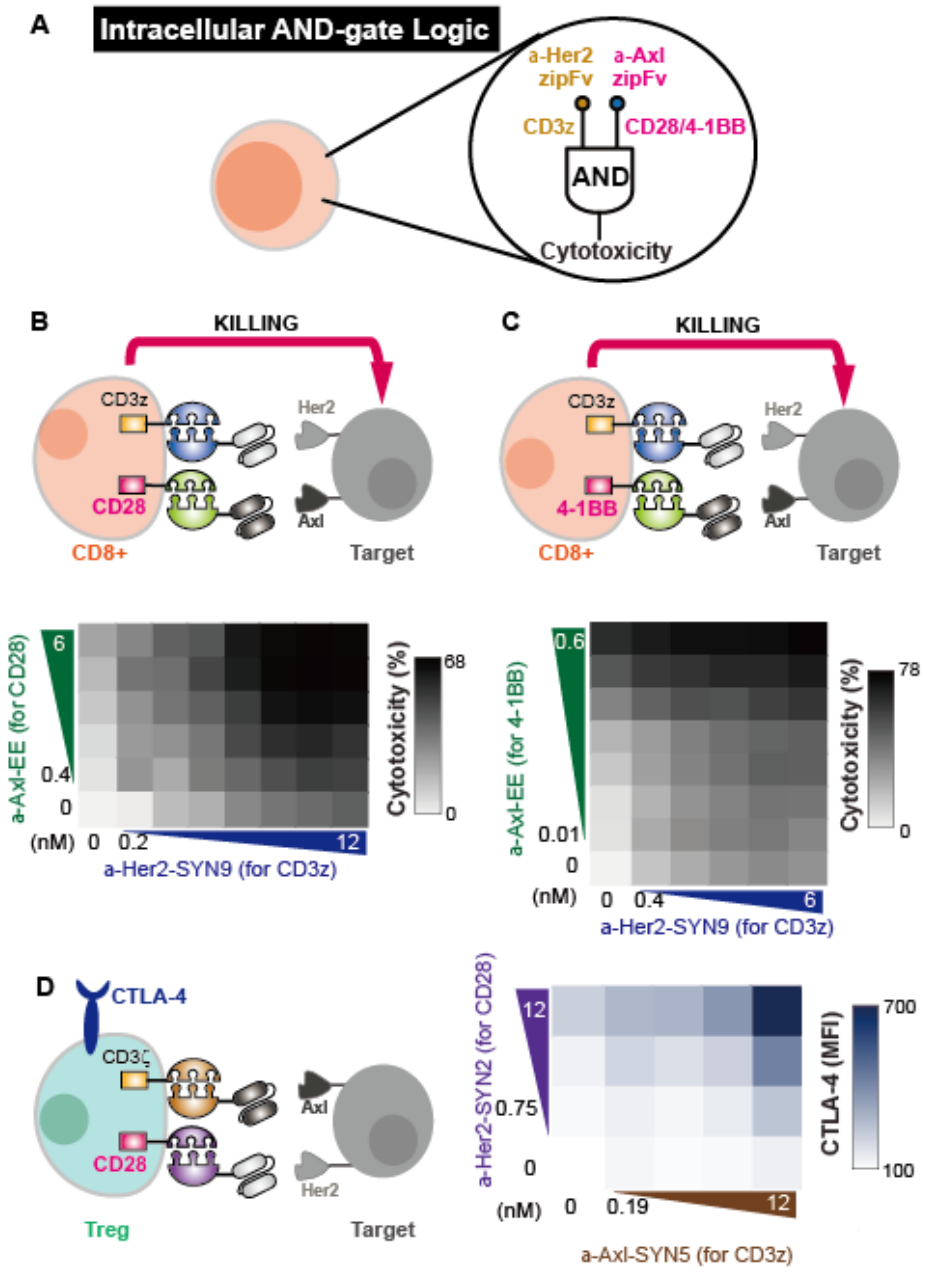

Figure 4.6.2. The Intracellular AND Logic with different signaling domains.

(A) Diagram of intracellular AND logic

(B) Primary human CD8+ T cells were transduced with FOS zipCAR containing CD3ζ domain and RR zipCAR containing CD28 domain. Cytotoxicity against Her2- and Axl-

expressing Nalm6 was measured 24 hours after adding anti-Her2-SYN9 and/or anti-Axl-EE zipFvs. The heat map indicates cytotoxicity at varying zipFv concentrations (n=3, data are represented as mean).

(C) Cytotoxicity of CD8+ T cells transduced with FOS zipCAR containing CD3ζ domain and RR zipCAR containing the 4-1BB domain. The heat map indicates cytotoxicity at varying zipFv concentrations (n=3, data are represented as mean).

(D) (Left) Isolated Treg cells were transduced with two zipCAR constructs: SYN6- CD3ζ -P2A-FOXP3 and SYN1-CD28-P2A-puro. After puromycin selection (2ug/ml), Treg cells were co-cultured with Her2- and Axl-expressing Nalm6 target cells (Right) The heat map shows surface CTLA-4 expression detected after 48 hours by flow cytometry at varying zipFv concentrations (α-Axl-SYN5 and α-Her2-SYN2) (n=3, data are represented as mean).

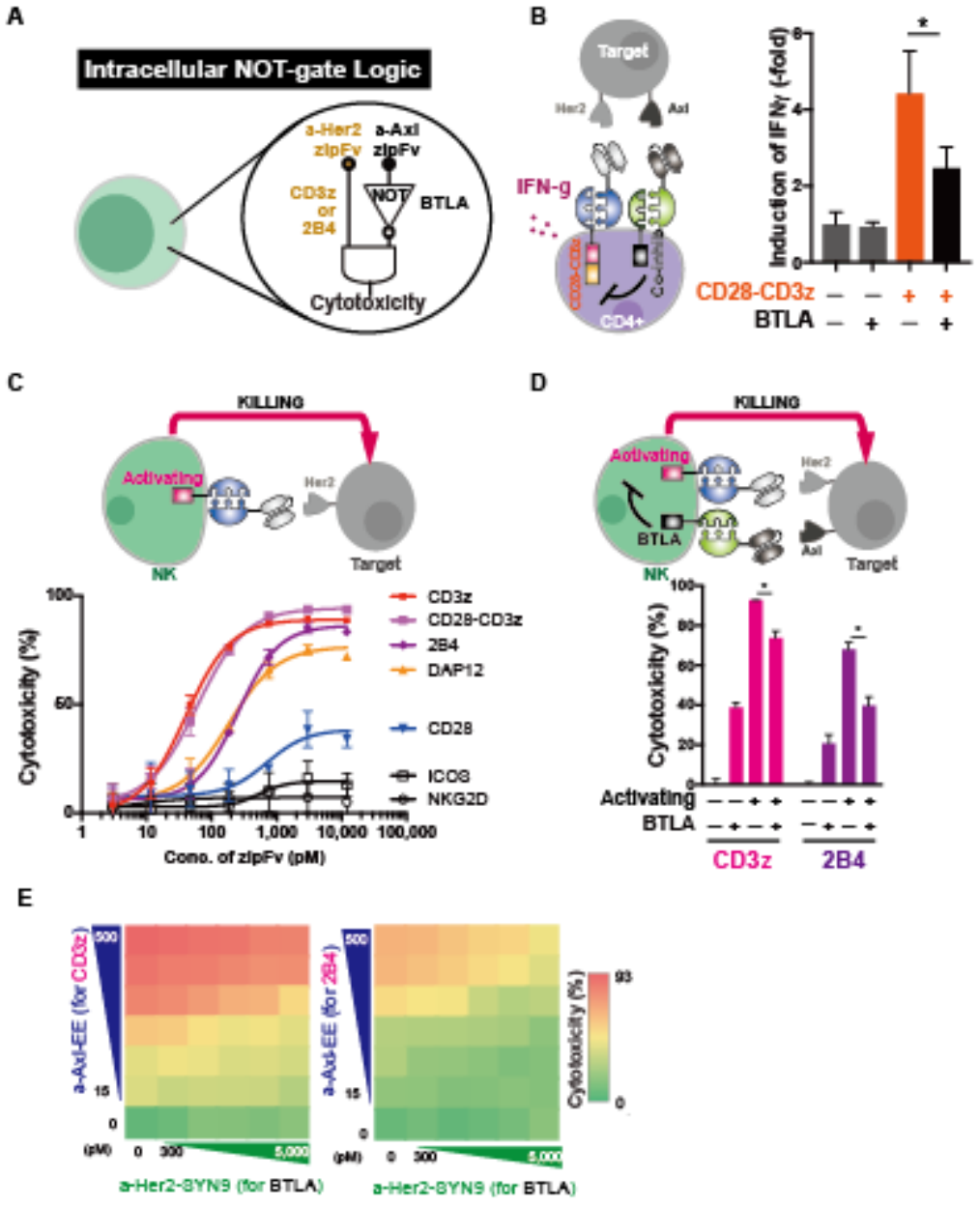

Figure 4.6.3. The Intracellular NOT Logic with BTLA in different cell types.

(A) Diagram of intracellular NOT logic using co-inhibitory signaling domains.

(B) IFN- γ production from CD4+ T cells transduced with FOS- CD3ζ and RR zipCAR with BTLA co-inhibitory domain. Supernatants were collected 24 hours after adding

1.2nM α-Her2-SYN9 zipFv and 12nM α-Axl-EE zipFv (n=3, data are represented as the mean ± SD).

(C) Effect of concentration of α-Her2-SYN9 zipFv on cytotoxicity performed by FOS zipCAR expressing NK-92MI cells with various activating domains (n=3, data are represented as the mean ± SD).

(D) Suppression of cytotoxicity by BTLA. NK-92MI cells expressing FOS zipCAR with two different activating domains (CD3ζ and 2B4) and RR zipCAR with BTLA co-inhibitory domain were co-cultured with Her2 and Axl expressing Nalm6 target cells in the presence or absence of α-Axl-SYN9 and α-Her2-EE. Living target cells were measured by flow cytometry 24 hours after starting co-culture (n=3, data are represented as the mean ± SD).

(E) Effect of concentration of α-Her2-SYN9 and α-Axl-EE zipFvs on cytotoxicity performed by NK-92MI cells. (Left) SUPRA CAR-engineered NK cells express RR zipCAR with BTLA co-inhibitory domain and FOS zipCAR with CD3ζ domain (Right) with 2B4 activation domain (n=3, data are represented as the mean).

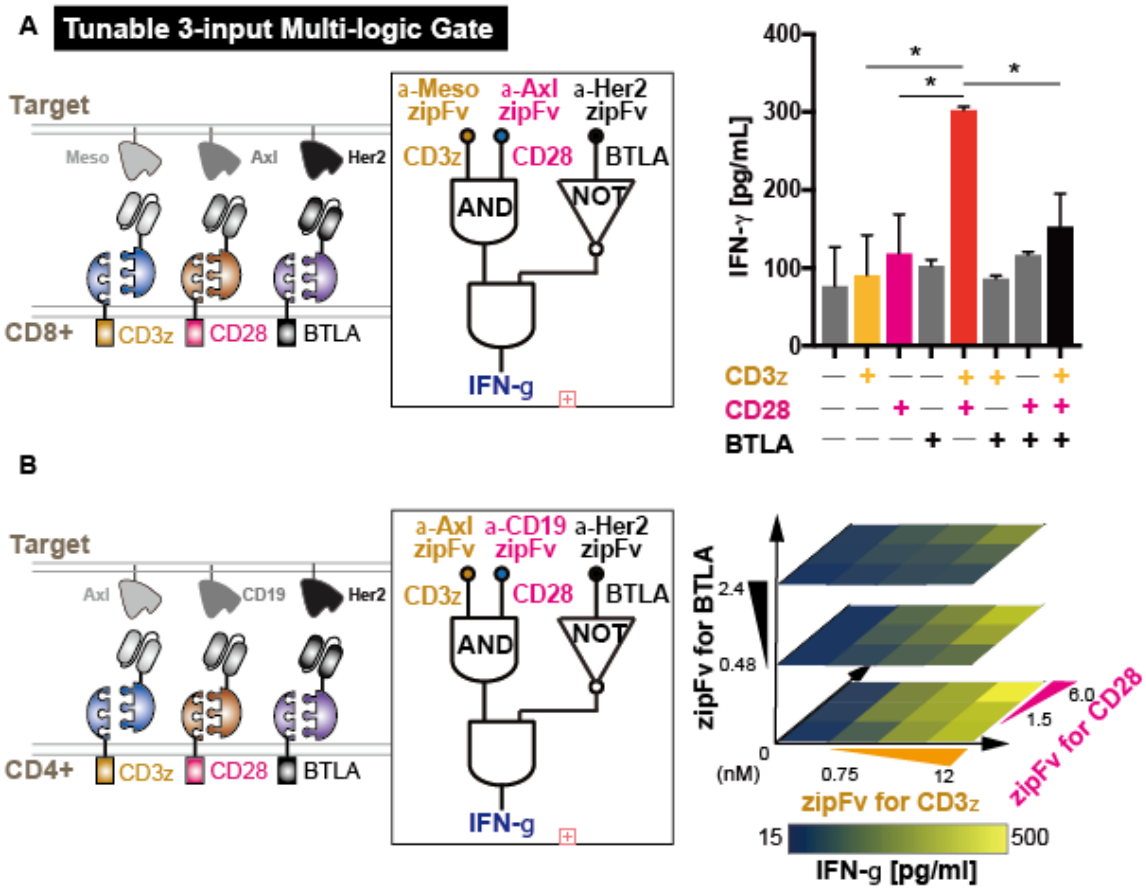

Figure 4.6.4. Tunable 3-input multi-logic in a single cell.

(A) Design of orthogonal SUPRA CARs that control CD3ζ, CD28, and BTLA signaling domains inducibly and independently. Primary CD8+ T cells were engineered to express FOS zipCAR, SYN6 zipCAR and SYN1 zipCAR that contain CD3ζ domain, CD28, and BTLA signaling domain, respectively. In addition, α-Meso-SYN9 zipFv, α-Axl-SYN5 zipFv, and α-SYN2-Her2 zipFv lead to activation of CD3ζ, CD28, and BTLA, respectively. IFN- γ secretion was measured after co-culturing with Her2, Axl, and Meso expressing Nalm6 target cells with different zipFv combinations (n=3, data are represented as the mean ± SD, the statistical significance was determined by Student's t-test, * = p

≤0.05).

(B) Primary CD4+ T cells expressing FOS- CD3ζ, SYN6-CD28, and SYN1-BTLA were co-cultured with Her2, Axl, and CD19 expressing Nalm6 target cells. The 3D heat map shows IFN-γ production from 3-input CD4+ T cells at varying concentrations of three different corresponding zipFvs (n=3, data are represented as the mean).

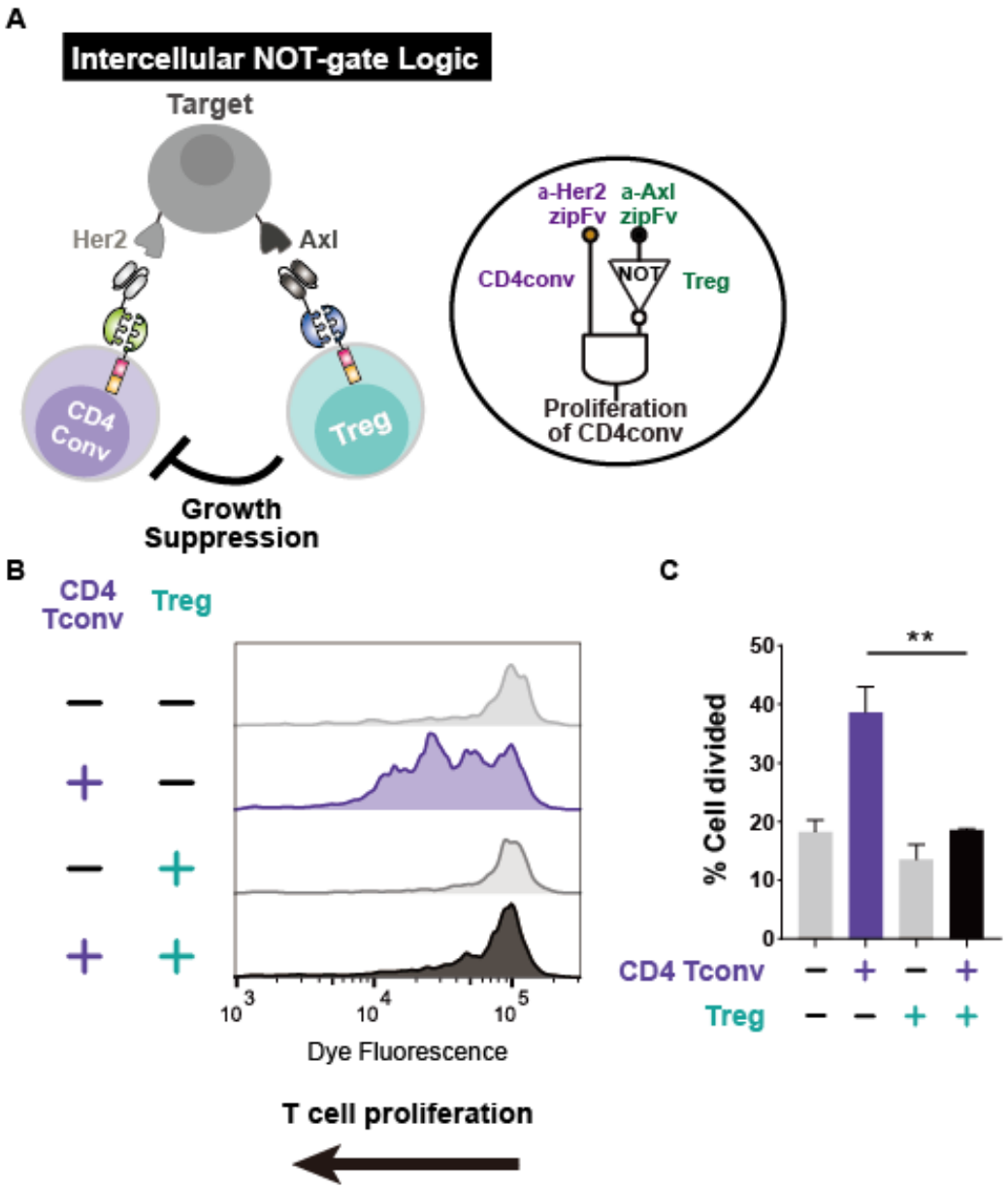

Figure 4.6.5. The Intercellular NOT-gate with Regulatory T (Treg) Cells.

(A) Diagram of intercellular NOT gate with Treg cells. The RR zipCAR and FOS zipCAR control the activity of Treg and conventional CD4+ T cells (Tconv), respectively. α-Axl-EE zipFv binds to RR zipCAR and activates Treg cells. α-Her2-SYN9 zipFv binds to the FOS zipCAR and activates CD4+ Tconv cells. Activation of Treg cells leads to suppression

of CD4+ Tconv cells.

(B) Suppression of growth of CD4+ Tconv cell by SUPRA CAR equipped Treg cells. CD4+ Tconv cells expressing FOS zipCAR were pre-labeled with the intracellular CellTrace Violet dye. When activated by CAR signaling, the fluorescence intensity of labeled cells will decrease with cellular growth. Cells were analyzed by flow cytometer after 4 days of the co-culture period. The shift of peaks to leftward indicates T cell proliferation. Each plot shows dye fluorescence of CD4+ Tconv cells with different zipFv combinations (representative of three biological replicates).

(C) Quantified proliferation measurement of FACS plot shown in Figure 5B (n=3, data are represented as the mean ± SD, the statistical significance was determined by Student's t-test, **= $p \leq 0.01$).

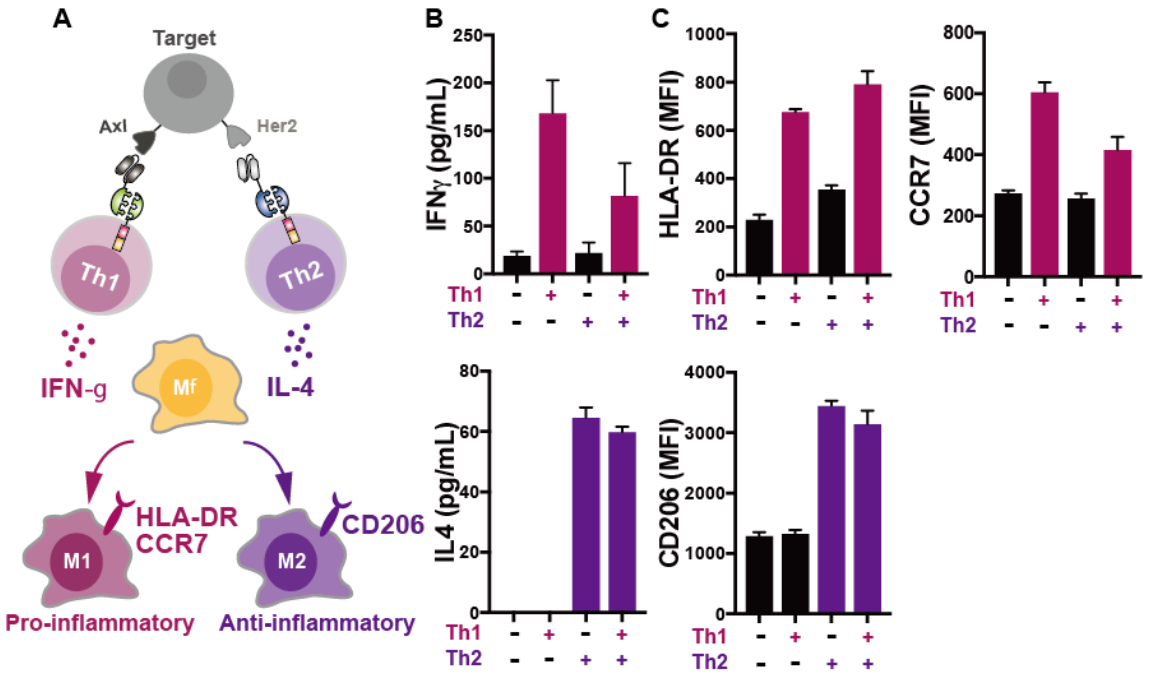

Figure 4.6.6. Engineering Endogenous Immune System with SUPRA CAR expressing different T cell subtypes.

(A) Schematic of controlling macrophage polarization by zipCAR expressing Th1 and Th2 cells. The RR zipCAR and FOS zipCAR control the activity of Th1 and Th2 cells, respectively. α-Axl-EE zipFv binds to RR zipCAR and activates Th1 cells. α-Her2-SYN9 zipFv binds to the FOS zipCAR and activates Th2 cells. Activation of Th1 and Th2 CD4+ T cells leads to secretion of IFN- γ and IL4, respectively. Macrophage polarizes to M1 (pro-inflammatory) when exposed to IFN- γ secreted by Th1 cell and it polarizes to M2 (anti-inflammatory) when exposed to IL-4 secreted by Th2 cells.

(B) IFN- γ (Top) and IL-4 (Bottom) production from RR zipCAR expressing Th1 cells and FOS zipCAR expressing Th2 cells with or without 5 nM anti-Her2-SYN9 zipFv and 5 nM anti-Axl-EE zipFv (n=3, data are represented as the mean ± SD).

(C) (Top) HLA-DR and CCR7 expression levels in THP-1 macrophages were measured by flow cytometer 24 hr after staring co-culture (Bottom) CD206 in THP-1 macrophages was also analyzed at the same time as detecting M2 marker (n=3, data are represented as the mean ± SD).

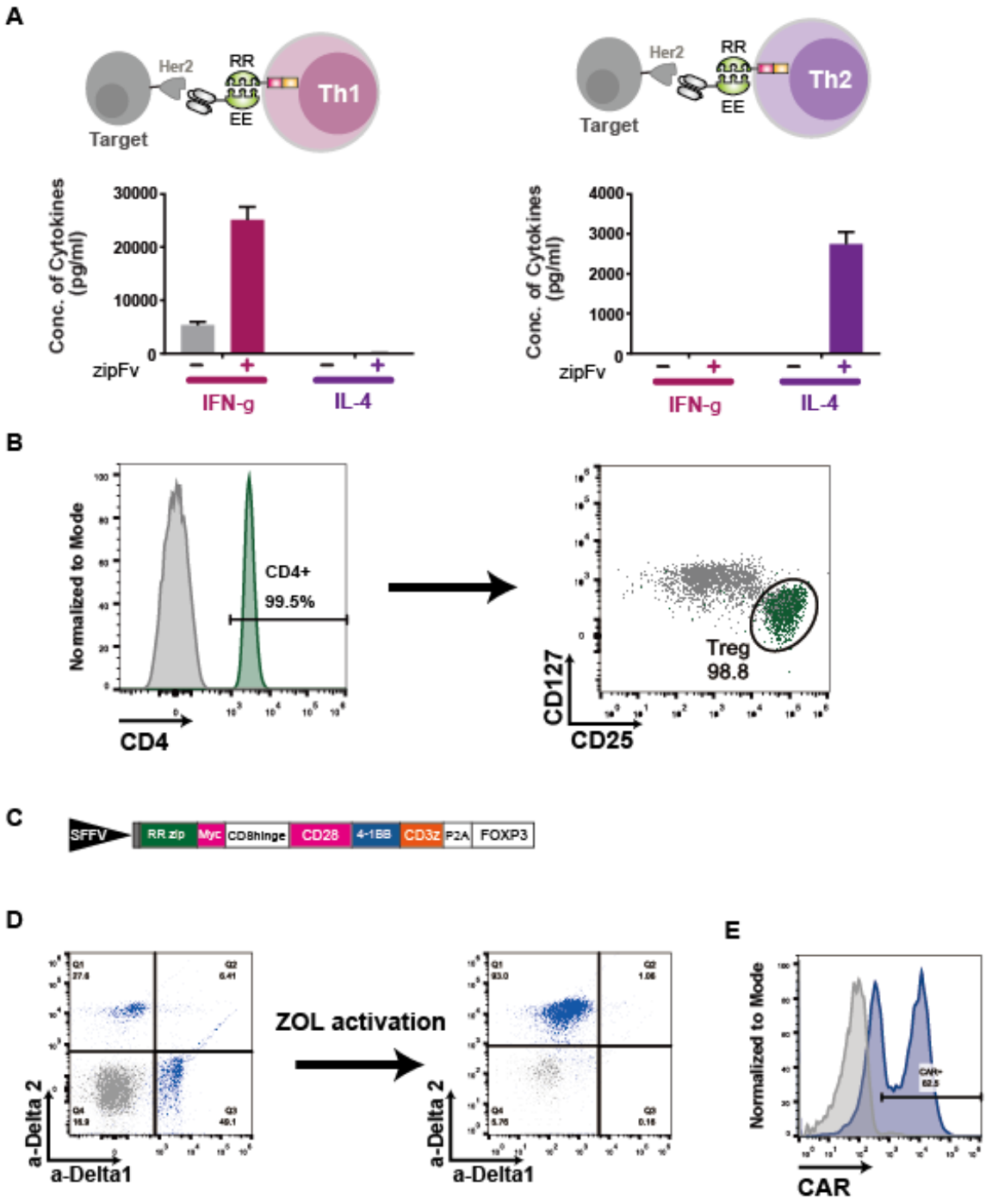

Figure 4.6.7. Different immune cell types expressing SUPRA CAR.

(A) (Left) IFN-γ and IL-4 cytokine secretion from RR zipCAR expressing *in vitro*

differentiated Th1 cells (Right) IFN-γ and IL-4 cytokine level from RR zipCAR expressing *in vitro* differentiated Th2 cells. NALM6 cells expressing Her2 were co-cultured with RR zipCAR expressing Th1 and Th2 cells with and without α-Her2-EE zipFv (n=3, data are represented as mean ± SD).

(B) Verification of the isolated CD4+CD25+highCD127low Treg. Once Treg has been isolated using "EasySep™ Human CD4+CD127lowCD25+ Regulatory T Cell Isolation Kit" (STEMCELL cat#18063), Treg surface markers (CD4, CD127, and CD25) have been verified using flow cytometry (Isolated Treg population is colored in green) (representative of three biological replicates).

(C) Schematic of zipCAR construct used for Treg experiments. FOXP3 transcription factor was coexpressed with zipCAR using P2A ribosomal skipping sequence to enhance Treg stability.

(D) Verification of γδ T cell surface marker after ZOL activation. Once γδ T cells were isolated using EasySep™ Human Gamma/Delta T Cell Isolation Kit (STEMCELL Car#19255), isolated cells were activated using zoledronic acid. γδ T specific surface markers (both Vδ1 and Vδ2) were used to verify the expression of delta TCR from isolated γδ T cells.

(E) After isolation and expansion, CAR expression was verified by expression of mCherry that was fused to zipCAR.

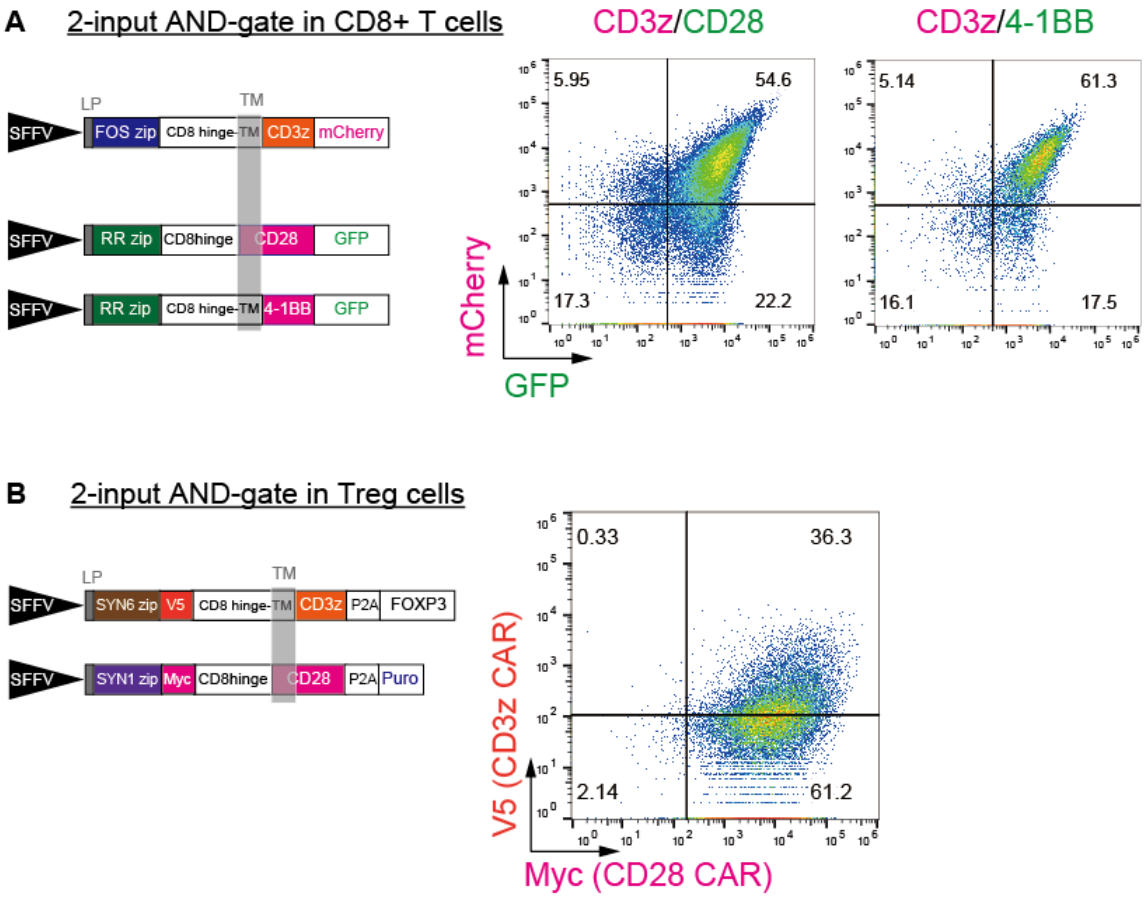

Figure 4.6.8 Schematics of SUPRA CARs used for 2-input AND gates.

(A) (Left) Schematics of 2 input AND gate constructs. Fos zipCAR is used to control the CD3ζ domain and RR zipCAR is used to control CD28 or 4-1BB co-stimulatory domains. Both zipCARs are fused to GFP or mCherry for visualization (Right) FACS diagram that shows the expression of two different receptors in a single cell (representative of three biological replicates).

(B) (Left) Schematics of 2 input AND gate construct designs. SYN5 zipCAR is used to control the CD3ζ domain and SYN1 zipCAR is used to control the CD28 co-stimulatory

domain. FOXP3 transcription factor and puromycin resistance gene are co-expressed with zipCARs using P2A ribosomal skipping sequence. After transduction of primary T cells, cells were treated with 2ug/ml puromycin to select for positive cells (Right) FACS diagram that shows the expression of two different receptors in a single cell (representative of three biological replicates).

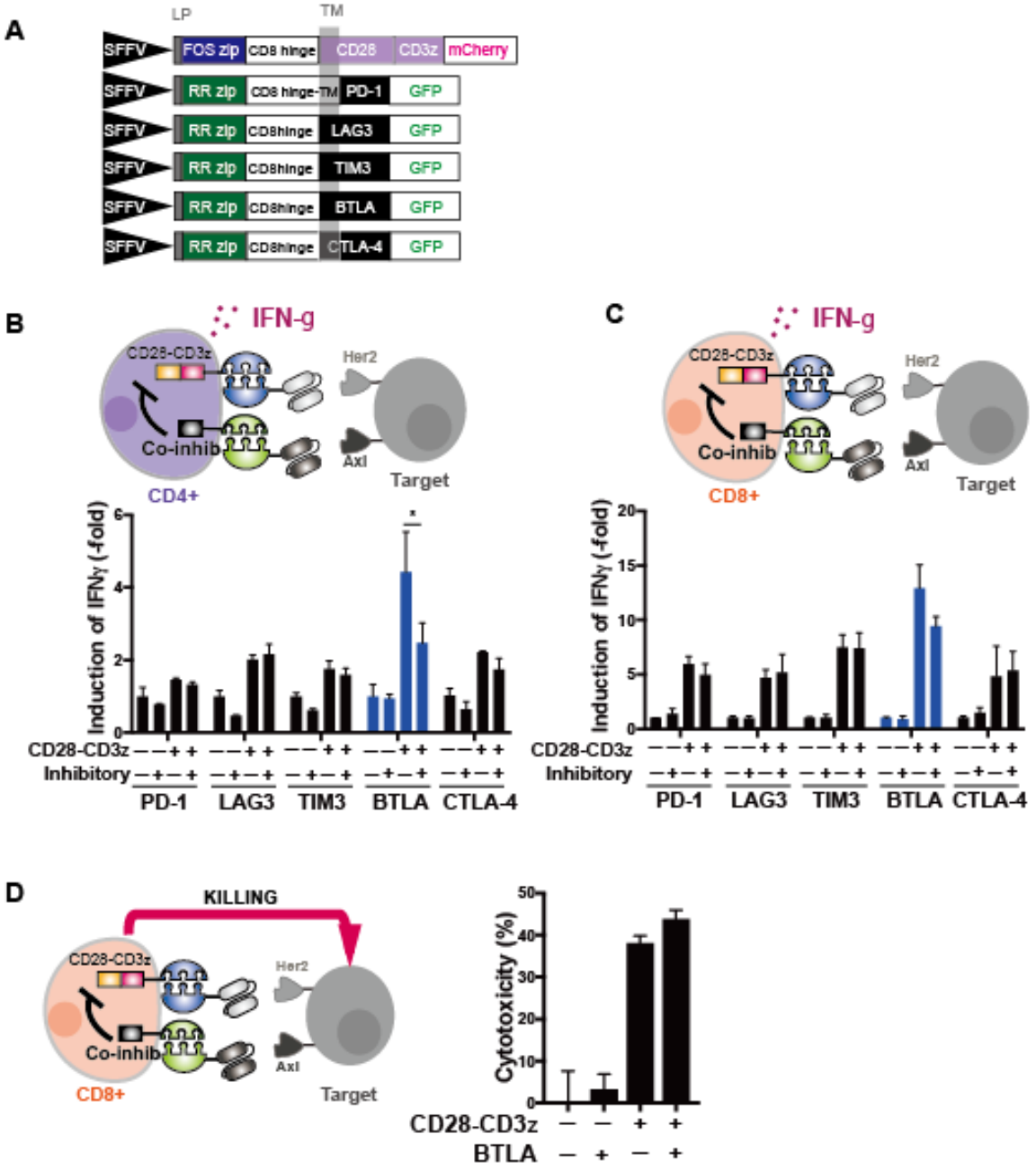

Figure 4.6.9. Co-Inhibitory domain screening in T cells.

(A) Schematics of co-inhibitory domain constructs. FOS zipCAR controls CD28- CD3ζ domain and RR zipCAR regulates different co-inhibitory domains including PD-1, LAG3,

TIM3, BTLA, and CTLA-4.

(B, C) Diagram of co-inhibitory screening in CD4+ T cells (B) and CD8+ T cells (C). CD4+ and CD8+ T cells are engineered to express FOS-CD28- CD3ζ zipCAR (binds to α-Her2-SYN9 zipFv) and RR zipCAR (binds to α-Axl-EE zipFv) with different co-inhibitory domains. IFN-γ cytokine level is measured after addition of different combinations of zipFvs (n=3, data are represented as mean ± SD).

(D) BTLA equipped SUPRA CD8+ T cell do not prevent the killing of target cells (n=3, data are represented as mean ± SD).

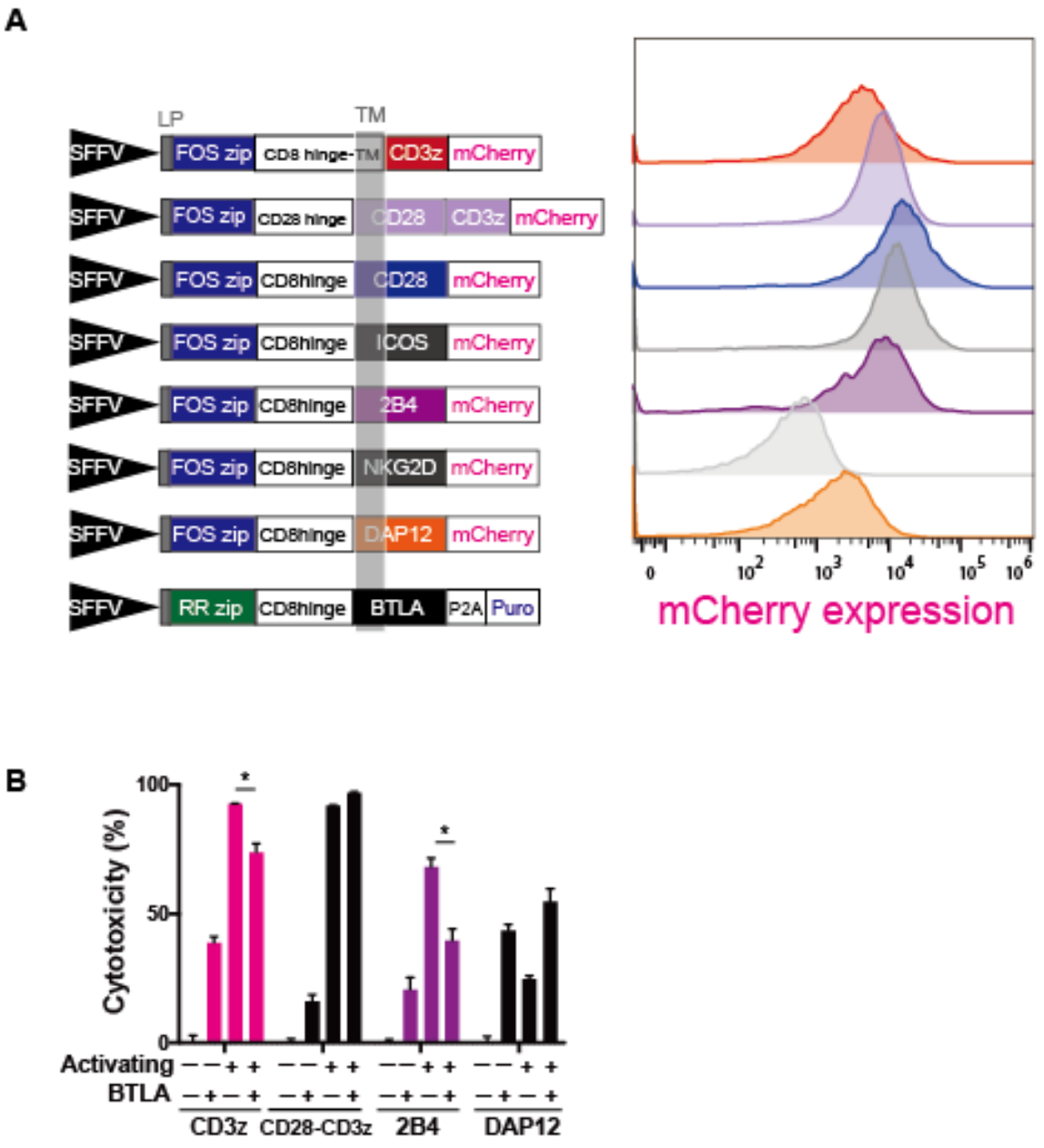

Figure 4.6.10. Co-stimulatory and Co-Inhibitory domain screening in NK cells.

(A) (Left) Schematics of activating domains and co-inhibitory domain constructs used in NK cells. FOS zipCAR controls different activating domains including CD3ζ, CD28-CD3ζ, CD28, ICOS, 2B4, NKG2D, and DAP12. RR zipCAR regulates BTLA co-

inhibitory domain (Right) zipCAR expression level measured by flow cytometry (representative of three biological replicates).

(B) Effect of BTLA activation on different activating domains in NK cells (n=3, data are represented as mean ± SD).

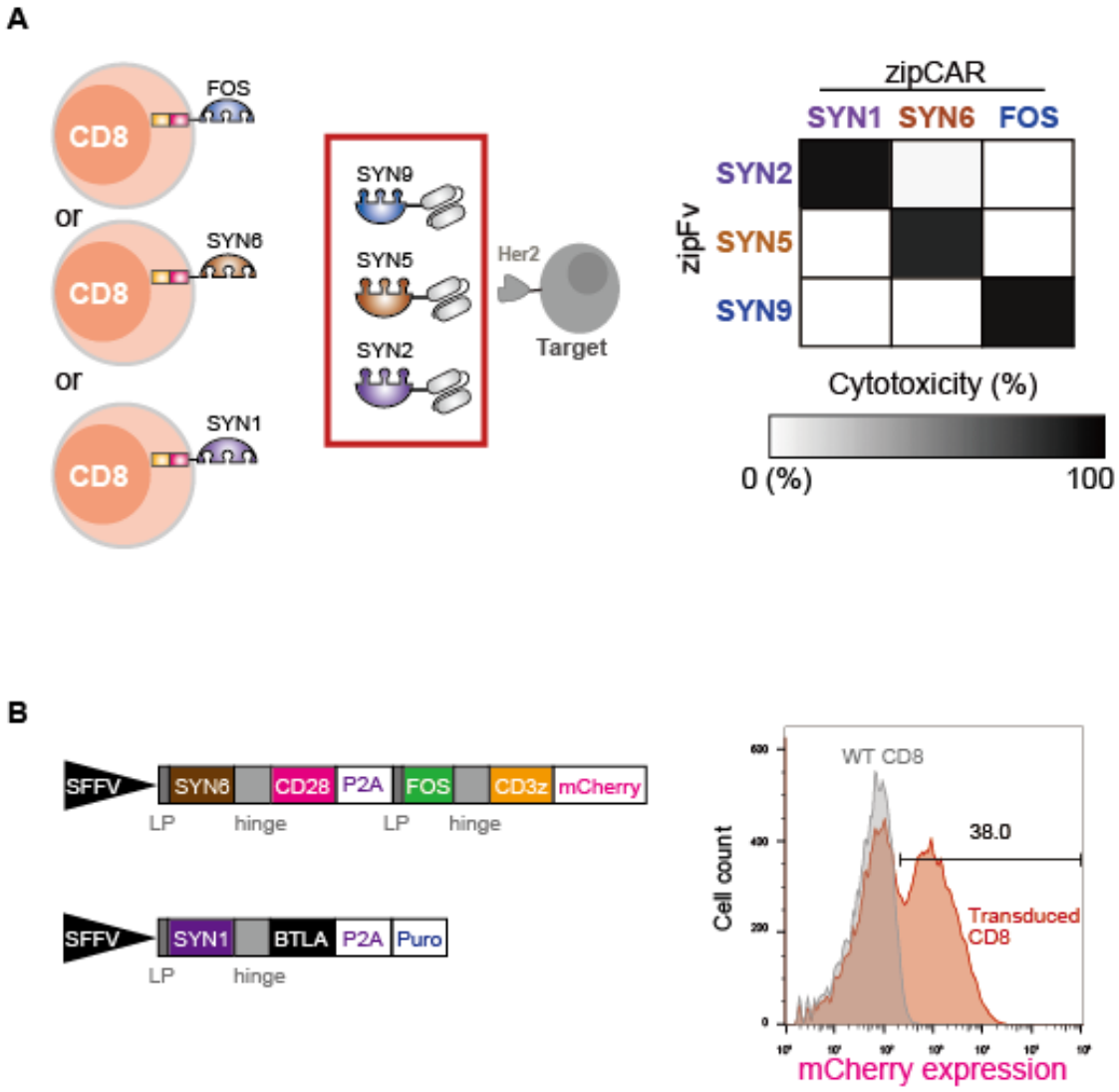

Figure 4.6.11. Orthogonal SUPRA pairs in primary human T cells and schematics construct designs used for 3 input logic circuit.

(A) Functional orthogonal SUPRA pairs in CD8+ T cells (n=3, data are represented as mean).

(B) (Left) Schematics of three different zipCAR constructs used for 3 input logic circuits (Right) zipCAR expression level measured by flow cytometry after puromycin selection.

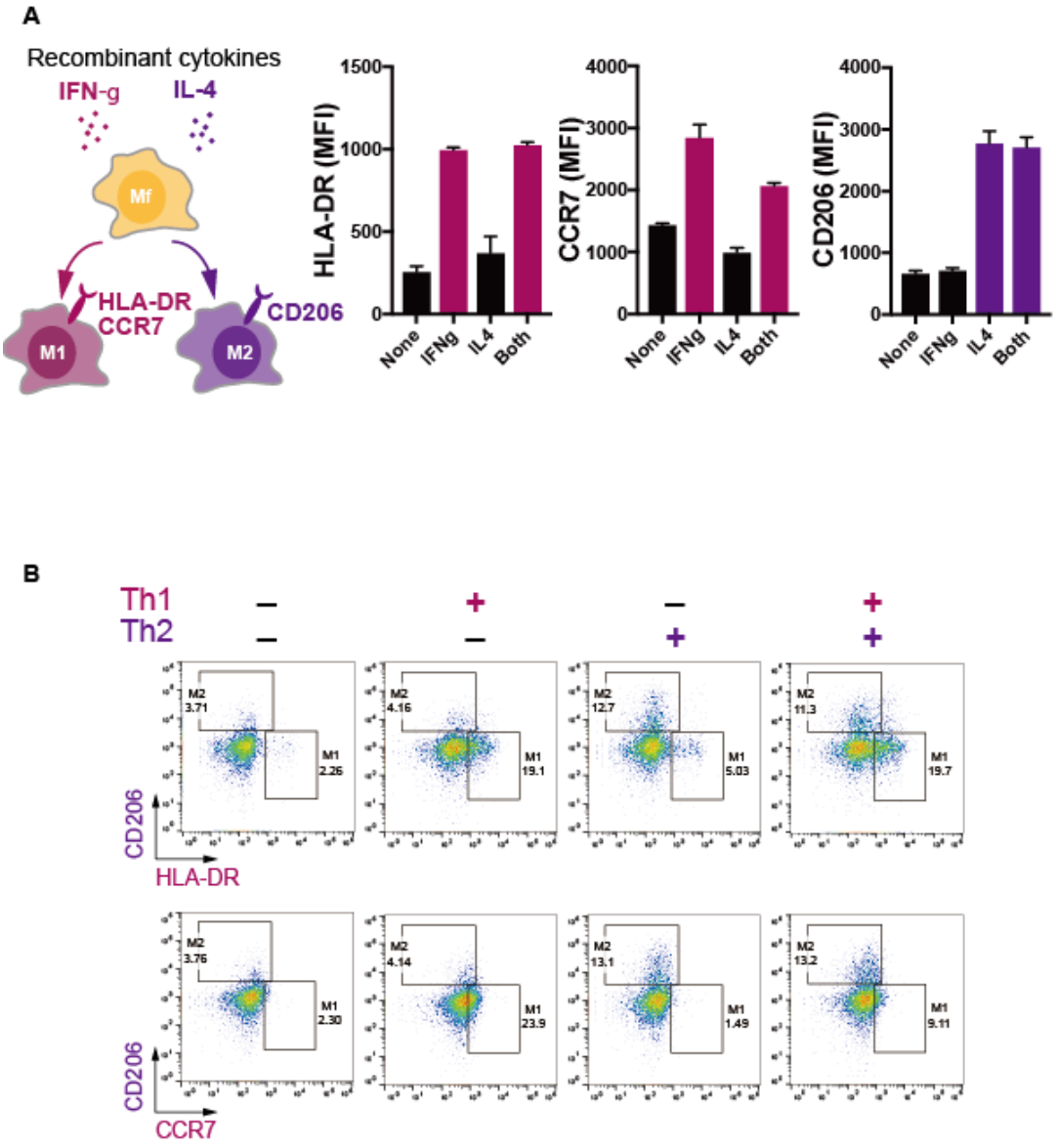

Figure 4.6.12. Effect of recombinant cytokines on macrophage differentiation.

(A) Effect of recombinant IFN-γ (10ng/ml) or IL-4 (10ng/ml) on in vitro macrophage differentiation measured by M1 and M2 macrophage surface markers (n=3, data are represented as mean ± SD).

(B) Flow cytometry plot shown in Figures 7B and 7C.

4.7 Acknowledgment

I want to acknowledge Dr. Atsushi Okuma, Dr. James Collins and Dr. Wilson Wong for their significant contributions including editing published manuscript to complete this chapter.

BIBLIOGRAPHY

1. Cameron DE, Bashor CJ, Collins JJ. A brief history of synthetic biology. Nature Reviews. Microbiology. 2014;12: 381–390. doi:10.1038/nrmicro3239

2. Chakravarti D, Cho JH, Weinberg BH, Wong NM, Wong WW. Synthetic biology approaches in cancer immunotherapy, genetic network engineering, and genome editing. Integrative Biology. 2016;8: 504–517. doi:10.1039/c5ib00325c

3. Bashor CJ, Collins JJ. Understanding biological regulation through synthetic biology. Annual Review of Biophysics. 2018;47: 399–423. doi:10.1146/annurev-biophys-070816-033903

4. Xie M, Fussenegger M. Designing cell function: assembly of synthetic gene circuits for cell biology applications. Nature Reviews. Molecular Cell Biology. 2018;19: 507–525. doi:10.1038/s41580-018-0024-z

5. Gardner TS, Cantor CR, Collins JJ. Construction of a genetic toggle switch in Escherichia coli. Nature. 2000;403: 339–342. doi:10.1038/35002131

6. Elowitz MB, Leibler S. A synthetic oscillatory network of transcriptional regulators. Nature. 2000;403: 335–338. doi:10.1038/35002125

7. Mondragón-Palomino O, Danino T, Selimkhanov J, Tsimring L, Hasty J. Entrainment of a population of synthetic genetic oscillators. Science. 2011;333: 1315–1319. doi:10.1126/science.1205369

8. Siuti P, Yazbek J, Lu TK. Synthetic circuits integrating logic and memory in living cells. Nature Biotechnology. 2013;31: 448–452. doi:10.1038/nbt.2510

9. Lienert F, Lohmueller JJ, Garg A, Silver PA. Synthetic biology in mammalian cells: next generation research tools and therapeutics. Nature Reviews. Molecular Cell Biology. 2014;15: 95–107. doi:10.1038/nrm3738

10. Rinaudo K, Bleris L, Maddamsetti R, Subramanian S, Weiss R, Benenson Y. A universal RNAi-based logic evaluator that operates in mammalian cells. Nature Biotechnology. 2007;25: 795–801. doi:10.1038/nbt1307

11. Xie Z, Liu SJ, Bleris L, Benenson Y. Logic integration of mRNA signals by an RNAi-based molecular computer. Nucleic Acids Research. 2010;38: 2692–2701. doi:10.1093/nar/gkq117

12. Nishimura K, Fukagawa T, Takisawa H, Kakimoto T, Kanemaki M. An auxin-based degron system for the rapid depletion of proteins in nonplant cells. Nature Methods. 2009;6: 917–922. doi:10.1038/nmeth.1401

13. Chung HK, Jacobs CL, Huo Y, Yang J, Krumm SA, Plemper RK, et al. Tunable and reversible drug control of protein production via a self-excising degron. Nature Chemical Biology. 2015;11: 713–720. doi:10.1038/nchembio.1869

14. Grimley JS, Chen DA, Banaszynski LA, Wandless TJ. Synthesis and analysis of stabilizing ligands for FKBP-derived destabilizing domains. Bioorganic & Medicinal Chemistry Letters. 2008;18: 759–761. doi:10.1016/j.bmcl.2007.11.044

15. Wu C-Y, Roybal KT, Puchner EM, Onuffer J, Lim WA. Remote control of therapeutic T cells through a small molecule-gated chimeric receptor. Science. 2015;350: aab4077. doi:10.1126/science.aab4077

16. Miyamoto T, DeRose R, Suarez A, Ueno T, Chen M, Sun T, et al. Rapid and orthogonal logic gating with a gibberellin-induced dimerization system. Nature Chemical Biology. 2012;8: 465–470. doi:10.1038/nchembio.922

17. Taslimi A, Zoltowski B, Miranda JG, Pathak GP, Hughes RM, Tucker CL. Optimized second-generation CRY2-CIB dimerizers and photoactivatable Cre recombinase. Nature Chemical Biology. 2016;12: 425–430. doi:10.1038/nchembio.2063

18. Inoue T, Heo WD, Grimley JS, Wandless TJ, Meyer T. An inducible translocation strategy to rapidly activate and inhibit small GTPase signaling pathways. Nature Methods. 2005;2: 415–418. doi:10.1038/nmeth763

19. Levskaya A, Weiner OD, Lim WA, Voigt CA. Spatiotemporal control of cell signalling using a light-switchable protein interaction. Nature. 2009;461: 997–1001. doi:10.1038/nature08446

20. Polstein LR, Gersbach CA. A light-inducible CRISPR-Cas9 system for control of endogenous gene activation. Nature Chemical Biology. 2015;11: 198–200. doi:10.1038/nchembio.1753

21. Niopek D, Benzinger D, Roensch J, Draebing T, Wehler P, Eils R, et al. Engineering light-inducible nuclear localization signals for precise spatiotemporal control of protein dynamics in living cells. Nature Communications. 2014;5: 4404. doi:10.1038/ncomms5404

22. Guntas G, Hallett RA, Zimmerman SP, Williams T, Yumerefendi H, Bear JE, et al. Engineering an improved light-induced dimer (iLID) for controlling the localization

and activity of signaling proteins. Proceedings of the National Academy of Sciences of the United States of America. 2015;112: 112–117. doi:10.1073/pnas.1417910112

23. Gossen M, Bujard H. Tight control of gene expression in mammalian cells by tetracycline-responsive promoters. Proceedings of the National Academy of Sciences of the United States of America. 1992;89: 5547–5551.

24. Brown M, Figge J, Hansen U, Wright C, Jeang KT, Khoury G, et al. lac repressor can regulate expression from a hybrid SV40 early promoter containing a lac operator in animal cells. Cell. 1987;49: 603–612.

25. Maeder ML, Thibodeau-Beganny S, Osiak A, Wright DA, Anthony RM, Eichtinger M, et al. Rapid "open-source" engineering of customized zinc-finger nucleases for highly efficient gene modification. Molecular Cell. 2008;31: 294–301. doi:10.1016/j.molcel.2008.06.016

26. Keung AJ, Bashor CJ, Kiriakov S, Collins JJ, Khalil AS. Using targeted chromatin regulators to engineer combinatorial and spatial transcriptional regulation. Cell. 2014;158: 110–120. doi:10.1016/j.cell.2014.04.047

27. Morbitzer R, Römer P, Boch J, Lahaye T. Regulation of selected genome loci using de novo-engineered transcription activator-like effector (TALE)-type transcription factors. Proceedings of the National Academy of Sciences of the United States of America. 2010;107: 21617–21622. doi:10.1073/pnas.1013133107

28. Garg A, Lohmueller JJ, Silver PA, Armel TZ. Engineering synthetic TAL effectors with orthogonal target sites. Nucleic Acids Research. 2012;40: 7584–7595. doi:10.1093/nar/gks404

29. Reyon D, Khayter C, Regan MR, Joung JK, Sander JD. Engineering designer transcription activator-like effector nucleases (TALENs) by REAL or REAL-Fast assembly. Current Protocols in Molecular Biology. 2012; Chapter 12: Unit 12.15. doi:10.1002/0471142727.mb1215s100

30. Qi LS, Larson MH, Gilbert LA, Doudna JA, Weissman JS, Arkin AP, et al. Repurposing CRISPR as an RNA-guided platform for sequence-specific control of gene expression. Cell. 2013;152: 1173–1183. doi:10.1016/j.cell.2013.02.022

31. Maeder ML, Linder SJ, Cascio VM, Fu Y, Ho QH, Joung JK. CRISPR RNA-guided activation of endogenous human genes. Nature Methods. 2013;10: 977–979. doi:10.1038/nmeth.2598

32. Perez-Pinera P, Kocak DD, Vockley CM, Adler AF, Kabadi AM, Polstein LR, et al. RNA-guided gene activation by CRISPR-Cas9-based transcription factors. Nature Methods. 2013;10: 973–976. doi:10.1038/nmeth.2600

33. Jinek M, East A, Cheng A, Lin S, Ma E, Doudna J. RNA-programmed genome editing in human cells. Elife. 2013;2: e00471. doi:10.7554/eLife.00471

34. Bibikova M, Beumer K, Trautman JK, Carroll D. Enhancing gene targeting with designed zinc finger nucleases. Science. 2003;300: 764. doi:10.1126/science.1079512

35. Eyquem J, Mansilla-Soto J, Giavridis T, van der Stegen SJC, Hamieh M, Cunanan KM, et al. Targeting a CAR to the TRAC locus with CRISPR/Cas9 enhances tumour rejection. Nature. 2017;543: 113–117. doi:10.1038/nature21405

36. Hale M, Mesojednik T, Romano Ibarra GS, Sahni J, Bernard A, Sommer K, et al. Engineering HIV-Resistant, Anti-HIV Chimeric Antigen Receptor T Cells. Molecular Therapy. 2017;25: 570–579. doi:10.1016/j.ymthe.2016.12.023

37. Conklin BR, Hsiao EC, Claeysen S, Dumuis A, Srinivasan S, Forsayeth JR, et al. Engineering GPCR signaling pathways with RASSLs. Nature Methods. 2008;5: 673–678. doi:10.1038/nmeth.1232

38. Barnea G, Strapps W, Herrada G, Berman Y, Ong J, Kloss B, et al. The genetic design of signaling cascades to record receptor activation. Proceedings of the National Academy of Sciences of the United States of America. 2008;105: 64–69. doi:10.1073/pnas.0710487105

39. Roybal KT, Williams JZ, Morsut L, Rupp LJ, Kolinko I, Choe JH, et al. Engineering T Cells with Customized Therapeutic Response Programs Using Synthetic Notch Receptors. Cell. 2016;167: 419–432.e16. doi:10.1016/j.cell.2016.09.011

40. LUXTURNA. In: LUXTURNA [Internet]. [cited 28 Jan 2019]. Available: https://www.fda.gov/BiologicsBloodVaccines/CellularGeneTherapyProducts/ApprovedProducts/ucm589507.htm

41. Mullard A. FDA approves landmark RNAi drug. Nature Reviews. Drug Discovery. 2018;17: 613–613. doi:10.1038/nrd.2018.152

42. thalassemia. In: CRISPR is coming to the clinic this year [Internet]. [cited 28 Jan 2019]. Available: https://cen.acs.org/content/cen/articles/96/i2/CRISPR-coming-clinic-year.html

43. Zheng P-P, Kros JM, Li J. Approved CAR T cell therapies: ice bucket challenges on glaring safety risks and long-term impacts. Drug Discovery Today. 2018;23: 1175–1182. doi:10.1016/j.drudis.2018.02.012

44. Roybal KT, Lim WA. Synthetic immunology: hacking immune cells to expand their therapeutic capabilities. Annual Review of Immunology. 2017;35: 229–253. doi:10.1146/annurev-immunol-051116-052302

45. Lim WA, June CH. The principles of engineering immune cells to treat cancer. Cell. 2017;168: 724–740. doi:10.1016/j.cell.2017.01.016

46. Ott PA, Hu Z, Keskin DB, Shukla SA, Sun J, Bozym DJ, et al. An immunogenic personal neoantigen vaccine for patients with melanoma. Nature. 2017;547: 217–221. doi:10.1038/nature22991

47. Keskin DB, Anandappa AJ, Sun J, Tirosh I, Mathewson ND, Li S, et al. Neoantigen vaccine generates intratumoral T cell responses in phase Ib glioblastoma trial. Nature. 2019;565: 234–239. doi:10.1038/s41586-018-0792-9

48. Handy CE, Antonarakis ES. Sipuleucel-T for the treatment of prostate cancer: novel insights and future directions. Future Oncology. 2018;14: 907–917. doi:10.2217/fon-2017-0531

49. Vacchelli E, Aranda F, Bloy N, Buqué A, Cremer I, Eggermont A, et al. Trial Watch-Immunostimulation with cytokines in cancer therapy. Oncoimmunology. 2016;5: e1115942. doi:10.1080/2162402X.2015.1115942

50. Wei SC, Duffy CR, Allison JP. Fundamental mechanisms of immune checkpoint blockade therapy. Cancer Discovery. 2018;8: 1069–1086. doi:10.1158/2159-8290.CD-18-0367

51. Rosenberg SA, Restifo NP, Yang JC, Morgan RA, Dudley ME. Adoptive cell transfer: a clinical path to effective cancer immunotherapy. Nature Reviews. Cancer. 2008;8: 299–308. doi:10.1038/nrc2355

52. Brenner MJ, Cho JH, Wong NML, Wong WW. Synthetic biology: immunotherapy by design. Annual Review of Biomedical Engineering. 2018;20: 95–118. doi:10.1146/annurev-bioeng-062117-121147

53. June CH, O'Connor RS, Kawalekar OU, Ghassemi S, Milone MC. CAR T cell immunotherapy for human cancer. Science. 2018;359: 1361–1365. doi:10.1126/science.aar6711

54. Rosenberg SA, Packard BS, Aebersold PM, Solomon D, Topalian SL, Toy ST, et al. Use of tumor-infiltrating lymphocytes and interleukin-2 in the immunotherapy of patients with metastatic melanoma. A preliminary report. New England Journal of Medicine. 1988;319: 1676–1680. doi:10.1056/NEJM198812223192527

55. Restifo NP, Dudley ME, Rosenberg SA. Adoptive immunotherapy for cancer: harnessing the T cell response. Nature Reviews. Immunology. 2012;12: 269–281. doi:10.1038/nri3191

56. Sadelain M, Brentjens R, Rivière I. The basic principles of chimeric antigen receptor design. Cancer Discovery. 2013;3: 388–398. doi:10.1158/2159-8290.CD-12-0548

57. Maude SL, Barrett D, Teachey DT, Grupp SA. Managing cytokine release syndrome associated with novel T cell-engaging therapies. Cancer Journal. 2014;20: 119–122. doi:10.1097/PPO.0000000000000035

58. Brudno JN, Kochenderfer JN. Toxicities of chimeric antigen receptor T cells: recognition and management. Blood. 2016;127: 3321–3330. doi:10.1182/blood-2016-04-703751

59. Bonifant CL, Jackson HJ, Brentjens RJ, Curran KJ. Toxicity and management in CAR T-cell therapy. Molecular Therapy Oncolytics. 2016;3: 16011. doi:10.1038/mto.2016.11

60. Morgan RA, Yang JC, Kitano M, Dudley ME, Laurencot CM, Rosenberg SA. Case report of a serious adverse event following the administration of T cells transduced with a chimeric antigen receptor recognizing ERBB2. Molecular Therapy. 2010;18: 843–851. doi:10.1038/mt.2010.24

61. Rooney C, Sauer T. Modeling cytokine release syndrome. Nature Medicine. 2018; 24: 705–706. doi:10.1038/s41591-018-0068-9

62. Kloss CC, Condomines M, Cartellieri M, Bachmann M, Sadelain M. Combinatorial antigen recognition with balanced signaling promotes selective tumor eradication by engineered T cells. Nature Biotechnology. 2013;31: 71–75. doi:10.1038/nbt.2459

63. Roybal KT, Rupp LJ, Morsut L, Walker WJ, McNally KA, Park JS, et al. Precision Tumor Recognition by T Cells With Combinatorial Antigen-Sensing Circuits. Cell. 2016;164: 770–779. doi:10.1016/j.cell.2016.01.011

64. Cho JH, Collins JJ, Wong WW. Universal chimeric antigen receptors for multiplexed and logical control of T cell responses. Cell. 2018;173: 1426–1438.e11. doi:10.1016/j.cell.2018.03.038

65. Zah E, Lin M-Y, Silva-Benedict A, Jensen MC, Chen YY. T cells expressing CD19/CD20 bispecific chimeric antigen receptors prevent antigen escape by malignant B cells. Cancer Immunology Research. 2016;4: 498–508. doi:10.1158/2326-6066.CIR-15-0231

66. Fry TJ, Shah NN, Orentas RJ, Stetler-Stevenson M, Yuan CM, Ramakrishna S, et al. CD22-targeted CAR T cells induce remission in B-ALL that is naive or resistant to CD19-targeted CAR immunotherapy. Nature Medicine. 2018;24: 20–28. doi:10.1038/nm.4441

67. Ruella M, Barrett DM, Kenderian SS, Shestova O, Hofmann TJ, Perazzelli J, et al. Dual CD19 and CD123 targeting prevents antigen-loss relapses after CD19-directed immunotherapies. Journal of Clinical Investigation. 2016;126: 3814–3826. doi:10.1172/JCI87366

68. Li J, Li W, Huang K, Zhang Y, Kupfer G, Zhao Q. Chimeric antigen receptor T cell (CAR-T) immunotherapy for solid tumors: lessons learned and strategies for moving forward. Journal of Hematology & Oncology. 2018;11: 22. doi:10.1186/s13045-018-0568-6

69. Knochelmann HM, Smith AS, Dwyer CJ, Wyatt MM, Mehrotra S, Paulos CM. CAR T cells in solid tumors: blueprints for building effective therapies. Frontiers in Immunology. 2018;9: 1740. doi:10.3389/fimmu.2018.01740

70. D'Aloia MM, Zizzari IG, Sacchetti B, Pierelli L, Alimandi M. CAR-T cells: the long and winding road to solid tumors. Cell Death Discovery. 2018;9: 282. doi:10.1038/s41419-018-0278-6

71. Gilham DE, Debets R, Pule M, Hawkins RE, Abken H. CAR-T cells and solid tumors: tuning T cells to challenge an inveterate foe. Trends in Molecular Medicine. 2012;18: 377–384. doi:10.1016/j.molmed.2012.04.009

72. Binnewies M, Roberts EW, Kersten K, Chan V, Fearon DF, Merad M, et al. Understanding the tumor immune microenvironment (TIME) for effective therapy. Nature Medicine. 2018;24: 541–550. doi:10.1038/s41591-018-0014-x

73. Gowrishankar K, Birtwistle L, Micklethwaite K. Manipulating the tumor microenvironment by adoptive cell transfer of CAR T-cells. Mammalian Genome. 2018; doi:10.1007/s00335-018-9756-5

74. Scharping NE, Menk AV, Moreci RS, Whetstone RD, Dadey RE, Watkins SC, et al. The tumor microenvironment represses T cell mitochondrial biogenesis to drive intratumoral T cell metabolic insufficiency and dysfunction. Immunity. 2016;45: 374–388. doi:10.1016/j.immuni.2016.07.009

75. Hegde M, Corder A, Chow KKH, Mukherjee M, Ashoori A, Kew Y, et al. Combinational targeting offsets antigen escape and enhances effector functions of adoptively transferred T cells in glioblastoma. Molecular Therapy. 2013;21: 2087–2101. doi:10.1038/mt.2013.185

76. Grada Z, Hegde M, Byrd T, Shaffer DR, Ghazi A, Brawley VS, et al. Tancar: A novel bispecific chimeric antigen receptor for cancer immunotherapy. Molecular Therapy. Nucleic Acids. 2013;2: e105. doi:10.1038/mtna.2013.32

77. Wu C-Y, Rupp LJ, Roybal KT, Lim WA. Synthetic biology approaches to engineer T cells. Current Opinion in Immunology. 2015;35: 123–130. doi:10.1016/j.coi.2015.06.015

78. Rodgers DT, Mazagova M, Hampton EN, Cao Y, Ramadoss NS, Hardy IR, et al. Switch-mediated activation and retargeting of CAR-T cells for B-cell malignancies. Proceedings of the National Academy of Sciences of the United States of America. 2016;113: E459–68. doi:10.1073/pnas.1524155113

79. Ma JSY, Kim JY, Kazane SA, Choi S-H, Yun HY, Kim MS, et al. Versatile strategy for controlling the specificity and activity of engineered T cells. Proceedings of the National Academy of Sciences of the United States of America. 2016;113: E450–8. doi:10.1073/pnas.1524193113

80. Tamada K, Geng D, Sakoda Y, Bansal N, Srivastava R, Li Z, et al. Redirecting gene-modified T cells toward various cancer types using tagged antibodies. Clinical Cancer Research. 2012;18: 6436–6445. doi:10.1158/1078-0432.CCR-12-1449

81. Urbanska K, Lanitis E, Poussin M, Lynn RC, Gavin BP, Kelderman S, et al. A universal strategy for adoptive immunotherapy of cancer through use of a novel T-cell antigen receptor. Cancer Research. 2012;72: 1844–1852. doi:10.1158/0008-5472.CAN-11-3890

82. Fedorov VD, Themeli M, Sadelain M. PD-1- and CTLA-4-based inhibitory chimeric antigen receptors (iCARs) divert off-target immunotherapy responses. Science Translational Medicine. 2013;5: 215ra172. doi:10.1126/scitranslmed.3006597

83. Di Stasi A, Tey S-K, Dotti G, Fujita Y, Kennedy-Nasser A, Martinez C, et al. Inducible apoptosis as a safety switch for adoptive cell therapy. New England Journal of Medicine. 2011;365: 1673–1683. doi:10.1056/NEJMoa1106152

84. Straathof KC, Pulè MA, Yotnda P, Dotti G, Vanin EF, Brenner MK, et al. An inducible caspase 9 safety switch for T-cell therapy. Blood. 2005;105: 4247–4254. doi:10.1182/blood-2004-11-4564

85. Peng W, Ye Y, Rabinovich BA, Liu C, Lou Y, Zhang M, et al. Transduction of tumor-specific T cells with CXCR2 chemokine receptor improves migration to tumor and antitumor immune responses. Clinical Cancer Research. 2010;16: 5458–5468. doi:10.1158/1078-0432.CCR-10-0712

86. Moon EK, Carpenito C, Sun J, Wang L-CS, Kapoor V, Predina J, et al. Expression of a functional CCR2 receptor enhances tumor localization and tumor eradication by retargeted human T cells expressing a mesothelin-specific chimeric antibody receptor. Clinical Cancer Research. 2011;17: 4719–4730. doi:10.1158/1078-0432.CCR-11-0351

87. Xu Y, Hyun Y-M, Lim K, Lee H, Cummings RJ, Gerber SA, et al. Optogenetic control of chemokine receptor signal and T-cell migration. Proceedings of the National Academy of Sciences of the United States of America. 2014;111: 6371–6376. doi:10.1073/pnas.1319296111

88. Caruana I, Savoldo B, Hoyos V, Weber G, Liu H, Kim ES, et al. Heparanase promotes tumor infiltration and antitumor activity of CAR-redirected T lymphocytes. Nature Medicine. 2015;21: 524–529. doi:10.1038/nm.3833

89. Zhang L, Yu Z, Muranski P, Palmer DC, Restifo NP, Rosenberg SA, et al. Inhibition of TGF-β signaling in genetically engineered tumor antigen-reactive T cells significantly enhances tumor treatment efficacy. Gene Therapy. 2013;20: 575–580. doi:10.1038/gt.2012.75

90. Leen AM, Sukumaran S, Watanabe N, Mohammed S, Keirnan J, Yanagisawa R, et al. Reversal of tumor immune inhibition using a chimeric cytokine receptor. Molecular Therapy. 2014;22: 1211–1220. doi:10.1038/mt.2014.47

91. Prosser ME, Brown CE, Shami AF, Forman SJ, Jensen MC. Tumor PD-L1 co-stimulates primary human CD8(+) cytotoxic T cells modified to express a PD1:CD28 chimeric receptor. Molecular Immunology. 2012;51: 263–272. doi:10.1016/j.molimm.2012.03.023

92. Komita H, Zhao X, Katakam AK, Kumar P, Kawabe M, Okada H, et al. Conditional interleukin-12 gene therapy promotes safe and effective antitumor immunity. Cancer Gene Therapy. 2009;16: 883–891. doi:10.1038/cgt.2009.33

93. Zhang L, Morgan RA, Beane JD, Zheng Z, Dudley ME, Kassim SH, et al. Tumor-infiltrating lymphocytes genetically engineered with an inducible gene encoding interleukin-12 for the immunotherapy of metastatic melanoma. Clinical Cancer Research. 2015;21: 2278–2288. doi:10.1158/1078-0432.CCR-14-2085

94. Lemmon MA, Schlessinger J. Cell signaling by receptor tyrosine kinases. Cell. 2010;141: 1117–1134. doi:10.1016/j.cell.2010.06.011

95. Myers SH, Brunton VG, Unciti-Broceta A. AXL inhibitors in cancer: A medicinal chemistry perspective. Journal of Medicinal Chemistry. 2016;59: 3593–3608. doi:10.1021/acs.jmedchem.5b01273

96. Wu X, Liu X, Koul S, Lee CY, Zhang Z, Halmos B. AXL kinase as a novel target for cancer therapy. Oncotarget. 2014;5: 9546–9563. doi:10.18632/oncotarget.2542

97. Ye X, Li Y, Stawicki S, Couto S, Eastham-Anderson J, Kallop D, et al. An anti-Axl monoclonal antibody attenuates xenograft tumor growth and enhances the effect of multiple anticancer therapies. Oncogene. 2010;29: 5254–5264. doi:10.1038/onc.2010.268

98. Meric F, Lee W-P, Sahin A, Zhang H, Kung H-J, Hung M-C. Expression profile of tyrosine kinases in breast cancer. Clinical Cancer Research. 2002;8: 361–367.

99. Paccez JD, Vasques GJ, Correa RG, Vasconcellos JF, Duncan K, Gu X, et al. The receptor tyrosine kinase Axl is an essential regulator of prostate cancer proliferation and tumor growth and represents a new therapeutic target. Oncogene. 2013;32: 689–698. doi:10.1038/onc.2012.89

100. Yu H, Liu R, Ma B, Li X, Yen HY, Zhou Y, et al. Axl receptor tyrosine kinase is a potential therapeutic target in renal cell carcinoma. British Journal of Cancer. 2015;113: 616–625. doi:10.1038/bjc.2015.237

101. Han J, Tian R, Yong B, Luo C, Tan P, Shen J, et al. Gas6/Axl mediates tumor cell apoptosis, migration and invasion and predicts the clinical outcome of osteosarcoma patients. Biochemical and Biophysical Research Communications. 2013;435: 493–500. doi:10.1016/j.bbrc.2013.05.019

102. Cichoń MA, Szentpetery Z, Caley MP, Papadakis ES, Mackenzie IC, Brennan CH, et al. The receptor tyrosine kinase Axl regulates cell-cell adhesion and stemness in cutaneous squamous cell carcinoma. Oncogene. 2014;33: 4185–4192. doi:10.1038/onc.2013.388

103. Byers LA, Diao L, Wang J, Saintigny P, Girard L, Peyton M, et al. An epithelial-mesenchymal transition gene signature predicts resistance to EGFR and PI3K inhibitors and identifies Axl as a therapeutic target for overcoming EGFR inhibitor resistance. Clinical Cancer Research. 2013;19: 279–290. doi:10.1158/1078-0432.CCR-12-1558

104. Zhang Z, Lee JC, Lin L, Olivas V, Au V, LaFramboise T, et al. Activation of the AXL kinase causes resistance to EGFR-targeted therapy in lung cancer. Nature Genetics. 2012;44: 852–860. doi:10.1038/ng.2330

105. Brand TM, Iida M, Stein AP, Corrigan KL, Braverman CM, Luthar N, et al. AXL mediates resistance to cetuximab therapy. Cancer Research. 2014;74: 5152–5164. doi:10.1158/0008-5472.CAN-14-0294

106. Gay CM, Balaji K, Byers LA. Giving AXL the axe: targeting AXL in human malignancy. British Journal of Cancer. 2017;116: 415–423. doi:10.1038/bjc.2016.428

107. Davila ML, Riviere I, Wang X, Bartido S, Park J, Curran K, et al. Efficacy and toxicity management of 19-28z CAR T cell therapy in B cell acute lymphoblastic leukemia. Science Translational Medicine. 2014;6: 224ra25. doi:10.1126/scitranslmed.3008226

108. Maude SL, Frey N, Shaw PA, Aplenc R, Barrett DM, Bunin NJ, et al. Chimeric antigen receptor T cells for sustained remissions in leukemia. New England Journal of Medicine. 2014;371: 1507–1517. doi:10.1056/NEJMoa1407222

109. Grupp SA, Kalos M, Barrett D, Aplenc R, Porter DL, Rheingold SR, et al. Chimeric antigen receptor-modified T cells for acute lymphoid leukemia. New England Journal of Medicine. 2013;368: 1509–1518. doi:10.1056/NEJMoa1215134

110. Brentjens RJ, Davila ML, Riviere I, Park J, Wang X, Cowell LG, et al. CD19-targeted T cells rapidly induce molecular remissions in adults with chemotherapy-refractory acute lymphoblastic leukemia. Science Translational Medicine. 2013;5: 177ra38. doi:10.1126/scitranslmed.3005930

111. Barrett DM, Singh N, Porter DL, Grupp SA, June CH. Chimeric antigen receptor therapy for cancer. Annual Review of Medicine. 2014;65: 333–347. doi:10.1146/annurev-med-060512-150254

112. Li D, Liu S, Liu R, Park R, Yu H, Krasnoperov V, et al. Axl-targeted cancer imaging with humanized antibody h173. Molecular Imaging & Biology. 2014;16: 511–518. doi:10.1007/s11307-013-0714-z

113. Tang X-Y, Sun Y, Zhang A, Hu G-L, Cao W, Wang D-H, et al. Third-generation CD28/4-1BB chimeric antigen receptor T cells for chemotherapy relapsed or refractory acute lymphoblastic leukaemia: a non-randomised, open-label phase I trial protocol. BMJ Open. 2016;6: e013904. doi:10.1136/bmjopen-2016-013904

114. Wilson MH, Coates CJ, George AL. PiggyBac transposon-mediated gene transfer in human cells. Molecular Therapy. 2007;15: 139–145. doi:10.1038/sj.mt.6300028

115. Ziegler SF, Ramsdell F, Alderson MR. The activation antigen CD69. Stem Cells. 1994;12: 456–465. doi:10.1002/stem.5530120502

116. Daringer NM, Dudek RM, Schwarz KA, Leonard JN. Modular extracellular sensor architecture for engineering mammalian cell-based devices. ACS Synthetic Biology. 2014;3: 892–902. doi:10.1021/sb400128g

117. Chowdhury F, Li ITS, Ngo TTM, Leslie BJ, Kim BC, Sokoloski JE, et al. Defining single molecular forces required for notch activation using nano yoyo. Nano Letters. 2016;16: 3892–3897. doi:10.1021/acs.nanolett.6b01403

118. Wang X, Ha T. Defining single molecular forces required to activate integrin and notch signaling. Science. 2013;340: 991–994. doi:10.1126/science.1231041

119. Kopan R, Ilagan MXG. The canonical Notch signaling pathway: unfolding the activation mechanism. Cell. 2009;137: 216–233. doi:10.1016/j.cell.2009.03.045

120. Brentjens RJ, Rivière I, Park JH, Davila ML, Wang X, Stefanski J, et al. Safety and persistence of adoptively transferred autologous CD19-targeted T cells in patients with relapsed or chemotherapy refractory B-cell leukemias. Blood. 2011;118: 4817–4828. doi:10.1182/blood-2011-04-348540

121. Kochenderfer JN, Dudley ME, Feldman SA, Wilson WH, Spaner DE, Maric I, et al. B-cell depletion and remissions of malignancy along with cytokine-associated toxicity in a clinical trial of anti-CD19 chimeric-antigen-receptor-transduced T cells. Blood. 2012;119: 2709–2720. doi:10.1182/blood-2011-10-384388

122. Scholler J, Brady TL, Binder-Scholl G, Hwang W-T, Plesa G, Hege KM, et al. Decade-long safety and function of retroviral-modified chimeric antigen receptor T cells. Science Translational Medicine. 2012;4: 132ra53. doi:10.1126/scitranslmed.3003761

123. Liu X, Jiang S, Fang C, Yang S, Olalere D, Pequignot EC, et al. Affinity-Tuned ErbB2 or EGFR Chimeric Antigen Receptor T Cells Exhibit an Increased Therapeutic Index against Tumors in Mice. Cancer Research. 2015;75: 3596–3607. doi:10.1158/0008-5472.CAN-15-0159

124. Caruso HG, Hurton LV, Najjar A, Rushworth D, Ang S, Olivares S, et al. Tuning sensitivity of CAR to EGFR density limits recognition of normal tissue while maintaining potent antitumor activity. Cancer Research. 2015;75: 3505–3518. doi:10.1158/0008-5472.CAN-15-0139

125. Zhao Z, Condomines M, van der Stegen SJC, Perna F, Kloss CC, Gunset G, et al. Structural design of engineered costimulation determines tumor rejection kinetics and persistence of CAR T cells. Cancer Cell. 2015;28: 415–428. doi:10.1016/j.ccell.2015.09.004

126. Lanitis E, Poussin M, Klattenhoff AW, Song D, Sandaltzopoulos R, June CH, et al. Chimeric antigen receptor T Cells with dissociated signaling domains exhibit focused antitumor activity with reduced potential for toxicity in vivo. Cancer Immunology Research. 2013;1: 43–53. doi:10.1158/2326-6066.CIR-13-0008

127. Zhu Y, Zhu G, Luo L, Flies AS, Chen L. CD137 stimulation delivers an antigen-independent growth signal for T lymphocytes with memory phenotype. Blood. 2007;109: 4882–4889. doi:10.1182/blood-2006-10-043463

128. Skapenko A, Lipsky PE, Kraetsch HG, Kalden JR, Schulze-Koops H. Antigen-independent Th2 cell differentiation by stimulation of CD28: regulation via IL-4 gene expression and mitogen-activated protein kinase activation. Journal of Immunology. 2001;166: 4283–4292. doi:10.4049/jimmunol.166.7.4283

129. Kawalekar OU, O'Connor RS, Fraietta JA, Guo L, McGettigan SE, Posey AD, et al. Distinct signaling of coreceptors regulates specific metabolism pathways and impacts memory development in CAR T cells. Immunity. 2016;44: 380–390. doi:10.1016/j.immuni.2016.01.021

130. Turtle CJ, Hanafi L-A, Berger C, Gooley TA, Cherian S, Hudecek M, et al. CD19 CAR-T cells of defined CD4+:CD8+ composition in adult B cell ALL patients. Journal of Clinical Investigation. 2016;126: 2123–2138. doi:10.1172/JCI85309

131. Sadelain M, Rivière I, Riddell S. Therapeutic T cell engineering. Nature. 2017;545: 423–431. doi:10.1038/nature22395

132. Cartellieri M, Feldmann A, Koristka S, Arndt C, Loff S, Ehninger A, et al. Switching CAR T cells on and off: a novel modular platform for retargeting of T cells to AML blasts. Blood Cancer Journal. 2016;6: e458. doi:10.1038/bcj.2016.61

133. Reinke AW, Grant RA, Keating AE. A synthetic coiled-coil interactome provides heterospecific modules for molecular engineering. Journal of the American Chemical Society. 2010;132: 6025–6031. doi:10.1021/ja907617a

134. Thompson KE, Bashor CJ, Lim WA, Keating AE. SYNZIP protein interaction toolbox: in vitro and in vivo specifications of heterospecific coiled-coil interaction domains. ACS Synthetic Biology. 2012;1: 118–129. doi:10.1021/sb200015u

135. Chmielewski M, Hombach A, Heuser C, Adams GP, Abken H. T cell activation by antibody-like immunoreceptors: increase in affinity of the single-chain fragment domain above threshold does not increase T cell activation against antigen-positive target cells but decreases selectivity. Journal of Immunology. 2004;173: 7647–7653. doi:10.4049/jimmunol.173.12.7647

136. Scott AM, Wolchok JD, Old LJ. Antibody therapy of cancer. Nature Reviews. Cancer. 2012;12: 278–287. doi:10.1038/nrc3236

137. Perna F, Sadelain M. Myeloid leukemia switch as immune escape from CD19 chimeric antigen receptor (CAR) therapy. Translational Cancer Research. 2016;5: S221–S225. doi:10.21037/tcr.2016.08.15

138. Haso W, Lee DW, Shah NN, Stetler-Stevenson M, Yuan CM, Pastan IH, et al. Anti-CD22-chimeric antigen receptors targeting B-cell precursor acute lymphoblastic leukemia. Blood. 2013;121: 1165–1174. doi:10.1182/blood-2012-06-438002

139. Shaw TJ, Senterman MK, Dawson K, Crane CA, Vanderhyden BC. Characterization of intraperitoneal, orthotopic, and metastatic xenograft models of human ovarian cancer. Molecular Therapy. 2004;10: 1032–1042. doi:10.1016/j.ymthe.2004.08.013

140. Lee MJ, Cho SS, You JR, Lee Y, Kang BD, Choi JS, et al. Intraperitoneal gene delivery mediated by a novel cationic liposome in a peritoneal disseminated ovarian cancer model. Gene Therapy. 2002;9: 859–866. doi:10.1038/sj.gt.3301704

141. Lengyel E, Burdette JE, Kenny HA, Matei D, Pilrose J, Haluska P, et al. Epithelial ovarian cancer experimental models. Oncogene. 2014;33: 3619–3633. doi:10.1038/onc.2013.321

142. Geller MA, Knorr DA, Hermanson DA, Pribyl L, Bendzick L, McCullar V, et al. Intraperitoneal delivery of human natural killer cells for treatment of ovarian cancer in a mouse xenograft model. Cytotherapy. 2013;15: 1297–1306. doi:10.1016/j.jcyt.2013.05.022

143. Karin M, Liu Z g, Zandi E. AP-1 function and regulation. Current Opinion in Cell Biology. 1997;9: 240–246. doi:10.1016/S0955-0674(97)80068-3

144. Chen L, Flies DB. Molecular mechanisms of T cell co-stimulation and co-inhibition. Nature Reviews. Immunology. 2013;13: 227–242. doi:10.1038/nri3405

145. Zhu Y, Yao S, Chen L. Cell surface signaling molecules in the control of immune responses: a tide model. Immunity. 2011;34: 466–478. doi:10.1016/j.immuni.2011.04.008

146. Greenwald RJ, Freeman GJ, Sharpe AH. The B7 family revisited. Annual Review of Immunology. 2005;23: 515–548. doi:10.1146/annurev.immunol.23.021704.115611

147. Vandenberghe P, Verwilghen J, Van Vaeck F, Ceuppens JL. Ligation of the CD5 or CD28 molecules on resting human T cells induces expression of the early activation antigen CD69 by a calcium- and tyrosine kinase-dependent mechanism. Immunology. 1993;78: 210–217.

148. Kane LP, Andres PG, Howland KC, Abbas AK, Weiss A. Akt provides the CD28 costimulatory signal for up-regulation of IL-2 and IFN-gamma but not TH2 cytokines. Nature Immunology. 2001;2: 37–44. doi:10.1038/83144

149. Howland KC, Ausubel LJ, London CA, Abbas AK. The roles of CD28 and CD40 ligand in T cell activation and tolerance. Journal of Immunology. 2000;164: 4465–4470. doi:10.4049/jimmunol.164.9.4465

150. Lucas PJ, Negishi I, Nakayama K, Fields LE, Loh DY. Naive CD28-deficient T cells can initiate but not sustain an in vitro antigen-specific immune response. Journal of Immunology. 1995;154: 5757–5768.

151. Luckheeram RV, Zhou R, Verma AD, Xia B. $CD4^+$T cells: differentiation and functions. Clinical & Developmental Immunology. 2012;2012: 925135. doi:10.1155/2012/925135

152. Hombach A, Köhler H, Rappl G, Abken H. Human CD4+ T cells lyse target cells via granzyme/perforin upon circumvention of MHC class II restriction by an antibody-like immunoreceptor. Journal of Immunology. 2006;177: 5668–5675. doi:10.4049/jimmunol.177.8.5668

153. Kudo K, Imai C, Lorenzini P, Kamiya T, Kono K, Davidoff AM, et al. T lymphocytes expressing a CD16 signaling receptor exert antibody-dependent cancer cell killing. Cancer Research. 2014;74: 93–103. doi:10.1158/0008-5472.CAN-13-1365

154. Hudecek M, Sommermeyer D, Kosasih PL, Silva-Benedict A, Liu L, Rader C, et al. The nonsignaling extracellular spacer domain of chimeric antigen receptors is decisive for in vivo antitumor activity. Cancer Immunology Research. 2015;3: 125–135. doi:10.1158/2326-6066.CIR-14-0127

155. Gould LH, Sui J, Foellmer H, Oliphant T, Wang T, Ledizet M, et al. Protective and therapeutic capacity of human single-chain Fv-Fc fusion proteins against West Nile virus. Journal of Virology. 2005;79: 14606–14613. doi:10.1128/JVI.79.23.14606-14613.2005

156. Carter P. Improving the efficacy of antibody-based cancer therapies. Nature Reviews. Cancer. 2001;1: 118–129. doi:10.1038/35101072

157. Kontermann RE. Strategies for extended serum half-life of protein therapeutics. Current Opinion in Biotechnology. 2011;22: 868–876. doi:10.1016/j.copbio.2011.06.012

158. Strohl WR. Fusion Proteins for Half-Life Extension of Biologics as a Strategy to Make Biobetters. BioDrugs. 2015;29: 215–239. doi:10.1007/s40259-015-0133-6

159. Szlachcic A, Zakrzewska M, Otlewski J. Longer action means better drug: tuning up protein therapeutics. Biotechnology Advances. 2011;29: 436–441. doi:10.1016/j.biotechadv.2011.03.005

160. Kimchi-Sarfaty C, Schiller T, Hamasaki-Katagiri N, Khan MA, Yanover C, Sauna ZE. Building better drugs: developing and regulating engineered therapeutic proteins. Trends in Pharmacological Sciences. 2013;34: 534–548. doi:10.1016/j.tips.2013.08.005

161. MacDonald KG, Hoeppli RE, Huang Q, Gillies J, Luciani DS, Orban PC, et al. Alloantigen-specific regulatory T cells generated with a chimeric antigen receptor. Journal of Clinical Investigation. 2016;126: 1413–1424. doi:10.1172/JCI82771

162. Yoon J, Schmidt A, Zhang A-H, Königs C, Kim YC, Scott DW. FVIII-specific human chimeric antigen receptor T-regulatory cells suppress T- and B-cell responses to FVIII. Blood. 2017;129: 238–245. doi:10.1182/blood-2016-07-727834

163. Glienke W, Esser R, Priesner C, Suerth JD, Schambach A, Wels WS, et al. Advantages and applications of CAR-expressing natural killer cells. Frontiers in Pharmacology. 2015;6: 21. doi:10.3389/fphar.2015.00021

164. Klingemann H. Are natural killer cells superior CAR drivers? Oncoimmunology. 2014;3: e28147. doi:10.4161/onci.28147

165. Fu X, Tao L, Rivera A, Williamson S, Song X-T, Ahmed N, et al. A simple and sensitive method for measuring tumor-specific T cell cytotoxicity. PLoS One. 2010;5: e11867. doi:10.1371/journal.pone.0011867

166. Pardoll DM. The blockade of immune checkpoints in cancer immunotherapy. Nature Reviews. Cancer. 2012;12: 252–264. doi:10.1038/nrc3239

167. Ribas A, Wolchok JD. Cancer immunotherapy using checkpoint blockade. Science. 2018;359: 1350–1355. doi:10.1126/science.aar4060

168. Topalian SL, Drake CG, Pardoll DM. Immune checkpoint blockade: a common denominator approach to cancer therapy. Cancer Cell. 2015;27: 450–461. doi:10.1016/j.ccell.2015.03.001

169. Topalian SL, Hodi FS, Brahmer JR, Gettinger SN, Smith DC, McDermott DF, et al. Safety, activity, and immune correlates of anti-PD-1 antibody in cancer. New England Journal of Medicine. 2012;366: 2443–2454 . doi:10.1056/NEJMoa1200690

170. Prieto PA, Yang JC, Sherry RM, Hughes MS, Kammula US, White DE, et al. CTLA-4 blockade with ipilimumab: long-term follow-up of 177 patients with metastatic melanoma. Clinical Cancer Research. 2012;18: 2039–2047. doi:10.1158/1078-0432.CCR-11-1823

171. Rizvi NA, Hellmann MD, Snyder A, Kvistborg P, Makarov V, Havel JJ, et al. Cancer immunology. Mutational landscape determines sensitivity to PD-1 blockade in non-small cell lung cancer. Science. 2015;348: 124–128. doi:10.1126/science.aaa1348

172. Kochenderfer JN, Wilson WH, Janik JE, Dudley ME, Stetler-Stevenson M, Feldman SA, et al. Eradication of B-lineage cells and regression of lymphoma in a patient treated with autologous T cells genetically engineered to recognize CD19. Blood. 2010;116: 4099–4102. doi:10.1182/blood-2010-04-281931

173. Porter DL, Levine BL, Kalos M, Bagg A, June CH. Chimeric antigen receptor-modified T cells in chronic lymphoid leukemia. New England Journal of Medicine. 2011;365: 725–733. doi:10.1056/NEJMoa1103849

174. Ellebrecht CT, Bhoj VG, Nace A, Choi EJ, Mao X, Cho MJ, et al. Reengineering chimeric antigen receptor T cells for targeted therapy of autoimmune disease. Science. 2016;353: 179–184. doi:10.1126/science.aaf6756

175. Perna F, Berman SH, Soni RK, Mansilla-Soto J, Eyquem J, Hamieh M, et al. Integrating proteomics and transcriptomics for systematic combinatorial chimeric antigen receptor therapy of AML. Cancer Cell. 2017;32: 506–519.e5. doi:10.1016/j.ccell.2017.09.004

176. Engblom C, Pfirschke C, Pittet MJ. The role of myeloid cells in cancer therapies. Nature Reviews. Cancer. 2016;16: 447–462. doi:10.1038/nrc.2016.54

177. Barry KC, Hsu J, Broz ML, Cueto FJ, Binnewies M, Combes AJ, et al. A natural killer-dendritic cell axis defines checkpoint therapy-responsive tumor microenvironments. Nature Medicine. 2018;24: 1178–1191. doi:10.1038/s41591-018-0085-8

178. de Mingo Pulido Á, Gardner A, Hiebler S, Soliman H, Rugo HS, Krummel MF, et al. TIM-3 Regulates CD103+ Dendritic Cell Function and Response to Chemotherapy in Breast Cancer. Cancer Cell. 2018;33: 60–74.e6. doi:10.1016/j.ccell.2017.11.019

179. Mok S, Koya RC, Tsui C, Xu J, Robert L, Wu L, et al. Inhibition of CSF-1 receptor improves the antitumor efficacy of adoptive cell transfer immunotherapy. Cancer Research. 2014;74: 153–161. doi:10.1158/0008-5472.CAN-13-1816

180. Sluijter M, van der Sluis TC, van der Velden PA, Versluis M, West BL, van der Burg SH, et al. Inhibition of CSF-1R supports T-cell mediated melanoma therapy. PLoS One. 2014;9: e104230. doi:10.1371/journal.pone.0104230

181. Gentles AJ, Newman AM, Liu CL, Bratman SV, Feng W, Kim D, et al. The prognostic landscape of genes and infiltrating immune cells across human cancers. Nature Medicine. 2015;21: 938–945. doi:10.1038/nm.3909

182. Zhu J, Paul WE. CD4 T cells: fates, functions, and faults. Blood. 2008;112: 1557–1569. doi:10.1182/blood-2008-05-078154

183. Sakaguchi S, Yamaguchi T, Nomura T, Ono M. Regulatory T cells and immune tolerance. Cell. 2008;133: 775–787. doi:10.1016/j.cell.2008.05.009

184. Bluestone JA, Buckner JH, Fitch M, Gitelman SE, Gupta S, Hellerstein MK, et al. Type 1 diabetes immunotherapy using polyclonal regulatory T cells. Science Translational Medicine. 2015;7: 315ra189. doi:10.1126/scitranslmed.aad4134

185. Mirzaei HR, Mirzaei H, Lee SY, Hadjati J, Till BG. Prospects for chimeric antigen receptor (CAR) γδ T cells: A potential game changer for adoptive T cell cancer immunotherapy. Cancer Letters. 2016;380: 413–423. doi:10.1016/j.canlet.2016.07.001

186. Guillerey C, Huntington ND, Smyth MJ. Targeting natural killer cells in cancer immunotherapy. Nature Immunology. 2016;17: 1025–1036. doi:10.1038/ni.3518

187. Arai S, Meagher R, Swearingen M, Myint H, Rich E, Martinson J, et al. Infusion of the allogeneic cell line NK-92 in patients with advanced renal cell cancer or melanoma: a phase I trial. Cytotherapy. 2008;10: 625–632. doi:10.1080/14653240802301872

188. Tonn T, Schwabe D, Klingemann HG, Becker S, Esser R, Koehl U, et al. Treatment of patients with advanced cancer with the natural killer cell line NK-92. Cytotherapy. 2013;15: 1563–1570. doi:10.1016/j.jcyt.2013.06.017

189. Zhang C, Oberoi P, Oelsner S, Waldmann A, Lindner A, Tonn T, et al. Chimeric Antigen Receptor-Engineered NK-92 Cells: An Off-the-Shelf Cellular Therapeutic for Targeted Elimination of Cancer Cells and Induction of Protective Antitumor Immunity. Frontiers in Immunology. 2017;8: 533. doi:10.3389/fimmu.2017.00533

190. Morrissey MA, Williamson AP, Steinbach AM, Roberts EW, Kern N, Headley MB, et al. Chimeric antigen receptors that trigger phagocytosis. Elife. 2018;7. doi:10.7554/eLife.36688

191. Zhang S, Cordon-Cardo C, Zhang HS, Reuter VE, Adluri S, Hamilton WB, et al. Selection of tumor antigens as targets for immune attack using immunohistochemistry: I. Focus on gangliosides. International Journal of Cancer. 1997;73: 42–49. doi:10.1002/(SICI)1097-0215(19970926)73:1<42::AID-IJC8>3.0.CO;2-1

192. Lamers CHJ, Sleijfer S, Vulto AG, Kruit WHJ, Kliffen M, Debets R, et al. Treatment of metastatic renal cell carcinoma with autologous T-lymphocytes genetically retargeted against carbonic anhydrase IX: first clinical experience. Journal of Clinical Oncology. 2006;24: e20–2. doi:10.1200/JCO.2006.05.9964

193. Neelapu SS, Locke FL, Bartlett NL, Lekakis LJ, Miklos DB, Jacobson CA, et al. Axicabtagene Ciloleucel CAR T-Cell Therapy in Refractory Large B-Cell Lymphoma. New England Journal of Medicine. 2017;377: 2531–2544. doi:10.1056/NEJMoa1707447

194. Schuster SJ, Svoboda J, Chong EA, Nasta SD, Mato AR, Anak Ö, et al. Chimeric Antigen Receptor T Cells in Refractory B-Cell Lymphomas. New England Journal of Medicine. 2017;377: 2545–2554. doi:10.1056/NEJMoa1708566

195. Di Ianni M, Falzetti F, Carotti A, Terenzi A, Castellino F, Bonifacio E, et al. Tregs prevent GVHD and promote immune reconstitution in HLA-haploidentical transplantation. Blood. 2011;117: 3921–3928. doi:10.1182/blood-2010-10-311894

196. Biswas M, Kumar SRP, Terhorst C, Herzog RW. Gene therapy with regulatory T cells: A beneficial alliance. Frontiers in Immunology. 2018;9: 554. doi:10.3389/fimmu.2018.00554

197. Zhang Q, Lu W, Liang C-L, Chen Y, Liu H, Qiu F, et al. Chimeric antigen receptor (CAR) treg: A promising approach to inducing immunological tolerance. Frontiers in Immunology. 2018;9: 2359. doi:10.3389/fimmu.2018.02359

198. Brunstein CG, Blazar BR, Miller JS, Cao Q, Hippen KL, McKenna DH, et al. Adoptive transfer of umbilical cord blood-derived regulatory T cells and early viral reactivation. Biology of Blood and Marrow Transplantation. 2013;19: 1271–1273. doi:10.1016/j.bbmt.2013.06.004

199. Walker LSK. Treg and CTLA-4: two intertwining pathways to immune tolerance. Journal of Autoimmunity. 2013;45: 49–57. doi:10.1016/j.jaut.2013.06.006

200. Derré L, Rivals J-P, Jandus C, Pastor S, Rimoldi D, Romero P, et al. BTLA mediates inhibition of human tumor-specific CD8+ T cells that can be partially reversed by vaccination. Journal of Clinical Investigation. 2010;120: 157–167. doi:10.1172/JCI40070

201. Skuljec J, Chmielewski M, Happle C, Habener A, Busse M, Abken H, et al. Chimeric Antigen Receptor-Redirected Regulatory T Cells Suppress Experimental Allergic Airway Inflammation, a Model of Asthma. Frontiers in Immunology. 2017;8: 1125. doi:10.3389/fimmu.2017.01125

202. Norelli M, Camisa B, Barbiera G, Falcone L, Purevdorj A, Genua M, et al. Monocyte-derived IL-1 and IL-6 are differentially required for cytokine-release syndrome and neurotoxicity due to CAR T cells. Nature Medicine. 2018;24: 739–748. doi:10.1038/s41591-018-0036-4

203. Giavridis T, van der Stegen SJC, Eyquem J, Hamieh M, Piersigilli A, Sadelain M. CAR T cell-induced cytokine release syndrome is mediated by macrophages and abated by IL-1 blockade. Nature Medicine. 2018;24: 731–738. doi:10.1038/s41591-018-0041-7

CURRICULUM VITAE